Membrane Diffusion Barriers Localize Signal Amplification during Macropinocytosis

by

Timothy Welliver

A dissertation submitted in partial fulfillment
of the requirements for the degree of
Doctor of Philosophy
(Immunology)
in The University of Michigan
2011

Doctoral Committee:

Professor Joel A. Swanson, Chair
Professor Robert S. Fuller
Professor Ronald W. Holz
Associate Professor Kathleen L. Collins
Associate Professor Gary D. Luker

Acknowledgments

I am most thankful to Joel Swanson for the role he has had in my life and scientific career. Joel has been an exemplary mentor over the past three years. I have no doubts that being a member of his lab was a unique and ideal developmental opportunity. Joel is infinitely creative, consistently encouraging and resourceful, and a true role model. There are very few people as talented and gracious as Joel, and I am grateful to have known him.

I would also like to thank my previous mentor, Dr. Jennifer Reed. Jen was my supervisor at MedImmune, Inc., and she has had a tremendous impact on my scientific development. Jen inspired my initial interest in pursuing a PhD, and she has been a continued and invaluable source of guidance and encouragement.

I would like to thank my thesis committee for their guidance and suggestions.

I would finally like to thank my lab peers, past and present. In particular, Sam Straight and Lad Dombrowski answered millions of technical questions. I am very grateful to have been a member of the Swanson lab.

Table of Contents

List of Figures

Figure

Chapter One:

Introduction

1.1 Introduction to the Biology of the Thesis

The intention of this thesis is to define the signaling mechanisms that drive an important immunological process, macropinocytosis. The general finding of this thesis is that macropinocytic cups demonstrate novel signaling phenomena; specifically, macropinocytic cups are regions of the plasma membrane that inhibit lateral diffusion of membrane molecules. This inhibited diffusion functions in the creation of a tightly regulated signaling network that is based on the formation and conversion of phosphoinositide species.

This introductory chapter sets up the biological questions addressed by providing background information on a number of topics that appear in the experimental chapters. Primarily, this chapter aims to increase the reader's understanding of macrophages and macropinocytosis, with a focus on their importance to the immune system. The section on macrophages includes a brief synopsis of their lifecycle, from origin to mature effector. The discussion on macropinocytosis provides information on a number of topics, including the cellular membranes, ligand receptors, phosphoinositides, lipid-modifiers, and GTPases.

Finally, this introduction discusses experimental methodology like fluorescence microscopy and computer modeling.

1.2 Macrophages

1.2.1 Origin, Maturation, and Life Cycle

Macrophages are mononuclear leukocytes that are widely distributed throughout the body. Macrophages originate as monocytes in the bone marrow and circulate in the bloodstream for typically one to three days before being recruited to different body tissues. Recruitment of monocytes is enhanced by inflammatory and immune stimuli like cytokines (Gordon and Hughes, 1997).

As monocytes enter body tissues, they encounter stimuli that induce them to differentiate into macrophages or dendritic cells. Differentiation is controlled by growth factors (e.g. M-CSF, IL-3, IL-4) and interactions with stromal and other cells. Differentiation is a maturation process in which the cell becomes "activated" or "elicited." The macrophage is capable of directing immunological responses, and has much higher metabolic requirements than its monocyte precursor. As such, differentiation is a tightly regulated process (Gordon and Hughes, 1997; Gordon and Taylor, 2005).

Macrophages are terminally differentiated cells, and they are incapable of reentering the bloodstream for systemic recirculation. In normal adult tissue, macrophages typically do not divide due to their limited ability to replicate DNA,

although some tissue microenvironments (lung epidermis, pituitary) are exceptions. Macrophages can have relatively long lifespans, with "resident" cells surviving up to several months. Resident macrophages are found in many different tissue types, and are thought to function as alarm-response systems. They are capable of RNA and protein synthesis, and are effective as both primary immune effectors and in recruitment of other immune cells via the production of cytokines (Tacke and Randolph, 2006; van Furth, 1992).

In research use, primary macrophages are derived from monocytes using growth factors. Monocytes are harvested from animal sources such as mice, typically through exudation and collection of bone marrow. Macrophage Colony Stimulating Factor (M-CSF) is a growth factor that promotes the proliferation, survival, and differentiation of macrophages (Stanley et al., 1997). When monocytes are cultured in media supplemented with animal serum and M-CSF, they differentiate into macrophages over approximately seven days (Swanson, 1989).

1.2.2 Role in Immunology

Macrophages make many contributions to immunity, as part of both the innate and adaptive responses. Primarily, macrophages are scavenger cells that clear pathogens and cellular debris from the body (Henson et al., 2001; Reed et al., 2008). Macrophages can ingest these molecules through two general processes, phagocytosis and pinocytosis. The macrophage subjects internalized pathogens to lysosomal acids and NADPH oxidase-dependent "bursts" of reactive oxygen species

(ROS) (Hoppe and Swanson, 2004). Macrophages therefore have an essential role in limiting pathogen infections, and macrophage deficiencies have been linked to many chronic infections (Reed et al., 2008; Rosenzweig and Holland, 2004).

In addition to their direct effector functions, macrophages also participate in the production, activation, and regulation of other immune cells. Macrophages are important antigen-presenting cells. Following digestion of internalized pathogens, macrophages present sample peptides for the purpose of activating relevant lymphocytes (Perry et al., 1993). Macrophages also contribute to immunity by producing and secreting various proteins. Proinflammatory cytokines like IL-1 and TNFα mediate the acute phase response that limits pathogen spread. Additionally, the macrophage secretes many antimicrobial molecules, including lysozyme, proteinases, ROS, and reactive nitrogen intermediates (Nathan and Sieff, 1987).

1.3 Macropinocytosis

1.3.1 Role of Macropinocytosis in Immunology

Macropinocytosis is best known as the process by which cells ingest bulk amounts of extracellular fluid. A more complete definition is that various particles are also included in macropinosome formation, including viruses and bacteria (Swanson and Watts, 1995).

Macropinosomes provide a sequestered environment for trafficking and processing of pathogens. Soon after formation, the macropinosome becomes slightly

acidic, inhibiting pathogenic survival and replication. Fusion with lysosomes increases macropinosome acidity and delivers digestive enzymes like proteinases and lysozymes (Sieczkarski and Whittaker, 2002). Digested particles are then shuttled to the endoplasmic reticulum for antigen presentation. Macropinocytosis, then, is a central part of the normal response to pathogen invasion (Kerr and Teasdale, 2009a).

Macropinocytosis is traditionally defined as being non-selective, meaning the corresponding particle ingestion is not a response to activation of specific cognate receptors. Indeed, most macropinocytosis is either spontaneous or in response to growth factor stimulation. However, a variety of other particles including bacteria, viruses, and cellular debris can also trigger the process. Further, many pathogens initiate macropinocytosis to gain entry into cells (Mercer and Helenius, 2009).

Macropinocytois is also an avenue for administering therapeutics, thereby bolstering the immune system. By copying the methods microbes use to successfully manipulate macropinocytosis, viral vectors could be tailored to efficiently trigger macrophage activation. Cell-penetrating peptides have similar applicability, and could also be administered via macropinocytosis (Jones, 2007; Mercer and Helenius, 2009).

1.3.2 Cell Morphology of Macropinocytosis

Macropinocytosis is a dynamic process that involves drastic, cell-wide changes in morphology (Swanson, 2008). Later chapters of this thesis will show that changes in cellular structure in turn affect the behavior of signaling molecules.

1.3.2.1 Cellular Membrane Structure and Function

The cellular membrane is a selectively permeable structure that separates the intracellular and extracellular environments. The membrane is a bilayer of amphipathic phospholipids in mirror symmetry, with the hydrophobic tails in direct proximity and the phospholipid heads defining the hydrophilic surfaces. Protein and cholesterol molecules are commonly interspersed in the lipid bilayer. Proteins can be either transmembrane- spanning across the entire bilayer- or localized to either the inner (towards the intracellular environment) or outer (extracellular) leaflets of the membrane. Carbohydrates can also adorn the lipids and proteins (Simon et al., 1991).

Although it is a separate organelle, the cytoskeleton is heavily involved in the structure and function of the membrane. In particular, the cortical actin network is a meshwork of polymerized actin filaments that guides membrane shape through direct physical interactions (Doherty and McMahon, 2008). Macropinocytosis is one of many cellular processes that requires coordinated membrane reorganization, and the reorganization is driven by controlled actin polymerization. Changes in membrane shape are largely caused by changes in the underlying actin framework (Swanson, 2008).

The cellular membrane was originally thought to be a simple, essential barrier. It allowed the cell to exclude pathogens and to create a distinct internal environment (Singer and Nicolson, 1972). The membrane is now more appreciated as a dynamic participant in a variety of processes. Perhaps the most prominent of those is the role of the membrane in signal transduction. The "fluid mosaic model" posited a homogenous, freely diffusible membrane surface, but subsequent research identified discrete signaling subdomains. Subdomains can be regions where specific membrane components, such as surface receptors and cholesterols, are heavily concentrated (Simons and Toomre, 2000). The function of these domains might be to amplify signaling locally. For example, a high concentration of surface receptors increases their likelihood or efficiency in dimerizing (Brinkerhoff et al., 2004). And, the cholesterol molecules inhibit lateral membrane diffusion, so that once the activated receptors have triggered the formation of membrane second messengers, those molecules stay in close proximity and recruit cytoplasmic effectors. That general mechanism is used by lipid rafts, which are small (≤50 nm diameter) membrane subdomains noted for augmented signal transduction (Simons and Toomre, 2000).

The central intent of this thesis is to show that macropinocytosis involves the formation of membrane subdomains much larger than lipid rafts, also with the benefit of augmenting downstream receptor signaling. However, the macropinocytic subdomain is unprecedented, as it relies not on assymetrical distribution of membrane molecules, but on the 3-dimensional shape of the membrane itself.

1.3.2.2 Morphological Changes during Macropinocytosis

The process of macropinocytosis begins when the plasma membrane folds over onto itself, forming a membrane ruffle. The driving force of ruffle formation is polymerization of the cortical actin meshswork that lies just beneath the cellular membrane. Polymerized actin physically pushes out on the membrane, extending as far as 5 μm from the plane of the cell surface (Swanson, 2008). Despite the actin framework underneath, ruffles demonstrate significant instability. Many ruffles disappear back into the membrane soon after formation (Kerr and Teasdale, 2009b). Other ruffles, though, will expand in size, undergoing extension and curvature until they have formed nominal "c-shaped ruffles" (due to the resemblance to a letter "c" when viewed from above) (Swanson and Watts, 1995). As these ruffles continue to lengthen, they might eventually form what looks to be a complete circle in a process known as ruffle closure. These closed, circular ruffles are also known as membrane cups (Swanson et al., 1999). The membrane cup has major significance in the signaling that guides macropinocytosis. A primary focus of this thesis is how the membrane cup is able to act as a distinct membrane subdomain that augments signaling networks.

The membrane cup is initially part of the plasma membrane, facing the extracellular environment. However, its sides begin to extend and close over the cup opening. This process is thought to involve myosin motor proteins pulling on the polymerized actin filaments, causing constriction of the cup's distal margin (Lim and

Gleeson, 2011). The point at which the distal margin has completely constricted is called cup closure (Swanson, 2008). The result is the formation of an intracellular vacuole, the macropinosome (Figure 1.1).

1.3.3 Macropinocytic Signaling

Phagocytosis, the process by which cells "eat" particles from the surrounding environment, has many morphological similarities to macropinocytosis (Swanson, 2008). In phagocytosis, the ingested particle provides spatial guidance to the cell: as the extracellular particle binds to surface receptors, it provides a prompt as to where the relevant signaling molecules should be localized in the cell. Macropinocytosis, however, is a self-organized process. As will be discussed later in this chapter, interesting questions can be asked about how the cell can coordinate such a complex system of components into an elegant and efficient signaling network.

1.3.3.1 Signaling Components of Macropinocytosis

1.3.3.1.1 Ligand Receptors

Macropinocytosis is typically a response to growth factors like epidermal growth factor (EGF) or M-CSF. These ligands are detected by enzyme-linked receptors, which are transmembrane proteins that effectively link extracellular stimuli with intracellular signaling networks. Ligand binding causes cognate

receptors to dimerize, at which point they autophosphorylate each other. Tyrosine kinases in each receptor phosphorylate specific tyrosine residues in the other, creating binding sites for Src homology 2 (SH2) domain- and phosphotyrosine binding (PTB) domain-containing proteins. SH2 and PTB domains are found in kinases, phospholipases, and other signaling proteins. As a result, receptor activation causes the recruitment of those proteins to the membrane domain, where they can mediate downstream signaling pathways(Bryant et al., 2007; Murray et al., 2000).

1.3.3.1.2 Phosphoinositides

Phosphoinositides (PIs) are a subset of plasma membrane phospholipids that regulate a substantial number of cellular processes. PIs mostly act to recruit cytoplasmic proteins to the membrane domain, where those proteins can execute specific reactions that contribute to signaling pathways. PI functionality is partially a product of their scarcity. As a PI increases in concentration, it recruits or activates enzymatic proteins, with the effect of triggering or contributing to signaling pathways (DiNitto and Lambright, 2006). Tight control of PI concentrations is consequently essential to normal cellular behavior. Indeed, irregular fluctuations in membrane PI populations contribute to a host of health issues, ranging from breast cancer to bipolar disorder (Krauss and Haucke, 2007b).

All of the PIs derive from phosphatidylinositol (PtdIns). As part of cellular membranes, PtdIns has a headgroup that protrudes into the cytosol. This headgroup

includes an inositol ring in which three of the five hydroxyl groups (D3, D4, and D5) are subject to reversible phosphorylation. The hydroxyl groups can be phosphorylated in seven possible combinations, and each resulting PI has a distinct shape that allows it to interact with particular proteins. The inositol ring is an extension of the cytosolic leaflet of cellular membrane, making it accessible for interactions with intracellular proteins. Consequently, the appearance of a PI species causes the localized recruitment of specific effector proteins to the membrane domain (Krauss and Haucke, 2007a; Krauss and Haucke, 2007b).

Some PIs have been associated with certain cellular processes. PtdIns 4,5-bisphosphate ($PI(4,5)P_2$) has been shown to facilitate actin polymerization by dissociating capping proteins from barbed ends of filaments (Hinchliffe et al., 1998; Lassing and Lindberg, 1985). However, another report suggested that the disappearance of $PI(4,5)P_2$ contributed to the actin polymerization that drives phagocytosis (Scott et al., 2005). PI(4,5)P2 is removed from membrane in two ways. It is subject to hydrolysis by the γ isoform of phospholipase C (PLCγ) to produce diacylglycerol (DAG) and inositol trisphosphate (IP_3) (Hinchliffe et al., 1998). Or, type I phosphoinositide 3-kinase (PI3K) can phosphorylate $PI(4,5)P_2$, forming PtdIns 3,4,5-trisphosphate (PIP_3) (Vanhaesebroeck and Waterfield, 1999).

For most cell types, PIP_3 is only formed after cell stimulation, as with insulin receptor ligation (Kotani et al., 1994). The main function of PIP_3 is the dual recruitment of the proteins Pdk1 and Akt. Once recruited, Pdk1 phosphorylates and activates Akt. Akt is a protein kinase that contributes to signaling pathways

regulating cell growth and survival (Hinchliffe, 2001). PIP_3 also recruits proteins that control the activity of small GTPases. One such protein is Grp1, a guanine nucleotide exchange factor (GEF) that activates Arf1 (Klarlund et al., 1998). Arf1 functions in the transport of intracellular vesicles from the Golgi to the cellular membrane (Donaldson, 2003). Similarly, PIP_3 contributes to deactivation of Arf6 through interactions with its GTPase-activating protein (GAP) (Venkateswarlu et al., 2007). Arf6 counteracts the activity of Arf1, guiding vesicles to the Golgi from the plasma membrane. Additionally, Arf6 is thought to have a role in the reorganization of the cortical actin network (Donaldson, 2002). The presence of PIP_3 in membranes has also been linked to dissociation of Rac1 from its GDP dissociation inhibitor (GDI), facilitating Rac1 activation (Missy et al., 1998) (Ugolev et al., 2008). Rac1 and other Rho GTPases contribute to actin reorganization. PIP_3 is removed from the membrane through dephosphorylation at any of the 3', 4', or 5' positions of its inositol headgroup.

The phosphatase SHIP1 removes the 5' phosphate group from PIP_3, forming PtdIns 3,4-bisphosphate ($PI(3,4)P_2$) (Maehama and Dixon, 1998). $PI(3,4)P_2$ function is highly redundant with that of PIP_3. $PI(3,4)P_2$ also functions in the recruitment and activation of Akt (Franke et al., 1997). The ς, ε, and δ isoforms of protein kinase C (PKCς, PKCε, and PKCδ, respectively) are all activated by $PI(3,4)P_2$ and PIP_3 (Nakanishi et al., 1993) (Toker et al., 1994). These proteins collectively regulate a variety of processes, including actin polymerization and stimulation of the NADPH oxidase during phagocytosis (Aderem, 1992).

Proteins with Pleckstrin Homology (PH) domains bind to PIs with high affinity. The PH domain contains a lysine- and arginine-rich C-terminal α helix that forms electrostatic interactions with the negatively charged phosphates in the PI inositol ring. Individual PH domains bind only a subset of the PI species (De Matteis and Godi, 2004). Figure 1.2 lists the PI specificities for different PH domains (DiNitto and Lambright, 2006). Consequently, the abundance of a particular PI in the membrane causes recruitment of specific PH-containing proteins.

Another PI-binding domain is the FYVE domain (based on the Fab1, YOTB, Vac1, and EEA1 proteins), which binds only to PtdIns 3-phosphate (PI(3)P) (Gillooly et al., 2000). Although FYVE is named after four cysteine-rich proteins, the domain has been found in over 60 proteins. PI(3)P has only been found on intracellular vesicles, and many proteins that contain FYVE domains are known to participate in vesicular trafficking and other endosome behaviors.

Besides their functions in normal cellular behavior, PI-binding domains can be used as sensors for PI formation. PH and FYVE domains have been fused to fluorescent proteins. When the resulting constructs are transfected into cells, they allow visualization of PI localization during dynamic cellular processes (Botelho et al., 2000; Mercanti et al., 2006).

The aforementioned PI species have all been visualized during macropinocytosis in different cell types (Swanson, 2008; Yoshida et al., 2009). Most recently, PtdIns 3,4,5-trisphosphate (PIP_3) was found to have distinct spatiotemporal localization in newly formed circular membrane ruffles (Yoshida et

al., 2009). This localization invites several questions about how actin-rich membrane ruffles are able to regulate PI synthesis. Those questions are a major focus of this thesis.

1.3.3.1.3 Lipid-modifying Enzymes

As mentioned earlier, PIs control a number of cellular behaviors and distribution of its members must therefore be tightly regulated. This regulation is conferred by enzymatic proteins like kinases, phosphatases, and phospholipases. Kinases and phosphatases add and remove phosphate groups from the PI headgroup, respectively, while phospholipases hydrolyze PIs into different compounds. Examples of all of these enzymatic reactions appear in Chapter Three of this thesis.

The previous section noted that PI3K is responsible for phosphorylating $PI(4,5)P_2$ into PIP_3. There are three known isoforms of PI3K, Types I, II, or III (Wymann and Pirola, 1998). Type I PI3K functions at the plasma membrane, and is responsible for the phosphorylation of $PI(4,5)P_2$. Type II PI3K does not have any known function (Fruman et al., 1998), while Type III PI3K contributes to endosome trafficking and the associated oxidative burst (Wymann and Pirola, 1998). Type I PI3K is composed of two subunits. The p85 regulatory subunit has two C-terminal SH2 domains that allow PI3K to associate with phosphorylated surface receptors (Gillham et al., 1999). As PI3K binds to the receptor, conformational changes activate its other subunit, the catalytic p110. While activated PI3K can

phosphorylate several PI species, $PI(4,5)P_2$ is its preferred substrate (Hawkins et al., 1992).

Phosphatases clear PIP_3 by removing its phosphate groups. Phosphatase and tensin homologue (PTEN) dephosphorylates PIP_3 at its 3' position to generate $PI(4,5)P_2$ (Li et al., 1997), counteracting PI3K. PTEN contains an N-terminal series of proline-rich stretches and a central inositol phosphatase domain. PTEN is essential for proper signaling in both chemotaxis and phagocytosis (Cao et al., 2004; Dormann et al., 2004; Kim et al., 2002).

Src-homology 2 domain-containing inositol phosphatase-1 (SHIP-1) also dephosphorylates PIP_3, but removes the phosphate groups at the 5' position. SHIP-1 consists of an N-terminal SH2 domain, a central inositol phosphatase domain, and a C-terminal NPXY motif (Damen et al., 1996). Its SH2 domain causes SHIP-1 to be recruited to a variety of surface receptors (Nakamura et al., 2002). After recruitment to the membrane domain, Src kinases phosphorylate SHIP-1, activating its dephosphorylation capabilities (Tridandapani et al., 1997). Studies have shown that SHIP-1 is an important regulator of phagocytosis and the activity of the Rho GTPase Ras (Ganesan et al., 2006).

$PI(3,4)P_2$ can be further dephosphorylated at its 4' phosphate, generating PI(3)P. The phosphatase responsible for this reaction is the inositol polyphosphate 4-phosphatase (4-phosphatase II) (Norris et al., 1997). 4-phosphatase contains a catalytic "CX_5R" motif that is common in protein tyrosine phosphatases and dual specificity protein/lipid phosphatases (Norris et al., 1997). 4-phosphatases localize

to endosomal membranes, and thereby likely contribute to the distribution of PI(3)P on intracellular vesicles (Ivetac et al., 2005).

As mentioned in the previous section, PLCγ hydrolyzes $PI(4,5)P_2$ into DAG and IP_3. DAG is a membrane lipid with functional similarity to its PI precursor. DAG recruits cytoplasmic proteins, namely the PKC family, to the membrane domain. PKC proteins regulate signaling pathways for a variety of processes, including cell growth and receptor desensitization. IP_3 translocates to the endoplasmic reticulum, where it causes the release of intracellular Ca^{2+}. The Ca^{2+} flux activates some PKC isoforms, and other proteins (Merida et al., 2008; van Blitterswijk and Houssa, 2000).

1.3.3.1.4 GTPases

Several GTPases are involved in macropinocytosis. GTPases alternate between two structural conformations, acting as binary molecular switches (Wennerberg et al., 2005). When GDP is bound, the GTPase is in its inactive form. GEFs replace GDP with GTP, activating the GTPase. GAPs work opposite to GEFS, deactivating GTPases by stimulating the hydrolysis of GTP. GDIs also negatively regulate GTPase activity, disallowing GTPases from being activated by sequestering them from membranes. This diversity in regulatory actions has been linked to diverse temporal and spatial patterns of GTPase activity (Hoppe and Swanson, 2004).

The Ras superfamily of small GTPases has over 150 members. All superfamily proteins share a common catalytic G domain, responsible for GTP hydrolysis. The Ras superfamily is divided into branches based on structural and functional similarities. The GTPases within a branch use similar GAPs and GEFs (Wennerberg et al., 2005). Four of the superfamily branches are the Ras, Rho, Rab, and Arf subfamilies of proteins.

The proteins of the Ras subfamily are activated in response to diverse extracellular stimuli, including EGF and M-CSF. Ras proteins guide cell proliferation, differentiation, and survival, and they are thought to contribute to human oncogenesis. The protein Ras uses the effector molecules Raf and PI3K to carry out a variety of processes. One such process is the activation of Rab5, which Ras indirectly controls by interacting with the GEF Rin1. Further, Ras is known to signal from endosomal surfaces, where Rab5 localizes (Porat-Shliom et al., 2008; Tall et al., 2001; Wennerberg et al., 2005).

Rho GTPases like CDC42 and Rac1 are key regulators of cytoskeletal reorganization, and control cell shape and motility. Several GEFs and GAPs regulate Rho GTPases, and the GTPases similarly utilize a variety of downstream effectors (Bustelo et al., 2007). CDC42 functions in the formation of actin microspikes and filopodia. Rac1 promotes lamellipodium formation and membrane ruffles (Ridley, 2006). One report showed that Rac1 is activated soon after macropinocytic ruffle closure, possibly in response to the formation of PIP_3 (Yoshida et al., 2009). Rac1

might control the actin polymerization required in the later stages of macropinocytosis.

Rab GTPases regulate intracellular vesicular transport and the trafficking of proteins between different organelles of the endocytic and secretory pathways. Rab proteins localize to specific intracellular compartments consistent with their functions. They associate with membranes via prenylation, and their specificity in localization is dictated by divergent C-terminal sequences. Rabs control endosomal maturation by guiding vesicular fusion events, such as fusing phagosomes and lysosomes into phagolysosomes. Rab5 is the earliest of the Rabs that function in endocytosis, appearing immediately after endosome formation. Rab5 is thought to contribute to the formation of PI(3)P (Lanzetti et al., 2004; Zerial and McBride, 2001).

Arf GTPases are also involved in vesicular transport. In contrast to Rab proteins that each function at single steps in membrane, Arfs can act at multiple steps. Arf1 regulates the formation of vesicle coats at different steps in the exocytic and endocytic pathways. Additionally, at the Golgi, Arf1 recruits and stimulates PtdIns 4-kinase (PI4K), forming PI(4)P that is then inserted into the cellular membrane as part of normal trafficking. Arf6 regulates actin reorganization in addition to endocytosis. Further, Arf6 at the cellular membrane activates PI4P5K, generating PI(4,5)P_2 (Donaldson and Jackson, 2011; Donaldson and Klausner, 1994).

1.3.3.2 Signaling Events of Macropinocytosis

A primary goal of the experimental work in this thesis is to expand the understanding of the macropinocytic signaling network. This section provides only a summary of the published knowledge. Additionally, since the experimental work relies exclusively on responses to activation of M-CSF surface receptors, only those events are discussed.

Binding of M-CSF to the cognate receptors causes them to dimerize and phosphorylate each other, creating the binding site for PI3K. Once PI3K is recruited to the membrane domain, it phosphorylates any accessible $PI(4,5)P_2$ molecules, forming PIP_3. PIP_3 interacts with various GTPase-modifying proteins, and might have several contributions to macropinocytosis. However, Rac1 is activated soon after PIP_3 formation, suggesting that PIP_3 causes Rac1 to dissociate from its GDI, allowing its activation. Rac1 then activates downstream effectors involved in actin polyermization, triggering the actin and membrane reorganization required in cup closure (Figure 1.3) (Swanson, 2008) (Murray et al., 2000; Swanson, 1989).

1.4 Experimental Methods

1.4.1 Fluorescence Microscopy Techniques

Traditional biochemical and molecular biology methods are useful in showing if certain molecules participate in cellular processes. They can also show which molecules directly interact in a signaling network. However, full

understanding of a signaling mechanism requires not only identifying the molecules involved, but also determining when and where their activities occur.

Fluorescence microscopy techniques are more effective in identifying the molecular interactions that drive a cellular process. These techniques can be used to identify the molecules and interactions that make up a signaling network, but with the benefit of spatial and temporal context (Hoppe and Swanson, 2004).

1.4.1.1 Fluorescent Probes

Fluorescence microscopy is based on staining or transfecting cells with molecules with discernible fluorescence patterns. Proper fluorescence dictates that such molecules have distinct excitation and emission spectra: when the molecule is excited by light of a particular wavelength, it subsequently emits light at a significantly longer wavelength. If the wavelengths adequately differ, filters attached to the microscope can detect if incident light has passed through the fluorescent molecules. If so, microscopic photography can elucidate the cellular locations of those fluorophores. One application of fluorescent probes is in tracking the movements of cellular proteins.

1.4.1.1.1 GFP and its Derivatives

The original version of Green Fluorescent Protein (GFP) was extracted from the luminescent jellyfish *Aquorea victoria*. GFP is a 26.9 kDa protein that contains a

chromophore, allowing it to absorb 395-nm wavelength light and emit green, 509-nm light. Importantly, GFP retains its fluorescence ability when expressed in cells from other organisms. Coupled with its relatively small size, GFP's photostability means that it can be attached to other proteins to visualize *in vivo* localization of those chimeric proteins (Tsien and Miyawaki, 1998).

GFP has been modified to meet evolving research needs, such as for different fluorescent colors. Cyan fluorescent protein (CFP) and yellow fluorescent protein (YFP) were early variants, each derived through point mutations in the GFP gene sequence (Tsien and Miyawaki, 1998). CFP and YFP were subsequently mutated- into mCerulean and mCitrine, respectively- to improve their brightness, photostability, and efficiency in Förster Resonance Energy Transfer reactions (Griesbeck et al., 2001; Rizzo et al., 2004). Red fluorescent protein, another early variant (Fradkov et al., 2000), underwent similar improvements with the creation of mCherry (Shu et al., 2006). The spectra of mCerulean, mCitrine, and mCherry are sufficiently distinct to allow their simultaneous use in tracking different proteins in the same cell.

Photoactivatable GFP (PAGFP) is another important GFP derivative. After intense radiation with 413-nm light, the protein demonstrates approximately 100-fold fluorescence increase in response to excitation by 488-nm light. PAGFP has unique applicability for cellular imaging. Specifically, it allows for visualization of subpopulations of tagged molecules (Patterson and Lippincott-Schwartz, 2002). In Chapter II of this thesis, PAGFP is used to measure diffusion dynamics in the plasma

membrane. It was attached to MEM, a protein that localizes to the inner leaflet of the plasma membrane. Once expressed in the cell, only a small population of the PAGFP-MEM chimeras were activated, and then visualized over time. Tracking the movement of these molecules with respect to the entire membrane provided insight into how diffusion is altered in different portions of the membrane surface.

1.4.1.1.2 FM4-64

FM4-64 is a lipophilic dye that is commonly used to label the outer leaflet of exposed membrane surfaces. FM4-64 has negligible fluorescence when suspended in water, but its fluorescence increases significantly upon binding to plasma membranes. The result is that membranes are detectable even in dye-containing medium. FM4-64 has low photostability. However, membrane binding is rapid and reversible, meaning that depleted molecules are continuously replaced by new molecules from the extracellular medium. FM4-64 is excited by 555-nm light and emits 605-nm light, giving it red fluorescence (Yoshida et al., 2009).

1.4.1.2 Ratiometric Fluorescence Microscopy

Path length, the distance that light travels through a fluorophore-containing sample, is an important consideration in fluorescence microscopy. Most measurements of the localization of a fluorescent-tagged protein try to determine where the relevant fluorescence is brightest in the cell. However, as in the example

of a cytosolic protein, bright areas might not be caused by localization but by increases in path length (i.e. cell thickness). Changes in cell morphology often involve the cell undergoing temporal, local expansions in cytosolic volume, as is the case with macropinocytic ruffling. In a ruffle, the incident light might encounter a greater number of cytosolic fluorophores. The result is increased brightness and an erroneous measurement of protein "localization."

Ratiometric imaging addresses this problem by normalizing for cell thickness (Figure 1.4). Here, a different fluorophore is coexpressed to act as a volume marker. In the above example, this protein would have cytosolic localization. The ratiometric aspect is to divide the fluorescence intensity of the protein of interest by the fluorescence intensity of the volume marker. In the resulting ratiometric image, changes in path length effectively cancel, and areas of brightness indicate genuine protein localization (Hoppe et al., 2002).

1.4.1.3 Förster Resonance Energy Transfer (FRET) Microscopy

In live cell imaging, visualization of protein interactions was historically a matter of inference. If fluorescence patterns showed colocalization of two proteins, those proteins might be interacting. Förster resonance energy transfer (FRET) microscopy has provided a more definite and quantitative assessment. FRET measures the energy transfer that occurs between two fluorophores, a donor and an acceptor. FRET occurs when the resonance energy of an excited state donor

molecule is transferred to the acceptor. The acceptor is briefly excited before emitting the energy as fluorescent light (Kraynov et al., 2000).

To be a FRET pair, the emission spectrum of the donor molecule must overlap with the excitation spectrum of the acceptor. Greater spectral overlap increases the FRET signal, and CFP and its variants are often paired with YFP and its variants. FRET efficiency is inversely proportional to the sixth power of the distance between fluorophores. Consequently, the fluorophores have to be very close (<10 nm) for FRET to occur (Lakowicz et al., 1999). For the fluorophores to be in close enough proximity to generate the FRET signal, the proteins to which they are attached must be physically interacting (Hoppe et al., 2002).

FRET microscopy can also be used to measure activation of GTPases (Figure 1.5). These measurements rely on the conformational differences in the active and non-active forms of the GTPases. Many proteins only interact with the active, GTP-bound form of the GTPase. The relevant binding domains can be harvested from those proteins and fluorescently tagged. The GTPase is then tagged with the FRET partner fluorophore. In live cell imaging, the FRET donor and acceptor will only be close enough to interact when the GTPase has adopted the active (GTP-bound) conformation. Therefore, the FRET signal can be used to monitor the concentration and localization of GTPase activity in the cell (Hoppe and Swanson, 2004).

1.4.2 Computer Modeling

We used computer modeling to simulate plasma membrane dynamics during macropinocytosis. We specifically wanted to see if observed experimental diffusion patterns could be explained by path length, in this case the height of macropinocytic ruffles and cups. A stochastic approach for modeling this type of cell biology is the "particle method," in which diffusible "particles" are programmed to act as molecules in a continuous membrane. The particles diffuse at a programmed diffusion coefficient, and spatial variations (such as regions that lower the diffusion coefficient) can be included in the simulation surface (Andrews et al., 2010; Linderman, 2009).

Our simulations required a system that accounted for the lateral diffusion of molecules on 3-dimensional surfaces. COMSOL Multiphysics has shape construction software that allowed for creation of the flat and membrane cup shapes. COMSOL solves for the solutions of ordinary and partial differential equations at discrete points (Meyers et al., 2006). Our simulations used Fick's second law as its governing equation. Fick's second law:

$$\frac{\partial c}{\partial t} = D\nabla^2 c$$

Where "*c*" is the concentration of diffusible particles, and "*D*" is the diffusion coefficient. Fick's second law essentially predicts how diffusion will cause changes in particle concentration over time. The resulting COMSOL measurements quantified the number of diffusible particles that remained in the "activation region" at the time elapsed following initiation of the simulation.

COMSOL allowed us to measure the diffusion coefficient of a membrane-tethered fluorophore, PAGFP-MEM, and to test models of diffusion barriers in and around membrane ruffles.

1.5 Scope of the Thesis

This chapter has alluded to different questions that will be addressed later in this thesis. The first such question regards the spatial organization of signaling molecules during macropinocytosis. Phagocytosis is organized by the ingested particle, which causes receptor activation in distinct areas of the membrane. Macropinocytosis lacks such guidance. When stimulated by exogenous growth factors, receptor activation occurs throughout the entire membrane: the growth factor is equally accessible in any part of the membrane, and the receptors are evenly distributed. How, then, is macropinocytosis localized to distinct regions of the membrane? Chapter Two provides evidence that macropinocytosis involves establishing barriers to lateral diffusion in the plasma membrane. This chapter shows that macropinocytic cups are membrane subdomains in which membrane-tethered molecules are prevented from diffusing into the surrounding membrane.

Chapter Three investigates the functional significance of those diffusion barriers. Specifically, are there distinct signaling properties associated with the unique morphology of macropinocytosis? The chapter provides evidence that macropinocytosis has a high degree of spatial and temporal regulation. The efficiency of the signaling network is likely strongly reliant on the structure of the

macropinocytic cup, as the cup is effectively a partitioned region of the membrane that allows for efficient chemical reactions.

The Discussion in Chapter Four focuses on the implications of the membrane diffusion barriers and corresponding signaling chemistries.

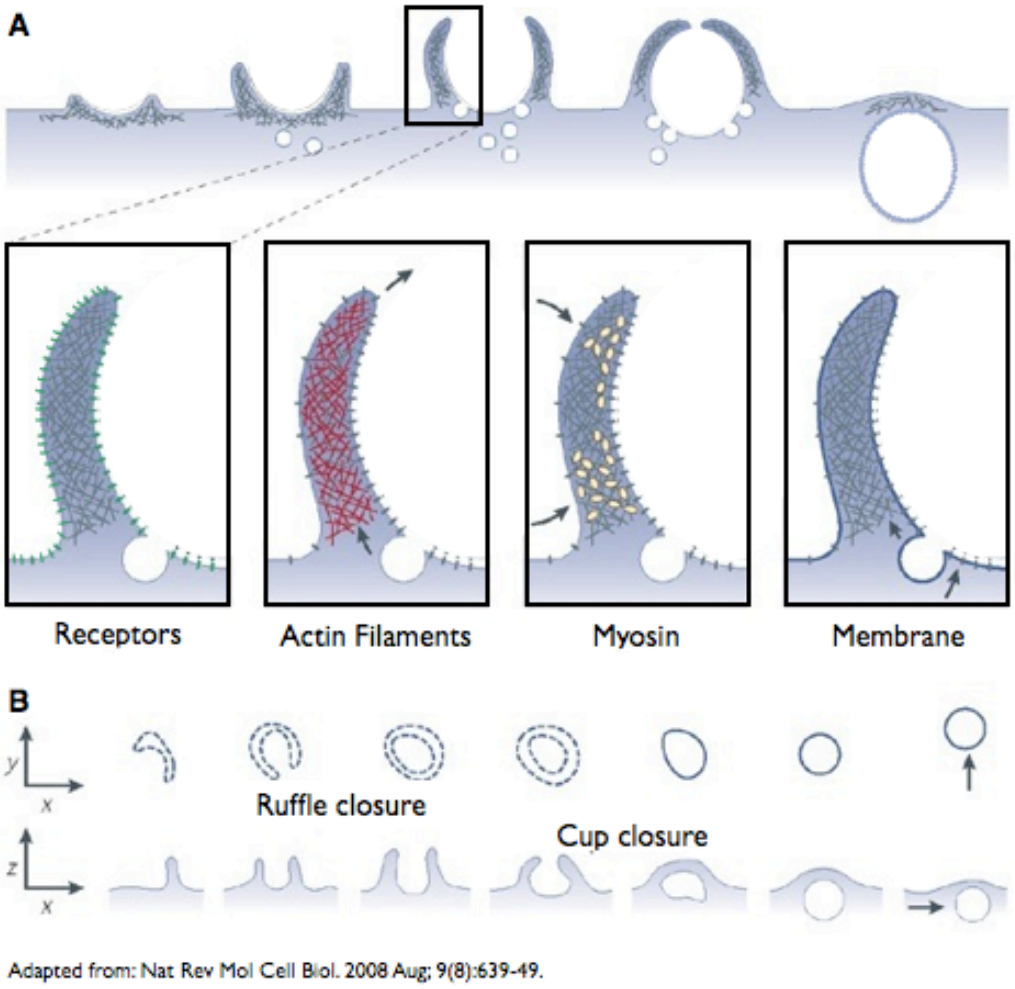

Figure 1.1 Morphological changes during macropinocytosis. (A) During macropinocytosis, the plasma membrane extends first to form a cup shape, then a full intracellular vacuole. Growth receptors (green) are evenly distributed inside and outside the forming macropinosome. Actin filaments (red) and myosin (yellow) are concentrated in the advancing cup. Membrane (blue) from intracellular compartments is inserted into the base of the forming macropinosome. In diagram for actin filaments, arrows indicate the net displacement of actin filaments by actin polymerization. In the myosin diagram, arrows indicate the contraction of the actin-myosin network. In the membrane diagram, arrows indicate the net flow of membrane into cups. (B) Macropinosomes at their distal margins form from cell-surface ruffles that close laterally into open cups (ruffle closure) and then into discrete intracellular vesicles (cup closure). Two aspects of macropinosome formation are presented: the XY projection indicates the 'top-down' view typically seen in light microscopy, and the XZ projection shows a side view of membrane movements. Dotted lines indicate folds in the plasma membrane. Ruffle closure is the formation of a circular, open cup of plasma membrane. Cup closure is the

separation of the macropinosome from the plasma membrane. Arrows indicate macropinosome displacement through the cytoplasm.

PH domain	Ligand	K_d (μM)
PLCδ1	$PI(4,5)P_2$	0.21
Btk	$PI(3,4,5)P_3$	0.040
PDK1	$PI(3)P$ $PI(3,4)P_2$ $PI(4,5)P_2$ $PI(3,4,5)P_3$	0.084 0.0052 0.024 00016
Akt	$PI(3,4)P_2$ $PI(4,5)P_2$ $PI(3,4,5)P_3$	2.5 0.57 0.40
DAPP1	$PI(3,4)P_2$ $PI(3,4,5)P_3$	not determined 0.003
PEPP1	$PI(3)P$	0.325
FAPP1	$PI(4)P$ $PI(4,5)P_2$	18.6 33.2
TAPP1	$PI(3,4)P_2$	0.005
TAPP2	$PI(3,4)P_2$	0.025
Dynamin	$PI(3,4)P_2$ $PI(4,5)P_2$ $PI(3,4,5)P_3$	64.0 63.0 43.0

Adapted from: Biochimica et Biophysica Acta. 2006; 1761: 850-867.

Figure 1.2 PH domains and their PI binding specificities.

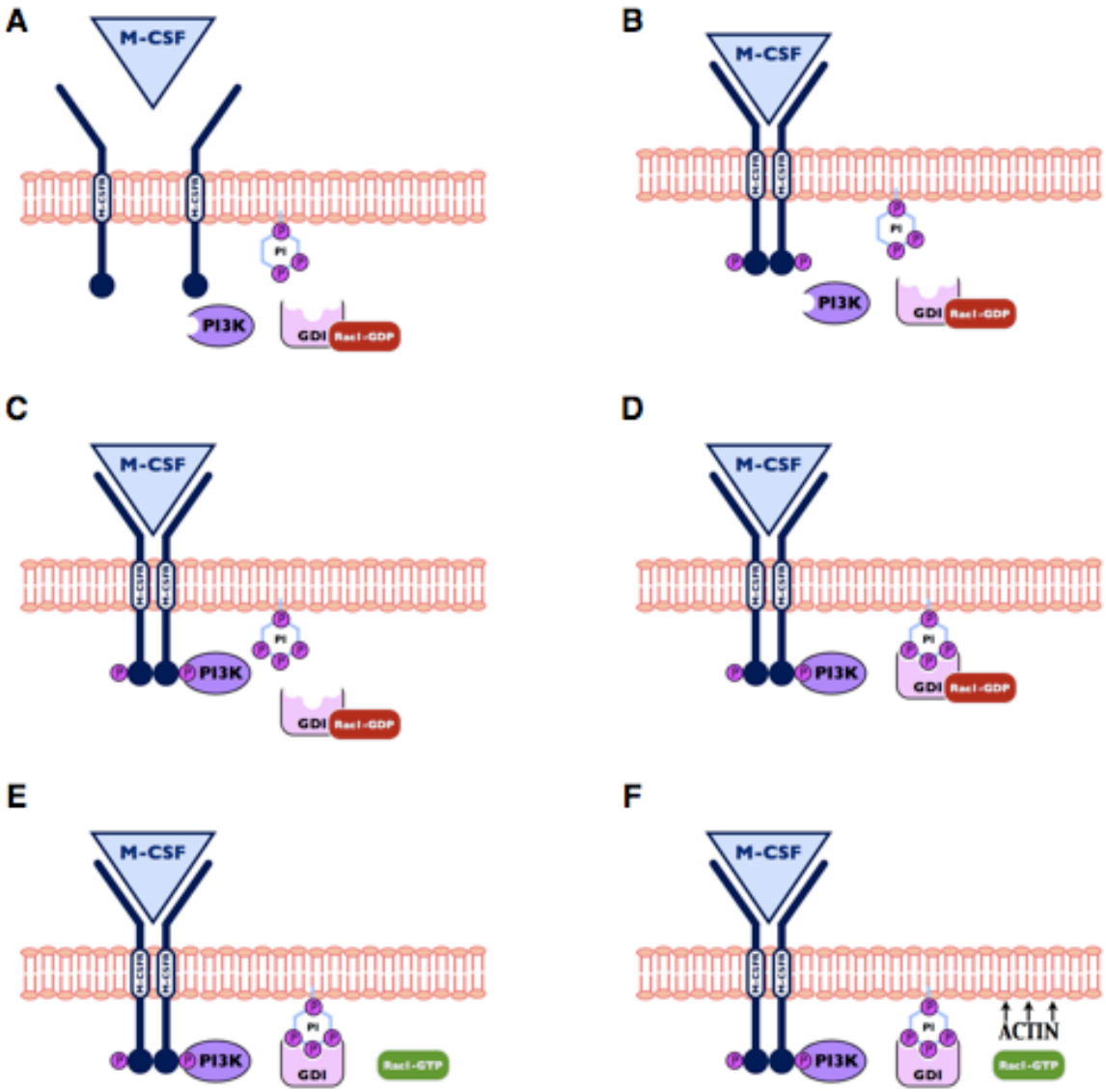

Figure 1.3 The macropinocytic signaling pathway. (A) Macropinocytosis occurs in response to growth factors like M-CSF. (B) After the growth factor binds to its cognate receptors, receptor dimerization causes autophosphorylation. (C) Phosphorylation of specific tyrosine residues creates binding sites for the cytosolic proteins like PI3K. As PI3K localizes to the membrane, it can phosphorylate PI(4,5)P2 into PIP3. (D) PIP3 interacts with the GDI for Rac1. Conformational changes cause dissociation between Rac1 and the GDI. (E) Rac1 can then be activated, through GTP binding. (F) Activation of Rac1 leads to downstream actin polymerization of the cortical actin network.

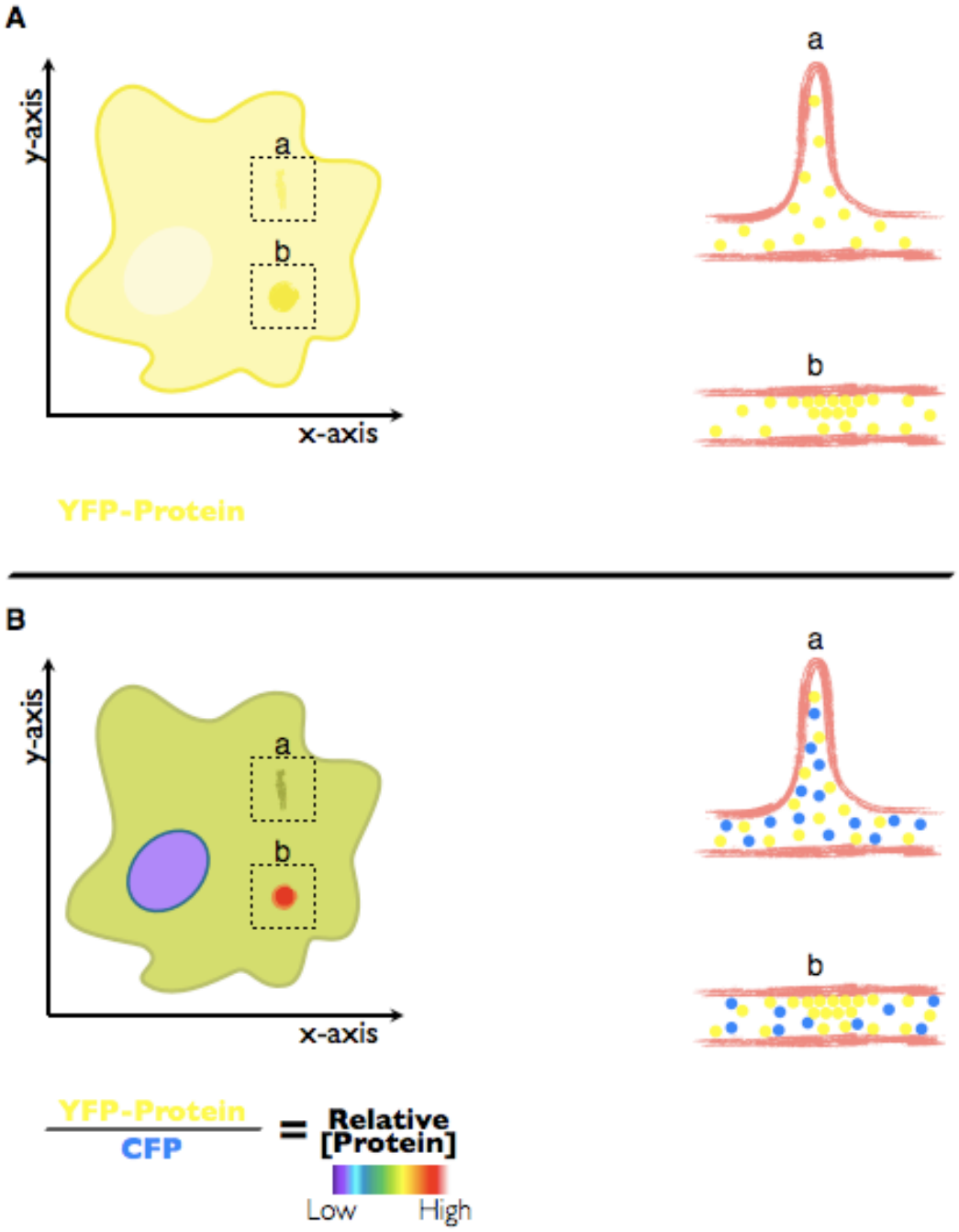

Figure 1.4 Ratiometric imaging. (A) Cell expressing fluorescent YFP-tagged protein chimera for a cytosolic protein. Image on left shows XY view of the cell, with two "bright" areas, a and b. Images on right show side (XZ) views for a and b, revealing a to be a ruffle, and b to be a region of protein localization. (B) Ratiometric image generated in cell expressing same YFP-tagged protein chimera and a CFP "volume marker." The CFP protein normalizes the brightness caused by path length, as in region a. Region b still registers as high protein localization, since the brightness for YFP is higher than that for the CFP comparator.

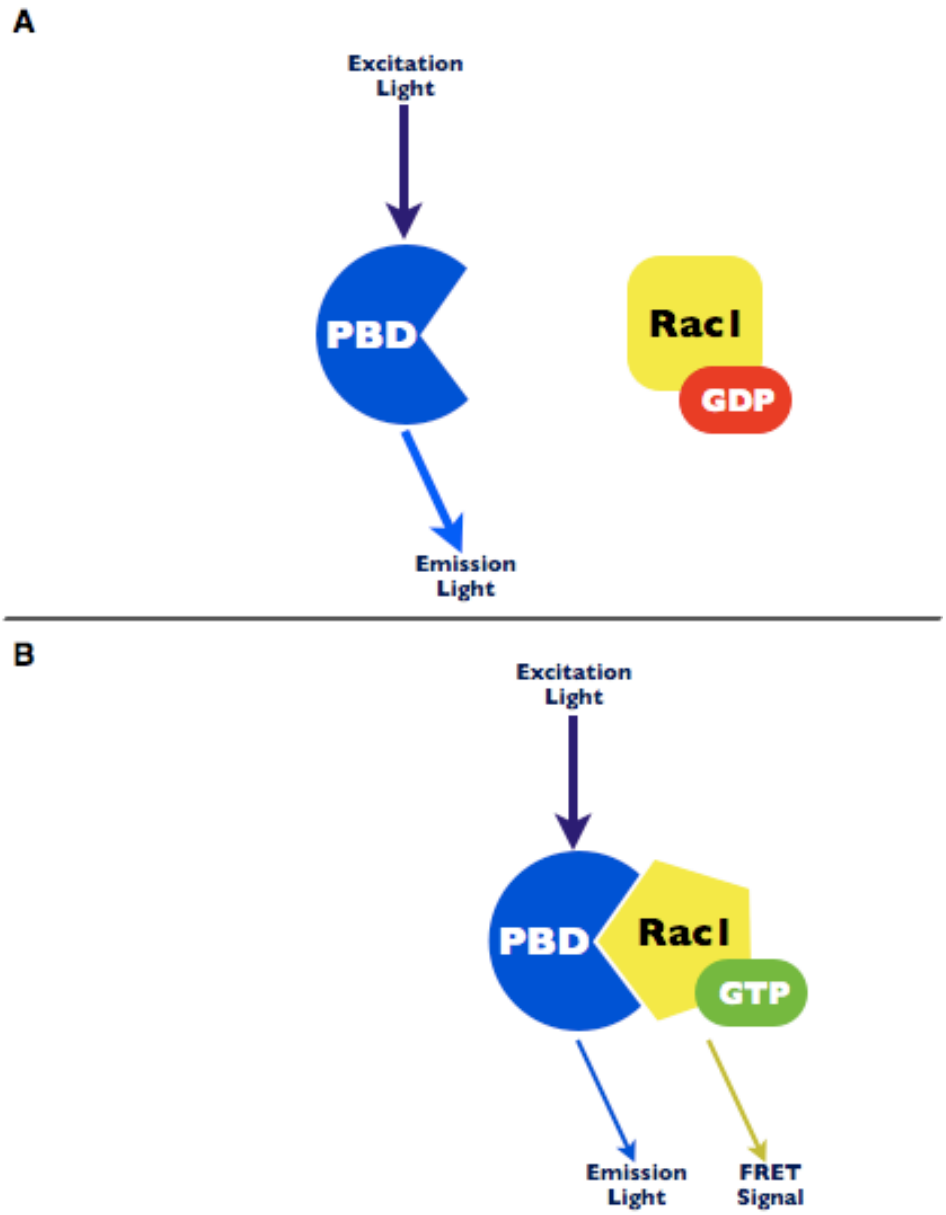

Figure 1.5 Using FRET microscopy to detect GTPase activation. FRET interactions occur when donor and acceptor fluorophores are very close together (≤10 nm). Pak1 binding domain is a protein subdomain that binds only the active, GTP-bound form of Rac1. In this example, PBD is tagged with CFP, and Rac1 is tagged with YFP. (A) When Rac1 is in its inactive form, PBD will not bind. The donor (CFP) and acceptor (YFP) fluorophores will not be in close enough proximity to generate a FRET signal. Excitation of CFP leads only to the corresponding CFP emission light. (B) In its active form, Rac1 binds to PBD and the fluorophores are brought into close proximity. Excitation of CFP now leads to excitation of YFP through resonance. Consequently, YFP fluorescence increases and CFP fluorescence decreases.

1.6 References

Aderem, A. 1992. The role of myristoylated protein kinase C substrates in intracellular signaling pathways in macrophages. *Curr Top Microbiol Immunol*. 181:189-207.

Andrews, S.S., N.J. Addy, R. Brent, and A.P. Arkin. 2010. Detailed simulations of cell biology with Smoldyn 2.1. *PLoS computational biology*. 6:e1000705.

Botelho, R.J., M. Teruel, R. Dierckman, R. Anderson, A. Wells, J.D. York, T. Meyer, and S. Grinstein. 2000. Localized biphasic changes in phosphatidylinositol-4,5-bisphosphate at sites of phagocytosis. *The Journal of cell biology*. 151:1353-1368.

Brinkerhoff, C.J., P.J. Woolf, and J.J. Linderman. 2004. Monte Carlo simulations of receptor dynamics: insights into cell signaling. *J Mol Histol*. 35:667-677.

Bryant, D.M., M.C. Kerr, L.A. Hammond, S.R. Joseph, K.E. Mostov, R.D. Teasdale, and J.L. Stow. 2007. EGF induces macropinocytosis and SNX1-modulated recycling of E-cadherin. *J Cell Sci*. 120:1818-1828.

Bustelo, X.R., V. Sauzeau, and I.M. Berenjeno. 2007. GTP-binding proteins of the Rho/Rac family: regulation, effectors and functions in vivo. *Bioessays*. 29:356-370.

Cao, X., G. Wei, H. Fang, J. Guo, M. Weinstein, C.B. Marsh, M.C. Ostrowski, and S. Tridandapani. 2004. The inositol 3-phosphatase PTEN negatively regulates Fc gamma receptor signaling, but supports Toll-like receptor 4 signaling in murine peritoneal macrophages. *J Immunol*. 172:4851-4857.

Damen, J.E., L. Liu, P. Rosten, R.K. Humphries, A.B. Jefferson, P.W. Majerus, and G. Krystal. 1996. The 145-kDa protein induced to associate with Shc by multiple cytokines is an inositol tetraphosphate and phosphatidylinositol 3,4,5-triphosphate 5-phosphatase. *Proceedings of the National Academy of Sciences of the United States of America*. 93:1689-1693.

De Matteis, M.A., and A. Godi. 2004. PI-loting membrane traffic. *Nat Cell Biol*. 6:487-492.

DiNitto, J.P., and D.G. Lambright. 2006. Membrane and juxtamembrane targeting by PH and PTB domains. *Biochimica et biophysica acta*. 1761:850-867.

Doherty, G.J., and H.T. McMahon. 2008. Mediation, modulation, and consequences of membrane-cytoskeleton interactions. *Annu Rev Biophys*. 37:65-95.

Donaldson, J.G. 2002. Arf6 and its role in cytoskeletal modulation. *Methods Mol Biol*. 189:191-198.

Donaldson, J.G. 2003. Multiple roles for Arf6: sorting, structuring, and signaling at the plasma membrane. *The Journal of biological chemistry*. 278:41573-41576.

Donaldson, J.G., and C.L. Jackson. 2011. ARF family G proteins and their regulators: roles in membrane transport, development and disease. *Nature reviews*. 12:362-375.

Donaldson, J.G., and R.D. Klausner. 1994. ARF: a key regulatory switch in membrane traffic and organelle structure. *Curr Opin Cell Biol*. 6:527-532.

Dormann, D., G. Weijer, S. Dowler, and C.J. Weijer. 2004. In vivo analysis of 3-phosphoinositide dynamics during Dictyostelium phagocytosis and chemotaxis. *J Cell Sci*. 117:6497-6509.

Fradkov, A., Y. Chen, L. Ding, E. Barsova, M. Matz, and S. Lukyanov. 2000. Novel fluorescent protein from Discosoma coral and its mutants possesses a unique far-red fluorescence. *FEBS Letters*. 479:127-130.

Franke, T.F., D.R. Kaplan, L.C. Cantley, and A. Toker. 1997. Direct regulation of the Akt proto-oncogene product by phosphatidylinositol-3,4-bisphosphate. *Science*. 275:665-668.

Fruman, D.A., R.E. Meyers, and L.C. Cantley. 1998. Phosphoinositide kinases. *Annu Rev Biochem*. 67:481-507.

Ganesan, L.P., T. Joshi, H. Fang, V.K. Kutala, J. Roda, R. Trotta, A. Lehman, P. Kuppusamy, J.C. Byrd, W.E. Carson, M.A. Caligiuri, and S. Tridandapani. 2006. FcgammaR-induced production of superoxide and inflammatory cytokines is differentially regulated by SHIP through its influence on PI3K and/or Ras/Erk pathways. *Blood*. 108:718-725.

Gillham, H., M.C. Golding, R. Pepperkok, and W.J. Gullick. 1999. Intracellular movement of green fluorescent protein-tagged phosphatidylinositol 3-kinase in response to growth factor receptor signaling. *The Journal of cell biology*. 146:869-880.

Gillooly, D.J., I.C. Morrow, M. Lindsay, R. Gould, N.J. Bryant, J.M. Gaullier, R.G. Parton, and H. Stenmark. 2000. Localization of phosphatidylinositol 3-phosphate in yeast and mammalian cells. *The EMBO journal*. 19:4577-4588.

Gordon, S., and D. Hughes. 1997. Macrophages and their origins: heterogeneity in relation to tissue microenvironment. Marcel Dekker, New York.

Gordon, S., and P.R. Taylor. 2005. Monocyte and macrophage heterogeneity. *Nat Rev Immunol*. 5:953-964.

Griesbeck, O., G.S. Baird, R.E. Campbell, D.A. Zacharias, and R.Y. Tsien. 2001. Reducing the environmental sensitivity of yellow fluorescent protein. Mechanism and applications. *The Journal of biological chemistry*. 276:29188-29194.

Hawkins, P.T., T.R. Jackson, and L.R. Stephens. 1992. Platelet-derived growth factor stimulates synthesis of PtdIns(3,4,5)P3 by activating a PtdIns(4,5)P2 3-OH kinase. *Nature*. 358:157-159.

Henson, P.M., D.L. Bratton, and V.A. Fadok. 2001. Apoptotic cell removal. *Curr Biol*. 11:R795-805.

Hinchliffe, K.A. 2001. Cellular signalling: stressing the importance of PIP3. *Curr Biol*. 11:R371-372.

Hinchliffe, K.A., A. Ciruela, and R.F. Irvine. 1998. PIPkins1, their substrates and their products: new functions for old enzymes. *Biochimica et biophysica acta*. 1436:87-104.

Hoppe, A., K. Christensen, and J.A. Swanson. 2002. Fluorescence resonance energy transfer-based stoichiometry in living cells. *Biophys J*. 83:3652-3664.

Hoppe, A.D., and J.A. Swanson. 2004. Cdc42, Rac1, and Rac2 display distinct patterns of activation during phagocytosis. *Molecular Cell Biology*. 15:3509-3519.

Ivetac, I., A.D. Munday, M.V. Kisseleva, X.M. Zhang, S. Luff, T. Tiganis, J.C. Whisstock, T. Rowe, P.W. Majerus, and C.A. Mitchell. 2005. The type Ialpha inositol polyphosphate 4-phosphatase generates and terminates phosphoinositide 3-kinase signals on endosomes and the plasma membrane. *Molecular biology of the cell*. 16:2218-2233.

Jones, A.T. 2007. Macropinocytosis: searching for an endocytic identity and role in the uptake of cell penetrating peptides. *J Cell Mol Med*. 11:670-684.

Kerr, M.C., and R.D. Teasdale. 2009a. Defining macropinocytosis. *Traffic*. 10:364-371.

Kerr, M.C., and R.D. Teasdale. 2009b. Defining macropinocytosis. *Traffic*. 10:364-371.

Kim, J.S., X. Peng, P.K. De, R.L. Geahlen, and D.L. Durden. 2002. PTEN controls immunoreceptor (immunoreceptor tyrosine-based activation motif) signaling and the activation of Rac. *Blood*. 99:694-697.

Klarlund, J.K., L.E. Rameh, L.C. Cantley, J.M. Buxton, J.J. Holik, C. Sakelis, V. Patki, S. Corvera, and M.P. Czech. 1998. Regulation of GRP1-catalyzed ADP ribosylation factor guanine nucleotide exchange by phosphatidylinositol 3,4,5-trisphosphate. *The Journal of biological chemistry*. 273:1859-1862.

Kotani, K., K. Yonezawa, K. Hara, H. Ueda, Y. Kitamura, H. Sakaue, A. Ando, A. Chavanieu, B. Calas, F. Grigorescu, and et al. 1994. Involvement of phosphoinositide 3-kinase in insulin- or IGF-1-induced membrane ruffling. *The EMBO journal*. 13:2313-2321.

Krauss, M., and V. Haucke. 2007a. Phosphoinositide-metabolizing enzymes at the interface between membrane traffic and cell signalling. *EMBO reports*. 8:241-246.

Krauss, M., and V. Haucke. 2007b. Phosphoinositides: regulators of membrane traffic and protein function. *FEBS Lett*. 581:2105-2111.

Kraynov, V.S., C. Chamberlain, G.M. Bokoch, M.A. Schwartz, S. Slabaugh, and K.M. Hahn. 2000. Localized Rac activation dynamics visualized in living cells. *Science*. 290:333-337.

Lakowicz, J.R., I. Gryczynski, Z. Gryczynski, and J.D. Dattelbaum. 1999. Anisotropy-based sensing with reference fluorophores. *Anal Biochem*. 267:397-405.

Lanzetti, L., A. Palamidessi, L. Areces, G. Scita, and P.P. Di Fiore. 2004. Rab5 is a signalling GTPase involved in actin remodelling by receptor tyrosine kinases. *Nature*. 429:309-314.

Lassing, I., and U. Lindberg. 1985. Specific interaction between phosphatidylinositol 4,5-bisphosphate and profilactin. *Nature*. 314:472-474.

Li, J., C. Yen, D. Liaw, K. Podsypanina, S. Bose, S.I. Wang, J. Puc, C. Miliaresis, L. Rodgers, R. McCombie, S.H. Bigner, B.C. Giovanella, M. Ittmann, B. Tycko, H. Hibshoosh, M.H. Wigler, and R. Parsons. 1997. PTEN, a putative protein tyrosine phosphatase gene mutated in human brain, breast, and prostate cancer. *Science*. 275:1943-1947.

Lim, J.P., and P.A. Gleeson. 2011. Macropinocytosis: an endocytic pathway for internalising large gulps. *Immunol Cell Biol*.

Linderman, J.J. 2009. Modeling of G-protein-coupled receptor signaling pathways. *The Journal of biological chemistry*. 284:5427-5431.

Maehama, T., and J.E. Dixon. 1998. The tumor suppressor, PTEN/MMAC1, dephosphorylates the lipid second messenger, phosphatidylinositol 3,4,5-trisphosphate. *The Journal of biological chemistry*. 273:13375-13378.

Mercanti, V., S.J. Charette, N. Bennett, J.J. Ryckewaert, F. Letourneur, and P. Cosson. 2006. Selective membrane exclusion in phagocytic and macropinocytic cups. *J Cell Sci*. 119:4079-4087.

Mercer, J., and A. Helenius. 2009. Virus entry by macropinocytosis. *Nat Cell Biol*. 11:510-520.

Merida, I., A. Avila-Flores, and E. Merino. 2008. Diacylglycerol kinases: at the hub of cell signalling. *Biochem J*. 409:1-18.

Meyers, J., J. Craig, and D.J. Odde. 2006. Potential for control of signaling pathways via cell size and shape. *Curr Biol*. 16:1685-1693.

Missy, K., V. Van Poucke, P. Raynal, C. Viala, G. Mauco, M. Plantavid, H. Chap, and B. Payrastre. 1998. Lipid products of phosphoinositide 3-kinase interact with Rac1 GTPase and stimulate GDP dissociation. *The Journal of biological chemistry*. 273:30279-30286.

Murray, J., L. Wilson, and S. Kellie. 2000. Phosphatidylinositol-3' kinase-dependent vesicle formation in macrophages in response to macrophage colony stimulating factor. *J Cell Sci*. 113 Pt 2:337-348.

Nakamura, K., A. Malykhin, and K.M. Coggeshall. 2002. The Src homology 2 domain-containing inositol 5-phosphatase negatively regulates Fcgamma receptor-mediated phagocytosis through immunoreceptor tyrosine-based activation motif-bearing phagocytic receptors. *Blood*. 100:3374-3382.

Nakanishi, H., K.A. Brewer, and J.H. Exton. 1993. Activation of the zeta isozyme of protein kinase C by phosphatidylinositol 3,4,5-trisphosphate. *The Journal of biological chemistry*. 268:13-16.

Nathan, D.G., and C.A. Sieff. 1987. The biological activities and uses of recombinant granulocyte-macrophage and multi-colony stimulating factors. *Prog Hematol*. 15:1-18.

Norris, F.A., R.C. Atkins, and P.W. Majerus. 1997. The cDNA cloning and characterization of inositol polyphosphate 4-phosphatase type II. Evidence for conserved alternative splicing in the 4-phosphatase family. *The Journal of biological chemistry*. 272:23859-23864.

Patterson, G.H., and J.A. Lippincott-Schwartz. 2002. A photoactivatable GFP for selective photolabeling of proteins and cells. *Science*. 297:1873-1877.

Perry, V.H., P.B. Andersson, and S. Gordon. 1993. Macrophages and inflammation in the central nervous system. *Trends in neurosciences*. 16:268-273.

Porat-Shliom, N., Y. Kloog, and J.G. Donaldson. 2008. A unique platform for H-Ras signaling involving clathrin-independent endocytosis. *Molecular biology of the cell*. 19:765-775.

Reed, J.L., Y.A. Brewah, T. Delaney, T. Welliver, T. Burwell, E. Benjamin, E. Kuta, A. Kozhich, L. McKinney, J. Suzich, P.A. Kiener, L. Avendano, L. Velozo, A. Humbles, R.C. Welliver, Sr., and A.J. Coyle. 2008. Macrophage impairment underlies airway occlusion in primary respiratory syncytial virus bronchiolitis. *J Infect Dis*. 198:1783-1793.

Ridley, A.J. 2006. Rho GTPases and actin dynamics in membrane protrusions and vesicle trafficking. *Trends in cell biology*. 16:522-529.

Rizzo, M.A., G.H. Springer, B. Granada, and D.W. Piston. 2004. An improved cyan fluorescent protein variant useful for FRET. *Nature biotechnology*. 22:445-449.

Rosenzweig, S.D., and S.M. Holland. 2004. Phagocyte immunodeficiencies and their infections. *J Allergy Clin Immunol*. 113:620-626.

Scott, C.C., W. Dobson, R.J. Botelho, N. Coady-Osberg, P. Chavrier, D.A. Knecht, C. Heath, P. Stahl, and S. Grinstein. 2005. Phosphatidylinositol-4,5-bisphosphate hydrolysis directs actin remodeling during phagocytosis. *J Cell Biol*. 169:139-149.

Shu, X., N.C. Shaner, C.A. Yarbrough, R.Y. Tsien, and S.J. Remington. 2006. Novel chromophores and buried charges control color in mFruits. *Biochemistry*. 45:9639-9647.

Sieczkarski, S.B., and G.R. Whittaker. 2002. Dissecting virus entry via endocytosis. *J Gen Virol*. 83:1535-1545.

Simon, M.I., M.P. Strathmann, and N. Gautam. 1991. Diversity of G proteins in signal transduction. *Science*. 252:802-808.

Simons, K., and D. Toomre. 2000. Lipid rafts and signal transduction. *Nature Reviews Molecular Cell Biology*. 1:31-39.

Singer, S.J., and G.L. Nicolson. 1972. The fluid mosaic model of the structure of cell membranes. *Science*. 175:720-731.

Stanley, E.R., K.L. Berg, D.B. Einstein, P.S. Lee, F.J. Pixley, Y. Wang, and Y.G. Yeung. 1997. Biology and action of colony--stimulating factor-1. *Mol Reprod Dev*. 46:4-10.

Swanson, J.A. 1989. Phorbol esters stimulate macropinocytosis and solute flow through macrophages. *Journal of Cell Science*. 94:135-142.

Swanson, J.A. 2008. Shaping cups into phagosomes and macropinosomes. *Nature Reviews Molecular Cell Biology*. 9:639-649.

Swanson, J.A., M.T. Johnson, K. Beningo, P. Post, M. Mooseker, and N. Araki. 1999. A contractile activity that closes phagosomes in macrophages. *Journal of Cell Science*. 112:301-316.

Swanson, J.A., and C. Watts. 1995. Macropinocytosis. *Trends in cell biology*. 5:424-428.

Tacke, F., and G.J. Randolph. 2006. Migratory fate and differentiation of blood monocyte subsets. *Immunobiology*. 211:609-618.

Tall, G.G., M.A. Barbieri, P.D. Stahl, and B.F. Horazdovsky. 2001. Ras-activated endocytosis is mediated by the Rab5 guanine nucleotide exchange activity of RIN1. *Developmental cell*. 1:73-82.

Toker, A., M. Meyer, K.K. Reddy, J.R. Falck, R. Aneja, S. Aneja, A. Parra, D.J. Burns, L.M. Ballas, and L.C. Cantley. 1994. Activation of protein kinase C family members by the novel polyphosphoinositides PtdIns-3,4-P2 and PtdIns-3,4,5-P3. *The Journal of biological chemistry*. 269:32358-32367.

Tridandapani, S., T. Kelley, M. Pradhan, D. Cooney, L.B. Justement, and K.M. Coggeshall. 1997. Recruitment and phosphorylation of SH2-containing inositol phosphatase and Shc to the B-cell Fc gamma immunoreceptor

tyrosine-based inhibition motif peptide motif. *Molecular and cellular biology*. 17:4305-4311.

Tsien, R.Y., and A. Miyawaki. 1998. Seeing the machinery of live cells. *Science*. 280:1954-1955.

Ugolev, Y., Y. Berdichevsky, C. Weinbaum, and E. Pick. 2008. Dissociation of Rac1(GDP).RhoGDI complexes by the cooperative action of anionic liposomes containing phosphatidylinositol 3,4,5-trisphosphate, Rac guanine nucleotide exchange factor, and GTP. *The Journal of biological chemistry*. 283:22257-22271.

van Blitterswijk, W.J., and B. Houssa. 2000. Properties and functions of diacylglycerol kinases. *Cell Signal*. 12:595-605.

van Furth, E. 1992. Mononuclear phagocytes: biology of monocytes and macrophages. Kluwer, Dordrecht, Netherlands.

Vanhaesebroeck, B., and M.D. Waterfield. 1999. Signaling by distinct classes of phosphoinositide 3-kinases. *Experimental cell research*. 253:239-254.

Venkateswarlu, K., K.G. Brandom, and H. Yun. 2007. PI-3-kinase-dependent membrane recruitment of centaurin-alpha2 is essential for its effect on ARF6-mediated actin cytoskeleton reorganisation. *J Cell Sci*. 120:792-801.

Wennerberg, K., K.L. Rossman, and C.J. Der. 2005. The Ras superfamily at a glance. *J Cell Sci*. 118:843-846.

Wymann, M.P., and L. Pirola. 1998. Structure and function of phosphoinositide 3-kinases. *Biochimica et biophysica acta*. 1436:127-150.

Yoshida, S., A.D. Hoppe, N. Araki, and J.A. Swanson. 2009. Sequential signaling in plasma-membrane domains during macropinosome formation in macrophages. *Journal of Cell Science*. 122:3250-3261.

Zerial, M., and H. McBride. 2001. Rab proteins as membrane organizers. *Nature reviews*. 2:107-117.

Chapter Two:
Ruffles Limit Diffusion in the Plasma Membrane during Macropinosome Formation

2.1 Abstract

In murine macrophages stimulated with Macrophage-Colony-stimulating Factor (M-CSF), signals essential to macropinosome formation are restricted to the domain of plasma membrane enclosed within cup-shaped, circular ruffles. Consistent with a role for these actin-rich structures in signal amplification, microscopic measures of Rac1 activity determined that disruption of actin polymerization by latrunculin B inhibited ruffling and the localized activation of Rac1 in response to M-CSF. To test the hypothesis that circular ruffles restrict the lateral diffusion of membrane proteins that are essential for signaling, we monitored diffusion of membrane-tethered, photoactivatable green fluorescent protein (PAGFP-MEM) in ruffling and non-ruffling regions of cells. Although diffusion within macropinocytic cups was not inhibited, circular ruffles retained photoactivated PAGFP-MEM inside cup domains. Confinement of membrane molecules by circular ruffles could explain how actin facilitates positive feedback amplification of Rac1 in these relatively large domains of plasma membrane, thereby organizing the contractile activities that close macropinosomes.

2.2 Introduction

In response to stimulation by growth factors, many cells extend actin-rich, circular ruffles that close into endocytic vacuoles called macropinosomes. Macropinocytosis begins with deformation of the plasma membrane by actin-based motile activities, first into linear or curved ruffles, then into cup-shaped circular ruffles at the cell surface (Swanson, 2008). This ruffle closure is followed by cup closure, in which the circular ruffle constricts at its distal margin and separates from the plasma membrane as a macropinosome inside the cell (Li et al., 1997).

Previous studies identified molecules that regulate macropinocytosis, including phosphatidylinositol 3'-kinase (PI3K) and Rac1 (Araki et al., 1996; Yoshida et al., 2009). Activated growth factor receptors recruit and activate type I PI3K, which generates phosphatidylinositol 3,4,5-trisphosphate (PIP_3) in the inner leaflet of the plasma membrane. Inhibitors of PI3K allow ruffle closure but inhibit cup closure (Araki et al., 2003; Araki et al., 1996), indicating that PIP_3 directs the late stage of macropinosome formation. Rac1 is requisite in the macrophage ruffling response to macrophage colony-stimulating factor (M-CSF) (Cox et al., 1997; Wells et al., 2004).

How are the movements of the actin cytoskeleton organized to close cup-shaped extensions into intracellular vesicles? Concentrated PIP_3 or Rac1 in the macropinocytic cup could regulate actin-myosin-based contractions that close the cup. Imaging of signaling in response to M-CSF showed that PIP_3 generation and Rac1 activation closely follow ruffle closure and are confined within circular ruffles

(Yoshida et al., 2009). This indicates that circular ruffles create domains of plasma membrane that facilitate signal amplification and the contractile activities of cup closure. We hypothesize that molecules necessary for Rac1 signal amplification are confined to circular ruffles by an actin-based diffusion barrier in the cup. We therefore conducted experiments to probe the existence and location of diffusion barriers in the inner leaflet of ruffling plasma membrane.

2.3 Results

2.3.1 Role of Actin Polymerization in Rac1 Activation

The relationship between actin-rich membrane ruffles and Rac1 signal amplification was examined by measuring the effect of the actin-depolymerizing agent latrunculin B on Rac1 activity. Quantitative Förster resonance energy transfer (FRET) microscopy was used to observe bone marrow-derived macrophages (BMM) expressing Citrine-Rac1 and Cerulean-PBD. PBD, derived from Pak1, binds the active (GTP-bound) form of Rac1 (Edwards et al., 1999). The citrine and cerulean chimeras produce significant FRET interactions in regions of the cell where Rac1 is active. FRET stoichiometry was used to determine G*, which is the fraction of activated Citrine-Rac1 in any given region of the image (Hoppe and Swanson, 2004). G* values in forming macropinosomes were higher than in the surrounding cytoplasm, indicating that Rac1 amplification was restricted to the cup domain (Fig. 2.1A, C, and F). After M-CSF addition, cells treated with latrunculin B did not ruffle

(Fig. 2.1D) and the small increase of Rac1 activity was delocalized (Fig. 2.1B and E). This indicated that Rac1 signal amplification in cups was actin-dependent.

2.3.2 Membrane Diffusion Dynamics in Macropinocytic Structures

To test the hypothesis that ruffles create barriers to diffusion in the inner leaflet of the plasma membrane, we measured the redistribution of plasma membrane-localized, photoactivatable green fluorescent protein (PAGFP-MEM), whose fluorescence following photoactivation increases 100-fold (Patterson and Lippincott-Schwartz, 2002). We first investigated whether ruffles could retain PAGFP-MEM near an initial region of photoactivation. Coexpression and imaging of monomeric Cherry (mCherry)-MEM chimeras provided a reference fluorescence that reported plasma membrane distribution. Ratiometric images, generated by dividing pixel values in the PAGFP-MEM images by the corresponding values in the mCherry-MEM images, normalized PAGFP-MEM distribution in the various ruffling morphologies. We activated small patches of PAGFP-MEM molecules and measured the rates at which fluorescence intensity decreased by diffusion in the plasma membrane (Fig. 2.2A). Curve-fitting analyses of fluorescence loss in flat regions of cells obtained a diffusion coefficient for PAGFP-MEM of 1.1×10^{-9} cm^2/second (Fig. 2.2B, Fig. 2.3A and B). Near linear ruffles, diffusion of the activated molecules was slightly inhibited (Fig. 2.2C). However, PAGFP-MEM activated inside circular ruffles was retained much more than PAGFP-MEM in flat or ruffled membrane (Fig. 2.2D), indicating that ruffled surfaces created effective barriers to diffusion of PAGFP-

MEM. Quantitative measurements of the fluorescence depletion supported this observation (Fig. 2.2E). The retention pattern for membrane cups leveled off approximately 15 seconds after activation, suggesting that activated molecules were retained in the activation region. The steep initial decline in fluorescence retention in all of the membrane structures could be explained by the fact that PAGFP-MEM molecules were photoactivated in both the top and bottom (i.e., substrate-adherent) membranes of the cells. Accordingly, plots of fluorescence depletion reflect the dynamics of PAGFP-MEM in both membranes, including the unrestricted diffusion in the flat, bottom membrane.

The apparent retention of PAGFP-MEM in the cup could be a consequence of its topography. Diffusion of PAGFP-MEM molecules activated inside membrane cups entails travel up the inner cup wall and down the outer cup wall. Apparent retention of activated PAGFP-MEM could simply reflect diffusion in the z-axis. However, simulations of diffusion in macropinocytic cups of various heights indicated that, in the absence of some type of barrier, diffusion in the z-axis would increase the retention of molecules in the activation spot only slightly (Fig. 2.2F and 2.3C). The observed retention of PAGFP-MEM in cups could only be simulated by inclusion of a diffusion barrier (i.e., a region with a 10-100x lower diffusion coefficient) in the cup structure.

To verify that the circular structures we analyzed were not closed pinosomes, we visualized photoactivated PAGFP-MEM using through-focus image acquisition and 3D reconstruction by image deconvolution. These experiments

showed directly that open macropinocytic cups retained PAGFP-MEM. Activated PAGFP-MEM molecules were visible in macropinocytic cups at least 19.5 seconds after activation (Fig. 2.4A-C). Comparable 3D reconstructions of activated PAGFP-MEM in flat membrane regions showed rapid and complete loss of fluorescence (Fig. 2.5).

Diffusion inside cups was further characterized using fluorescence intensity linescans of widefield microscopic images. Cherry-MEM linescans showed membrane contours. For open macropinocytic cups, the pixel intensities for Cherry-MEM were roughly equivalent inside and outside the cup, as fluorescence in each region derived from two layers of membrane (Fig. 2.6A and B). In contrast, Cherry-MEM fluorescence from closed macropinosomes should include four layers of membrane: the top and bottom membranes of the cell plus the top and bottom membranes of the macropinosome. Accordingly, the Cherry-MEM pixel intensities measured from closed macropinosomes were 2.15 times the intensities of the surrounding area (Fig. 2.7). This allowed us to use fluorescence linescans of Cherry-MEM images to confirm that all of the circular structures included in the quantification for Figure 2E were unclosed cups.

Fluorescence linescans also allowed us to measure the extent to which different membrane structures inhibited lateral diffusion of activated PAGFP-MEM. The initial fluorescence profiles for patches of activated PAGFP-MEM showed Gaussian distributions. In flat membrane, the intensity decreased rapidly to that of the surrounding plasma membrane (Fig. 2.6D-F), suggesting that the activated

molecules diffused out of the activation region. For circular ruffles, the intensity profiles in the activation region remained elevated (Fig. 2.6C), indicating retention of the photoactivated PAGFP-MEM in the cup region.

2.3.3 Characterization of Macropinocytic Diffusion Barrier

Retention of activated PAGFP-MEM in macropinocytic cups could be explained either by decreased diffusivity throughout the entire cup or by barriers localized to the circular ruffles. To determine if diffusion in the base of the cup resembles diffusion outside of the cup, we activated PAGFP-MEM in subregions of the cup structures and observed fluorescence redistribution within the cup. Imaging (Fig. 2.8A) and intensity linescans (Fig. 2.8B and C) of ratio fluorescence revealed that the initially asymmetrical activation profiles rapidly leveled off inside the cup. Modeling simulated PAGFP-MEM redistribution by creating an initially hemispherical cohort of activated molecules that redistributed with the diffusion coefficients of flat membrane (10^{-9} cm^2/second) or barriers (10^{-11} cm^2/second or 0 cm^2/second) (Fig. 2.8E and F). Diffusion barriers were assigned to different regions of the cup structure: the base, the inner wall, the distal rim, and combinations of those regions. The model most resembled the experimental data when the walls and rim of circular ruffles were assigned a barrier function and the base of the cup resembled flat membrane (Fig. 2.8G and I). In contrast, simulations that assigned low diffusion coefficients to the base, walls and rim yielded results that did not resemble the observations (Fig. 2.8H and J). This is consistent with a mechanism in

which proteins diffuse freely in the membrane of the base of the cup but encounter barriers in the ruffles.

2.4 Discussion

This study demonstrates that circular ruffles create barriers to protein diffusion in membranes. Unlike the diffusion barriers previously described for cleavage furrows (Schmidt and Nichols, 2004) and the leading edge of cellular protrusions (Weisswange et al., 2005), the diffusion barriers of circular ruffles are capable of organizing microdomains for focused signal amplification.

The molecular basis of the barrier remains unknown. Diffusion of membrane proteins or phospholipids could be restricted at the distal margins of ruffles, either by specific fence-like structures that constrain the lateral movements of membrane-associated molecules or by physical constraints imposed by the high membrane curvature at the ruffle edge. In lipid rafts, tight packing of phospholipids reduces diffusivity (Simons and Toomre, 2000); raft-like structures at the distal margins of the macropinocytic cups could create effective barriers. Alternatively, the underlying actin meshwork could limit diffusion in the plasma membrane, although a similar study suggested that cortical actin does not directly influence membrane diffusion (Frick et al., 2007). The slight slowing of PAGFP-MEM diffusion observed in linear ruffles, relative to flat membrane (Figs. 2C, E), suggests that the barrier is intrinsic to ruffle structure. Actin or actin-associated proteins in ruffles could create effective barriers simply by slowing lateral diffusion of molecules along the broad

face of the ruffle. Regardless of its physical basis, the constraint on diffusion created by actin-rich ruffles could provide a mechanism for biasing signal amplification in self-organizing systems, leading to actin-dependent amplification of signals in ruffle-rich regions of the cell.

The efficacy of the barrier for signal amplification is maximized in the circular ruffle, where diffusion is inhibited in all directions. Functionally, as a patch of plasma membrane with amplified activity of signaling proteins (Yoshida et al., 2009), the circular ruffle represents a novel signaling domain. Activated receptors recruit and activate lipid-modifying enzymes, such as PI3K, which recruit other enzymatic proteins to the membrane domain through the formation of lipid or phospholipid species. Absent barriers, diffusion in the membrane could dissipate receptor-generated signals to subthreshold levels and the initial activation signal would be unable to reach concentrations needed to activate later signals. Barriers could allow concentrations of lipids or activated GTPases to remain high, thereby allowing the cell to recruit or activate the molecules that actuate the late stages of signaling. Accordingly, the actin-dependent amplification of Rac1 within circular ruffles indicates a positive feedback amplification mechanism in which restricted movement of diffusible signaling intermediates allows their concentration in the plasma membrane to exceed some transition threshold. Similarly, transient increases of PIP_3 that follow immediately after ruffle closure could locally activate guanine nucleotide exchange factors for Rac1 or other GTPases (Yoshida et al., 2009). Conversely, by stimulating actin polymerization necessary for circular ruffle formation, Rac1 could amplify PI3K activity through an actin-dependent mechanism.

This mechanism of localizing signal amplification would be distinct from processes such as chemotaxis or phagocytosis, because it is independent of external orienting factors. Moreover, this focal signal amplification through restricted diffusion could provide a mechanism for cells to respond to lower concentrations of growth factor.

2.5 Materials and Methods

2.5.1 Cell culture

Bone marrow-derived macrophages (BMM) were generated as previously described (Araki et al., 2003; Swanson, 1989). Bone marrow exudate was obtained from femurs of C57BL/6J mice. Marrow was cultured in medium (DMEM with 20% FBS and 30% L cell-conditioned medium) promoting the differentiation of macrophages. Bone marrow cultures were differentiated for 1 week with additions of fresh differentiation medium at days 3 and 6. Following differentiation, macrophages were transfected and plated onto 25-mm circular coverslips. Cultures were incubated overnight in medium lacking M-CSF (RPMI 1640 with 20% heat-inactivated FBS). All experiments were performed the day after plating.

2.5.2 Constructs and cell transfection

Fluorophores were localized to the inner leaflet of the plasma membrane using the membrane localization domain from neuromodulin (MEM), a protein that associates with membrane via prenylation (Moriyoshi et al., 1996). BMMs were

transfected with plasmids encoding PAGFP-MEM and mCherry-MEM via Amaxa Nucleofector II, using automated protocol Y-01. The conditions and reagents for macropinocytosis observation were 200 ng/mL M-CSF (R&D Systems) in Ringer's Buffer (155 mM NaCl, 5 mM KCl, 2 mM $CaCl_2$, 1 mM $MgCl_2$, 2 mM NaH_2PO_4, 10 mM glucose and 10 mM HEPES at pH 7.2). In some experiments, Latrunculin B (5 μM) was added to cells five minutes before addition of M-CSF. All imaging experiments were temperature controlled at 37°C.

2.5.3 XYT photoactivation experiments

Cells were imaged using an Olympus FV-500 Confocal microscope fitted with a 60x 1.45 NA oil immersion objective. The microscope was equipped with diode-pulse (for photoactivation), argon (for GFP imaging), and HeNe green (for mCherry imaging) lasers. Image collection used Fluoview FV500 imaging software. Images were acquired at 1 frame/second using line sequential scanning. Three pre-activation images were collected for each experiment: these images were averaged to provide a fluorescence baseline reading. Photoactivation of PAGFP-MEM required one image scan with the diode laser set to 100% intensity. Photoactivation in defined regions of the cell membrane created patches of GFP fluorescence, whose fluorescence intensity decreased quickly by molecule diffusion in the membrane.

Fluorescence intensities and PAGFP/mCherry ratiometric images were quantified using the "region mean intensity" measurement function in MetaMorph (Molecular Dynamics, Sunnyvale, CA). The averaged pre-activation images

established a baseline fluorescence that was subtracted from all post-activation images. A normalized fluorescence for each post-activation image was calculated by dividing its fluorescence by the initial post-activation timepoint fluorescence.

2.5.4 Computer modeling experiments

Three-dimensional models of the flat and cupped membranes were constructed using the transient diffusion module of COMSOL Multiphysics 3.4 (COMSOL Inc., Burlington, MA). The flat membrane (Fig. S1a) was represented by two disks of 5.0 μm radius, r_o, and 0.05 μm thickness, t, representing the top and bottom layers of the membrane, respectively. The outer radius, r_o, was chosen to ensure that no molecules reached the outer edge of the model geometry during the time simulated. The cupped membrane (Fig. S1c) was represented by a top layer geometry of an inner radius, r_i, of 1.1 μm; distance between inner and outer cup walls, w, of 150 nm; and cup height, h, variable from 0.5 μm to 5.0 μm. The membrane thickness, t, was 0.05 μm and the outer radius, r_o, was 5 μm. The bottom layer of the cupped membrane was represented by the same geometry as the flat membrane. COMSOL required specifying a membrane thickness to solve the cupped membrane, and this small value (0.05 μm) allowed us to mimic diffusion on the membrane surface. The software employs a finite element analysis to follow the time course of diffusion (solving $\frac{\partial c}{\partial t} = D\nabla^2 c$ where c is concentration and D is the diffusion coefficient) and to calculate the concentration of molecules at each point

within the model geometry as a function of time. The initial condition for each model was equal to 2000 molecules uniformly distributed within the activation spot (r_a = 1 μm), 1000 molecules each in the top and bottom membrane layers. To compare simulation results with the experimental data (normalized fluorescence ratio), the number of molecules within the activation spot was calculated at each time point and the computational ratio, *R*, was calculated as:

$$R = \frac{top(t) + bottom(t)}{top(0) + bottom(0)}$$

in which *top(t)* and *bottom(t)* are the number of molecules within the activation spot at time *t* on the top and bottom membrane layers, respectively.

Simulation results from a flat membrane were fit to experimental data and used to determine a diffusion coefficient, *D*, of 1.1 x 10^{-9} cm^2/s. *D* was then used in simulations with the cupped membrane.

2.5.5 XYZT photoactivation experiments

Three-dimensional reconstructions of membrane dynamics (XYZT) used the same microscope and software as the XYT experiments. Image Z-stacks used a step size of 250 nm between planes. Images were collected continuously in line sequential scanning mode. Collection of each Z-stack required approximately seven seconds. Image stacks were deconvolved using Huygens Essential software and the

deconvolved stacks were visualized using the 4D viewer and linescan function in MetaMorph.

2.5.6 FRET Microscopy

Fluorescence images were collected using a Nikon Eclipse TE-300 inverted microscope with a 60x numerical aperture 1.4, oil-immersion PlanApo objective lens (Nikon, Tokyo, Japan) and a Lambda LS xenon arc lamp for epifluorescence illumination (Sutter Instruments, Novato, CA). Fluorescence excitation and emission wavelengths were selected using a JP4v2 filter set (Chroma Technology, Rockingham, VT) and a Lambda 10-2 filter wheel controller (Shutter Instruments) equipped with a shutter for epifluorescence illumination control. Images were recorded with a Photometrics CoolSnap HQ cooled CCD camera (Roper Scientific, Tucson, AZ). Image acquisition and processing were performed using MetaMorph v6.3 (Molecular Devices, Sunnyvale, CA). Additional processing was performed using MATLAB v7.8.0 (The MathWorks, Inc., Natick, MA) and the equations of FRET stoichiometry (Hoppe et al., 2002).

FRET microscopy of macrophages expressing Citrine-Rac1 and Cerulean-PBD was carried out as previously described(Hoppe et al., 2002; Yoshida et al., 2009). Briefly, collected images were background-subtracted and shading-corrected. E_A, E_D, and Ratio images were then calculated using published FRET stoichiometry equations. G* images were calculated as previously described, using the coefficient values obtained from cells expressing Citrine-Rac1(L61) and Cerulean-PBD

(Beemiller et al., 2006; Hoppe and Swanson, 2004). G* values account for varying levels of donor and acceptor in a population of cells, and can therefore be used to accurately measure the fraction of active Citrine-Rac1 in cells that express variable relative amounts of Cerulean-PBD and Citrine-Rac1. A paired two-tailed Student's *t*-test was used to compare average G* values from macropinocytic cups and entire cells.

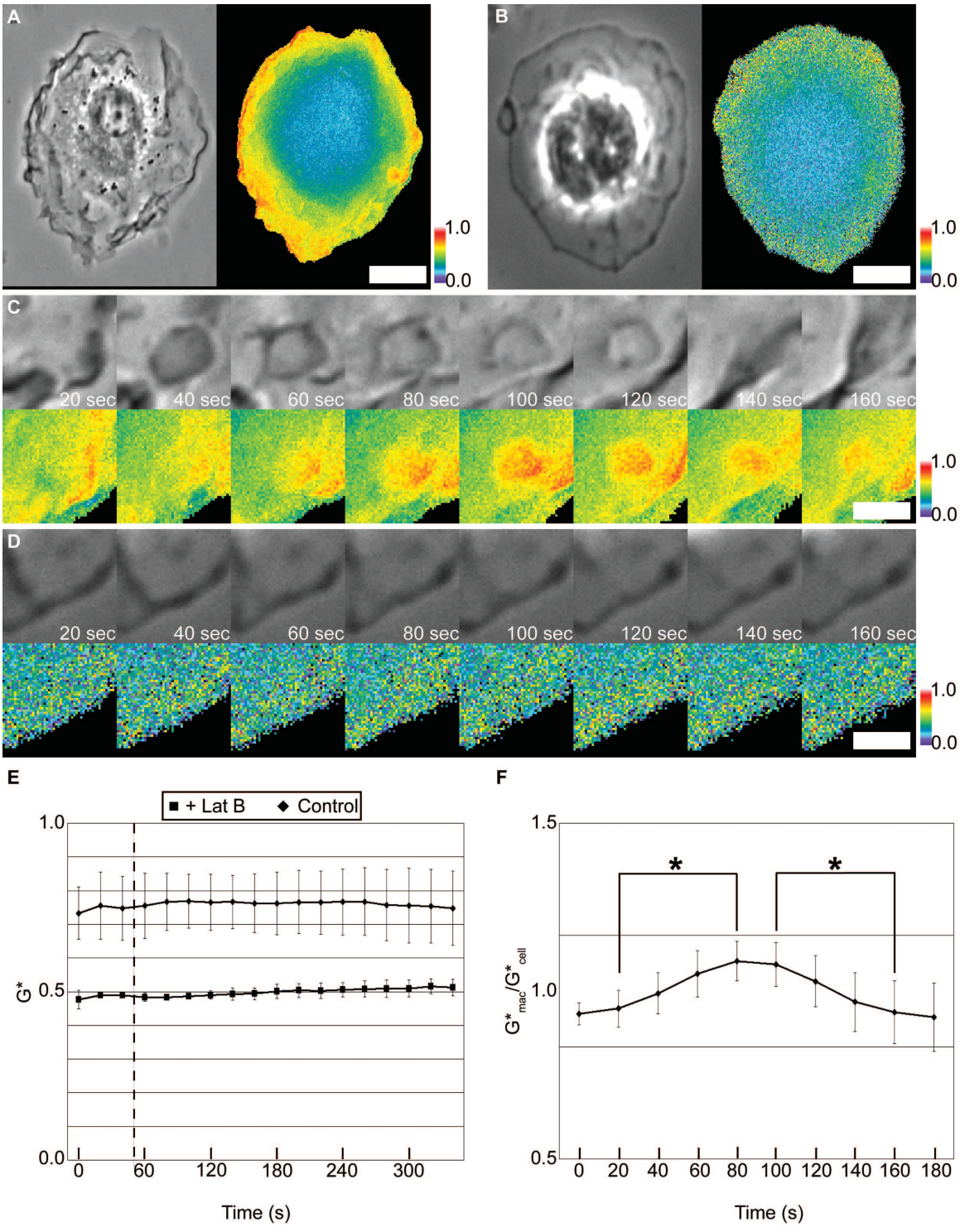

Figure 2.1 Focal activation of Rac1 during macropinocytosis. (A-D) FRET interactions of Cer-PBD and Cit-Rac1 in control (A and C) and latrunculin B-treated BMM (b and d) in response to M-CSF. (A and B) Left: Phase contrast; Right: G*. Scale bars = 4 mm. (C and D) Time series for subregions of the cells shown in panels a and b, highlighting a forming macropinosome (C), and a comparable region of a

latrunculin B-treated cell (D). Top: Phase Contrast; Bottom: G*. Scale bars = 1 mm. All color bars indicate G* values. (E) Quantification of total Cit-Rac1 activity in control and latrunculin B-treated BMM (*n*=5 for both conditions). Dotted line indicates when M-CSF was added. (F) To quantify Rac1 activation, the average G* in a forming macropinosome was divided by the average G* in the entire cell at each timepoint (*n*=14). The resulting ratio indicates the relative increase in Rac1 activity localized to the cup. Sequences were aligned by the timing of ruffle closure (t=80 seconds). Ratios were significantly higher than cytoplasm values (*P<0.001) from 80 seconds to 100 seconds following the beginning of macropinosome formation. Error bars indicate standard deviation.

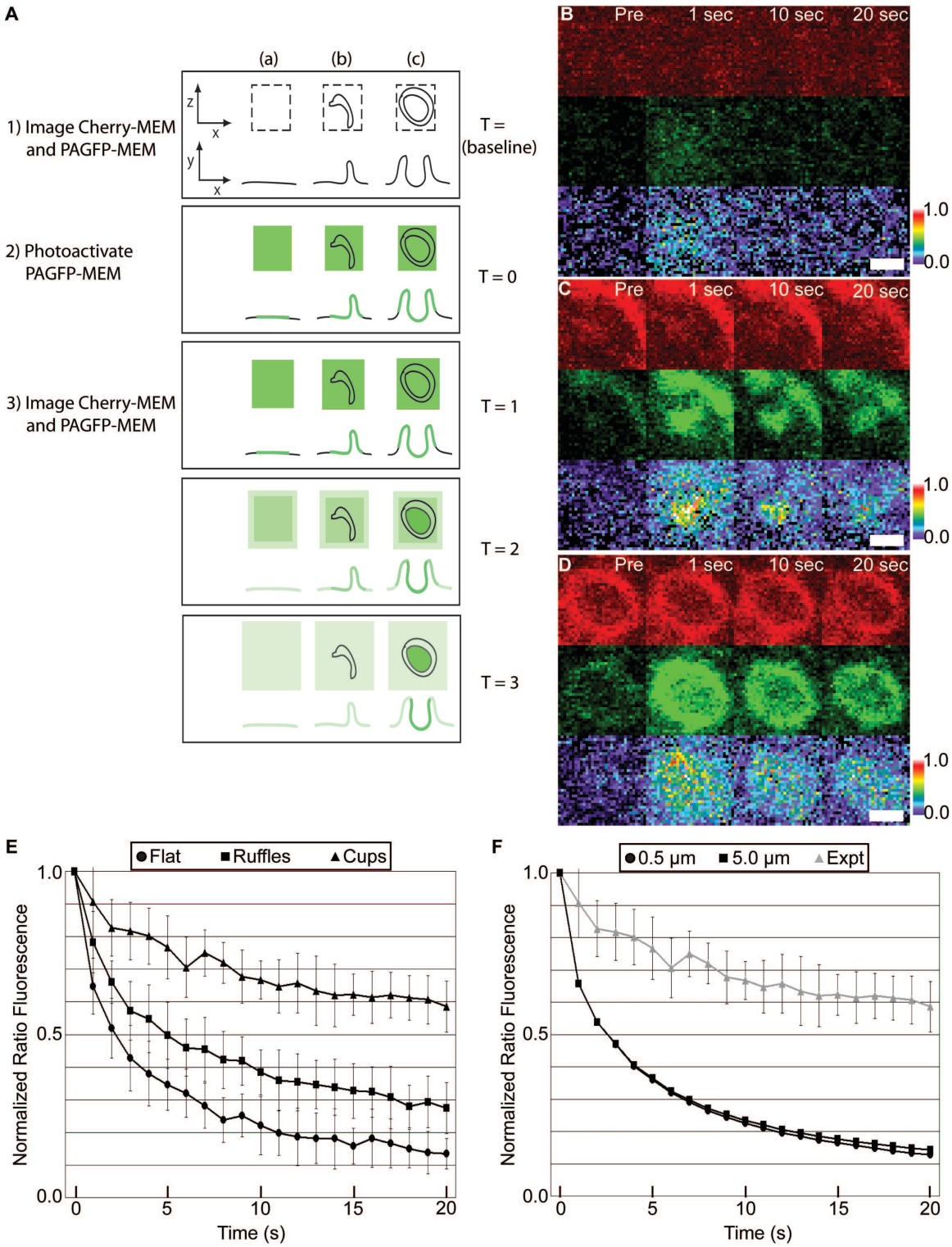

Figure 2.2 Selective photoactivation of PAGFP-MEM in plasma membranes. (A) Schematic of experimental protocol for XYT experiments. PAGFP-MEM was photoactivated in regions of flat (a), ruffled (b) or cupped membrane (c). Fluorescence intensities were collected in these activation regions over time. Loss of fluorescence indicated diffusion of activated PAGFP-MEM out of the activation

region; conversely, retention of activated PAGFP-MEM indicated restricted diffusion. (B-D) Images of different macropinocytic structures. Top: Cherry-MEM; Middle: PAGFP-MEM; Bottom: PAGFP/mCherry Ratio. From left to right: 1 second pre-activation, 1 second post-activation, 10 seconds post-activation, 20 seconds post-activation. Scale bars = 1 μm. Color bars indicate relative fluorescence intensities of ratio images. (B) Photoactivation in flat membrane. (C) Photoactivation in ruffle membrane. (D) Photoactivation in a macropinocytic cup. (E) Quantification of the fluorescence decrease in plasma membrane (n=5 for each condition). Membrane ruffles and cups demonstrate significant retention of photoactivated PAGFP-MEM. (F) Modeling of the effects of cup height on probe retention. Increasing cup height without adding a barrier or decreasing the diffusion coefficient did not affect molecule retention and could not account for the experimental values. Error bars indicate standard deviation.

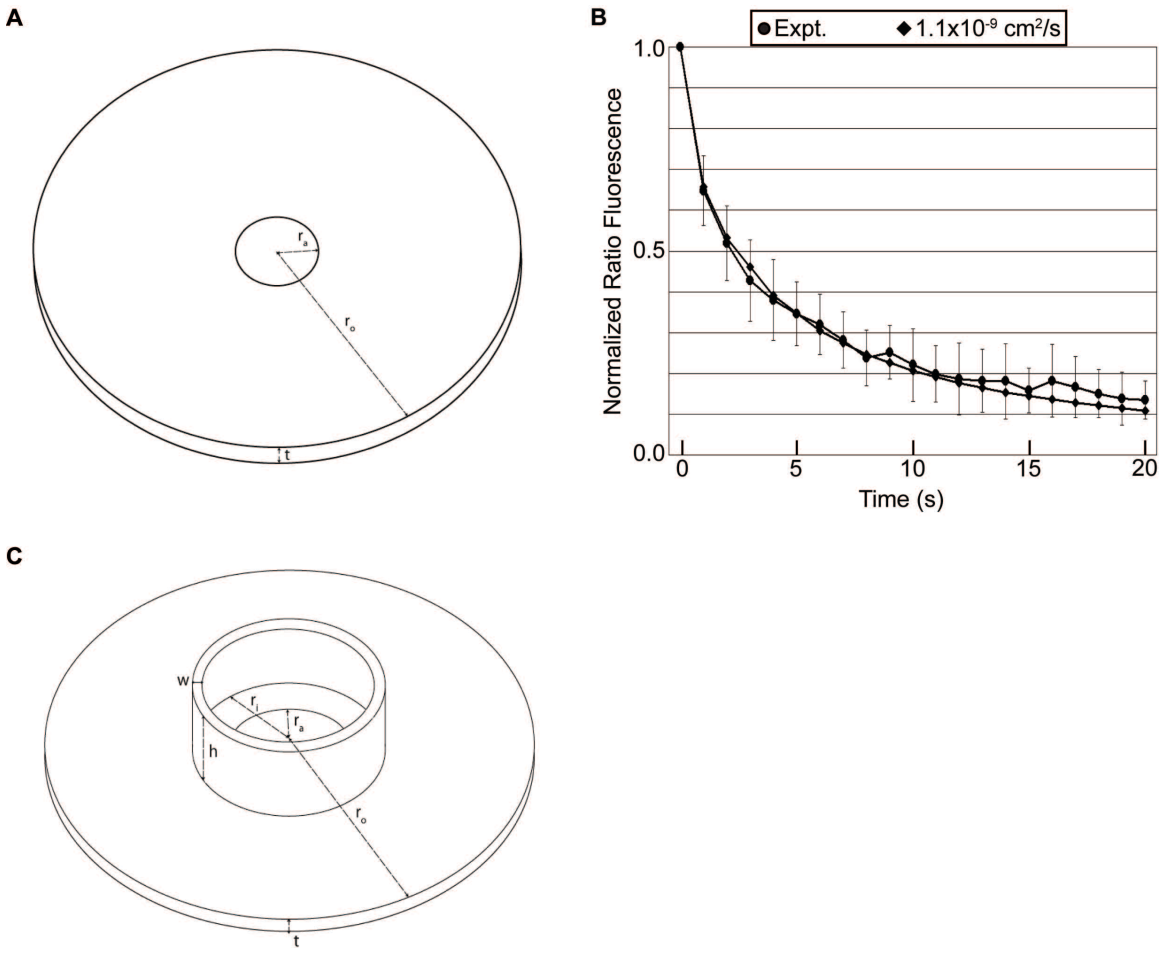

Figure 2.3 Computer modeling of diffusion experiments. (A) Schematic of model geometry showing activation spot on a flat membrane. (B) Fit of simulation to experimental data allowed determination of the diffusion coefficient value of 1.1×10^{-9} cm^2/second. (C) Schematic of geometry used for computer modeling of PAGFP-MEM diffusion in cups. For specific cup dimensions used, see Methods section.

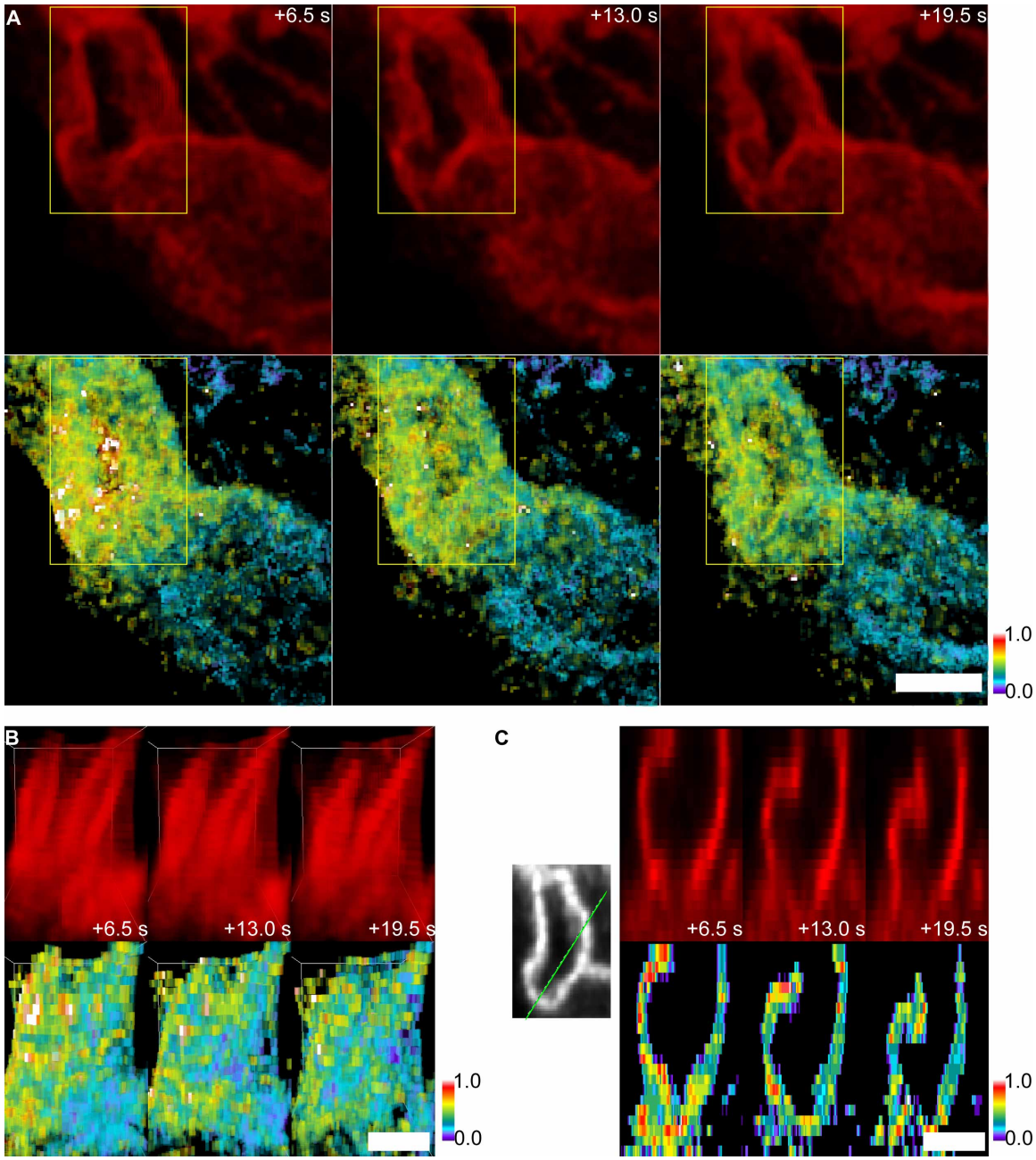

Figure 2.4 4D reconstruction of activated PAGFP-MEM in an open macropinocytic cup. Through-focus z-stacks were collected of PAGFP-MEM and mCherry at regular intervals after photoactivation of PAGFP-MEM in a cup. (A and B) Projections of a macropinocytic cup. Top: Cherry-MEM; Bottom: Ratio. From left to right: 6.5, 13.0, and 19.5 seconds after activation of PAGFP-MEM. (A) XY projection of a macropinocytic cup and surrounding cellular region. Yellow boxes delineate the macropinocytic cup. Scale bar = 1.0 µm. (B) XZ projections of the macropinocytic cup (side view). Fields correspond to the regions marked by the yellow boxes in (A). Scale bar = 1.0 µm. (C) Cross-sections of macropinocytic cups showing distribution of Cherry-MEM (red) and GFP/Cherry ratio (pseudocolor) at 13 seconds after photoactivation of PAGFP-MEM. Green line shows region of cross-

section. Scale bar = 1.0 μm. Color bars indicate relative fluorescence intensities of ratio images.

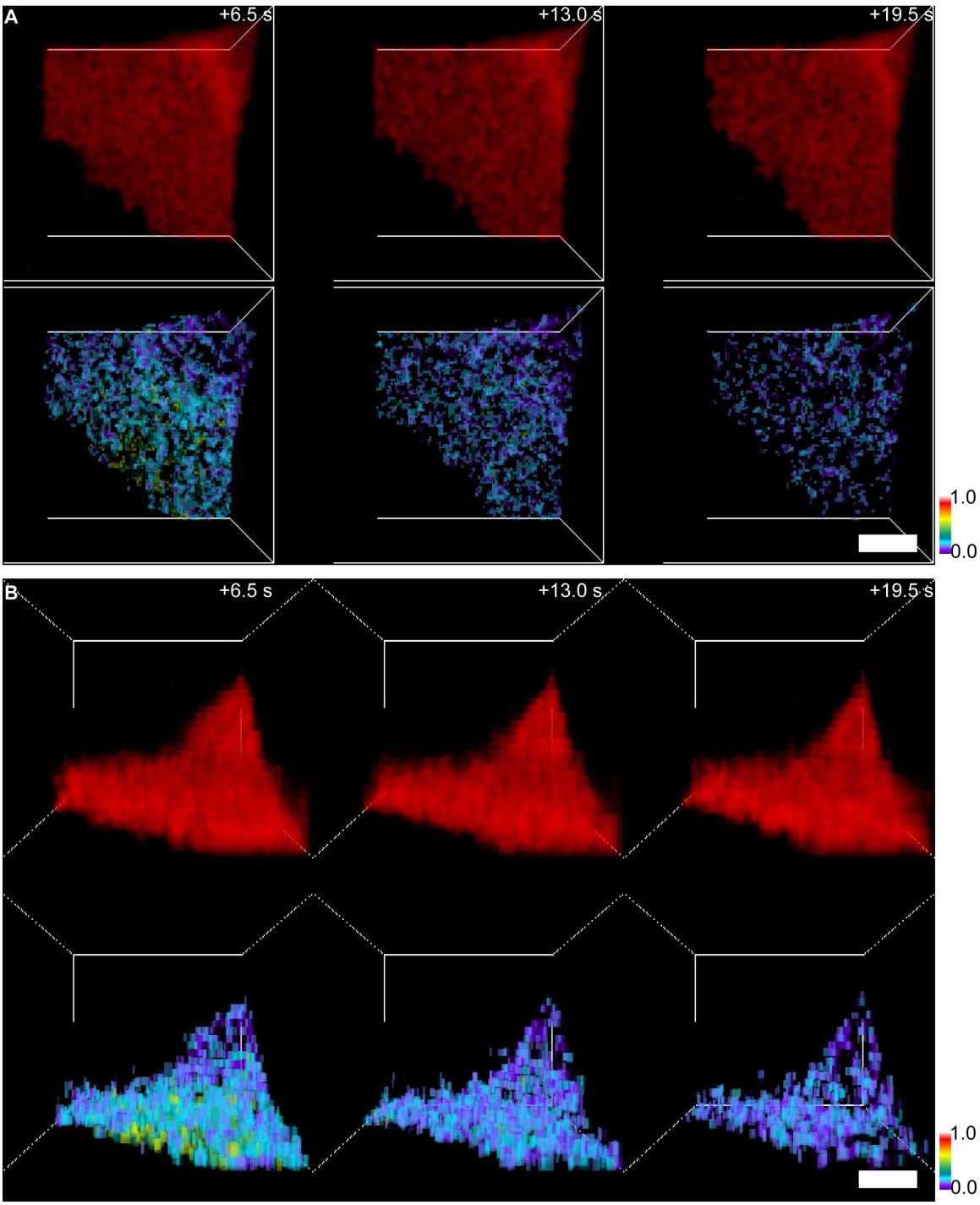

Figure 2.5 XYZT images of activated PAGFP-MEM in flat membrane. (A and B) Images of macropinocytic cup in the XY axis (a, top view) and XZ axis (b, side view). Top: Cherry-MEM; Bottom: Ratio. From left to right: 6.5, 13.0, and 19.5 seconds after activation of PAGFP-MEM. Scale bars = 1.0 μm. Color bars indicate relative fluorescence intensities of ratio images.

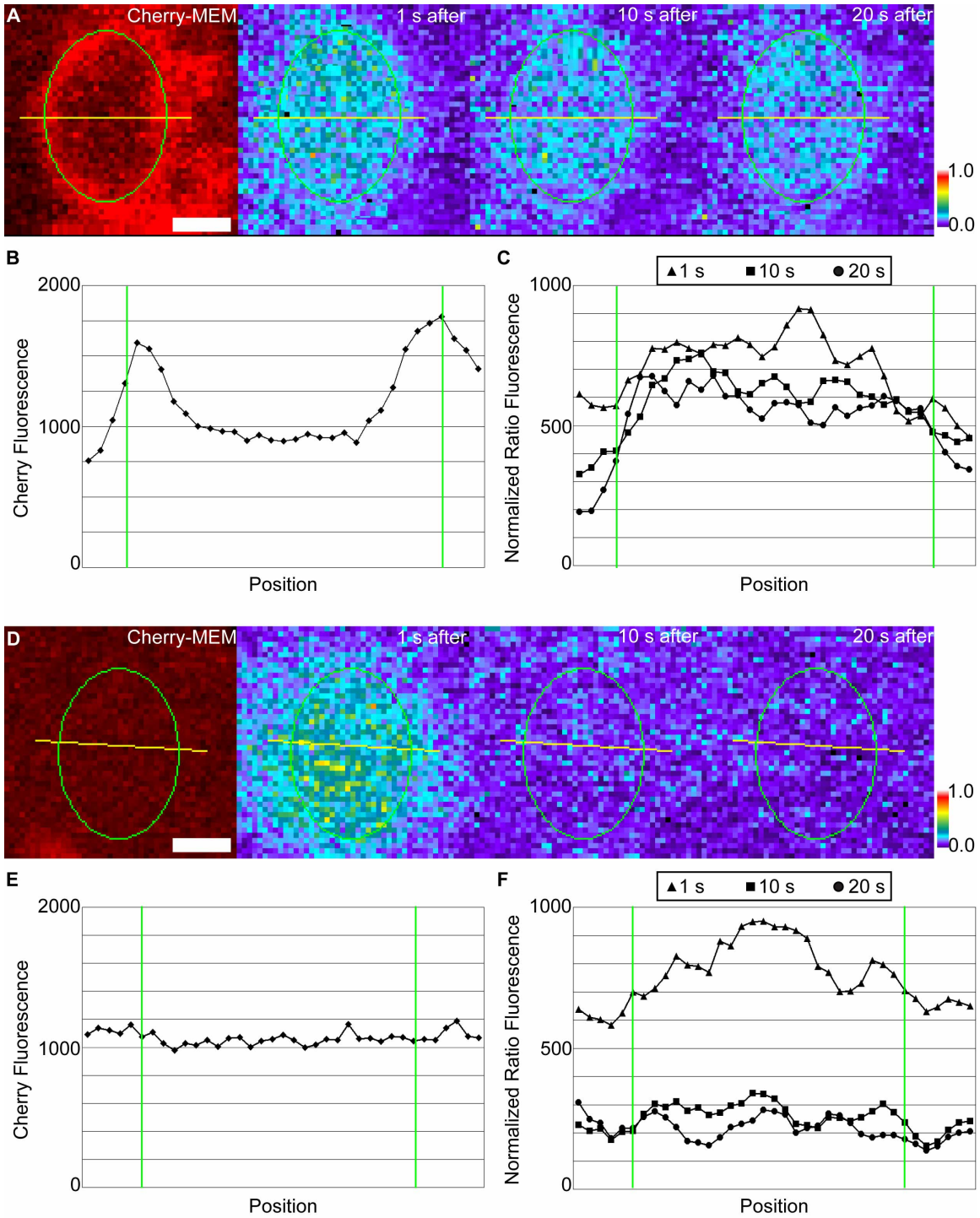

Figure 2.6 Fluorescence intensity linescans of cupped and flat membrane. (A and D) Representative linescans (yellow lines) in cupped and flat membrane, respectively. From left to right: Cherry-Mem image 1 second prior to activation, Ratio image 1 second after activation, Ratio image 10 seconds after activation, Ratio image 20 seconds after activation. Scale bars = 1.0 μm. Color bars indicate relative fluorescence intensities of ratio images. (B and E) Linescans of Cherry-MEM fluorescence intensities in cupped and flat membrane, respectively. (C and F)

Linescans of GFP/mCherry fluorescence ratios in cupped and flat membrane, respectively, at 1, 10 and 20 seconds after photoactivation. Green lines indicate the perimeter of the activation region. Similar fluorescence patterns were seen for seven macropinocytic cups and for ten regions of flat membrane.

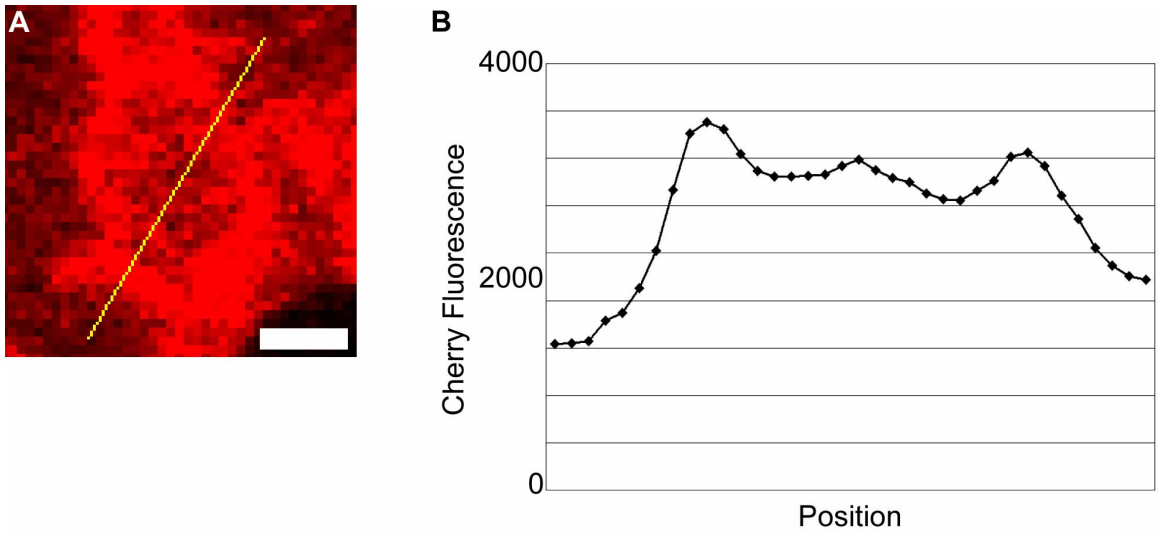

Figure 2.7 Fluorescence intensity linescan of a macropinocytic vacuole. (A) Representative linescan (yellow line) of a fully formed macropinosome in the cytoplasm. (B) Linescan measurements of Cherry-MEM fluorescence pixel intensities. Scale bar = 1 μm.

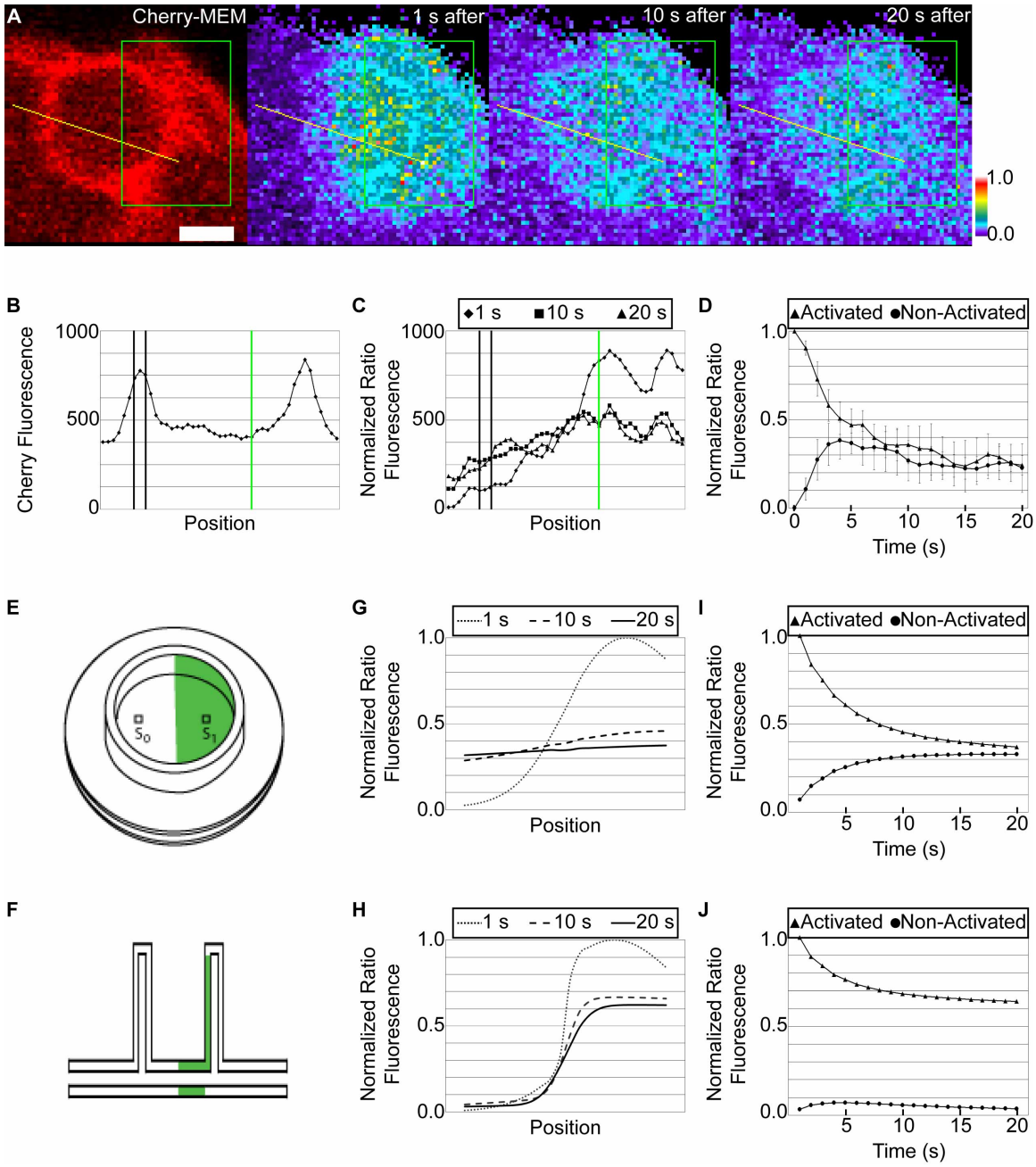

Figure 2.8 Diffusion dynamics within membrane cups indicate that the barrier localizes to the cup walls. (A-C) Fluorescence redistribution following asymmetric activation of PAGFP-MEM in macropinocytic cups. (A) Representative images. From left to right: Cherry-Mem image 1 second prior to activation, Ratio images 1 second, 10 seconds and 20 seconds after activation. Yellow lines indicate position of linescans. Green boxes indicate the perimeter of the activation region. Scale bar = 1.0 μm. Color bars indicate relative fluorescence intensities of ratio images. (B) Linescan measurements of Cherry-MEM pixel intensities. (C) Linescan measurements of Ratio values at 1, 10, and 20 seconds after photoactivation. Similar fluorescence patterns were seen in five macropinocytic cups. Dotted lines indicate the location of the cup wall. Green lines indicate the edge of the activation region.

(D) Fluorescence measurements of activated and non-activated regions in the base of the cup over time, *n*=5. (E-J) Modeling of diffusion within cups. (E, F) Diagrams of activation patterns used to model diffusion inside the cup, showing views from above (C) and in sagital section (F). (G, H) Distributions of molecules along the diameter of the base of the cup normal to the activation boundary, measured at 1, 10 and 20 seconds after activation. (G) When the diffusion coefficient in the walls is 10^{-11} cm^2/second (ie., a barrier) and in the base of the cup is 10^{-9} cm^2/second, fluorophore redistribution resembles the experimental data in 'C'. (H) When the diffusion coefficients of the walls and base are both set to 10^{-11} cm^2/second, fluorophore redistribution does not resemble the experimental data. (I, J) Modeling of the time course of fluorophore decrease from the activated region (triangles) and increase in the non-activated region (circles) when diffusion coefficients are set as in 'G' (I) and 'H' (J). The model resembles the experimental observations in 'D' when the base of the cup has the same diffusion coefficient as membrane outside the cup (I).

2.6 References

Araki, N., T. Hatae, A. Furuka, and J.A. Swanson. 2003. Phosphoinositide-3-kinase-independent contractile activities associated with fcgamma-receptor-mediated phagocytosis and macropinocytosis in macrophages. *Journal of Cell Science*. 116:247-257.

Araki, N., M.T. Johnson, and J.A. Swanson. 1996. A role for phosphoinositide 3-kinase in the completion of macropinocytosis and phagocytosis by macrophages. *Journal of Cell Biology*. 135:1249-1260.

Beemiller, P., A.D. Hoppe, and J.A. Swanson. 2006. A phosphatidylinositol-3-kinase-dependent signal transition regulates ARF1 and ARF6 during Fcgamma receptor-mediated phagocytosis. *PLoS biology*. 4:e162.

Cox, D., P. Chang, Q. Zhang, P.G. Reddy, G.M. Bokoch, and S. Greenberg. 1997. Requirements for both Rac1 and Cdc42 in membrane ruffling and phagocytosis in leukocytes. *Journal of Experimental Medicine*. 186:1487-1494.

Edwards, D.C., L.C. Sanders, G.M. Bokoch, and G.N. Gill. 1999. Activation of LIM-kinase by Pak1 couples Rac/CDC42 GTPase signalling to actin cytoskeletal dynamics. *Nature Cell Biology*:253-259.

Frick, M., K. Schmidt, and B.J. Nichols. 2007. Modulation of lateral diffusion in the plasma membrane by protein density. *Curr Biol*. 17:462-467.

Hoppe, A., K. Christensen, and J.A. Swanson. 2002. Fluorescence resonance energy transfer-based stoichiometry in living cells. *Biophys J*. 83:3652-3664.

Hoppe, A.D., and J.A. Swanson. 2004. Cdc42, Rac1, and Rac2 display distinct patterns of activation during phagocytosis. *Molecular Cell Biology*. 15:3509-3519.

Li, G., C. D'Souza-Schorey, M.A. Barbieri, J.A. Cooper, and P.D. Stahl. 1997. Uncoupling of membrane ruffling and pinocytosis durin ras signal transduction. *Journal of Biological Chemistry*. 272:10337-10340.

Moriyoshi, K., L.J. Richards, C. Akazawa, D.D. O'Leary, and S. Nakanishi. 1996. Labeling neural cells using adenoviral gene transfer of membrane-targeted GFP. *Neuron*. 16:255-260.

Patterson, G.H., and J.A. Lippincott-Schwartz. 2002. A photoactivatable GFP for selective photolabeling of proteins and cells. *Science*. 297:1873-1877.

Schmidt, K., and B.J. Nichols. 2004. A barrier to lateral diffusion in the cleavage furrow of dividing mammalian cells. *Current Biology*. 14:1002-1006.

Simons, K., and D. Toomre. 2000. Lipid rafts and signal transduction. *Nature Reviews Molecular Cell Biology*. 1:31-39.

Swanson, J.A. 1989. Phorbol esters stimulate macropinocytosis and solute flow through macrophages. *Journal of Cell Science*. 94:135-142.

Swanson, J.A. 2008. Shaping cups into phagosomes and macropinosomes. *Nature Reviews Molecular Cell Biology*. 9:639-649.

Weisswange, I., T. Bretschneider, and K.I. Anderson. 2005. The leading edge is a lipid diffusion barrier. *Journal of Cell Science*. 118:4375-4380.

Wells, C.M., M. Walmsley, S. Ooi, V. Tybulewicz, and A.J. Ridley. 2004. Rac1-deficient macrophages exhibit defects in cell spreading and membrane ruffling but not migration. *Journal of Cell Science*. 117:1259-1268.

Yoshida, S., A.D. Hoppe, N. Araki, and J.A. Swanson. 2009. Sequential signaling in plasma-membrane domains during macropinosome formation in macrophages. *Journal of Cell Science*. 122:3250-3261.

Chapter Three:
A Growth Factor Signaling Cascade Confined to Circular Ruffles in Macrophages

3.1 Abstract

Cell surface receptor signaling leads to coordinated cell movements such as migration, phagocytosis, ruffling and the formation of endocytic vesicles called macropinosomes. After stimulation by growth factors, macrophages form macropinosomes from circular ruffles in plasma membrane, which prompts the question of how the stochastic and molecular-scale activities of growth factor receptor activation are organized into micron-scale movements of macropinocytosis. Using quantitative fluorescence microscopy, we demonstrate that macropinosome formation is directed by a sequence of chemical changes within the cups of plasma membrane circular ruffles. Stages of receptor-dependent signaling were organized into distinct transient waves of phosphoinositides, diacylglycerol, PKCα, Rac and Ras activities, which preceded cup closure and peak recruitment of Rab5 to macropinosomes. Thus, circular ruffles enclose plasma membrane subdomains that focus receptor signal amplification and the signal transitions that coordinate cell movements.

3.2 Introduction

Early models of the cell membrane proposed it was a homogenous, neutral solvent with no role in protein function (Singer and Nicolson, 1972). A subsequent advance has been the identification of distinct subdomains, such as lipid rafts, that organize or regulate membrane proteins. These subdomains might contribute to signal transduction, wherein ligand activation of surface receptors is efficiently conveyed through intracellular signaling networks. Membrane subdomains aid transduction by localizing downstream signaling molecules (Simons and Toomre, 2000).

Macropincytosis is the process by which a cell ingests large amounts of fluid from its extracellular environment, typically in response to stimulation by growth factors. The process results in the formation of the macropinosome, a fluid-filled intracellular vacuole. Much of the signaling for macropinosome formation occurs in the cellular membrane. Activation of growth factor receptors triggers local phosphorylation of membrane lipids and proteins that activate cytoskeletal movements. The cytoskeleton in turn reshapes membrane topography, first through the formation of ruffles, then cups. Macropinocytic cups are self-contained regions of the plasma membrane in which proteins have limited lateral diffusion(Kerr and Teasdale, 2009; Swanson, 1989; Swanson, 2008).

In receptor-driven processes like macropinocytosis, surface receptors are presumably activated throughout the entire membrane. How, then, is this non-localized activation of surface receptors organized into signaling cascades limited to

distinct areas of the membrane? We previously showed that macropinocytic ruffles and cups limit lateral membrane diffusion (Chapter Two). We hypothesize that the spatial organization provided by these membrane subdomains allows for tight temporal regulation of signaling molecules. We conducted experiments attempting to identify discrete signaling events defining the progression of macropinocytosis. Our results demonstrate that receptor signaling networks are organized temporally into waves of membrane lipids.

3.3 Results

3.3.1 Rab5 as a Marker of Macropinosome Cup Closure

We used live cell fluorescence imaging to outline the signaling cascade that follows receptor activation in macropinocytosis. Fluorescence imaging is useful not only in identifying which molecules are involved in a signaling network, but also when and where those molecules appear. However, a key limitation of live cell fluorescence imaging is that it only allows for the simultaneous visualization of at most three different fluorophores. As macropinocytosis might involve dozens of signaling molecules, we needed a method for comparing the timing of events in different experiments. One solution was to use consistent, visible time markers of different stages of macropinocytosis, such as the beginning and end of the membrane cup phase. Time markers provide temporal context for different experiments by acting as fiduciary marks for aligning time series obtained different cells.

In phase-contrast microscopy, membrane ruffles form dark lines, in part because distortions or the membrane push it out of the microscopic plane of focus. Therefore, the appearance of a fully circular structure marks the formation of the membrane cup (Swanson, 1989). The membrane cup phase ends with the process known as cup closure, when the distal margin of the open cup closes to form the intracellular macropinosome (Swanson and Watts, 1995). Cup closure is not clearly identifiable in phase-contrast imaging. Instead, we used a molecular marker to indicate that closure had occurred.

Rab5 is a Ras superfamily GTPase that functions to mediate fusion between early endocytic vesicles. It accumulates on early endosomes, with maximal recruitment occurring soon after the vesicle is completely formed (Lanzetti et al., 2004) (Zerial and McBride, 2001). We used two methods to test whether Rab5 was a reliable marker of macropinosome closure. We first looked at the timing of Rab5 localization using 4-dimensional fluorescence imaging. Bone marrow-derived macrophages (BMMs) were transfected with the fluorescent protein chimeras CFP-MEM and Cherry-Rab5. MEM is a plasma membrane-localized protein, and expression of its fluorescent chimera allowed for visualization of plasma membrane distribution and morphology during macropinocytosis. Rab5 weakly localized to forming macropinocytic cups; only after complete closure did Rab5 localization reach peak intensity (Fig. 3.1).

As a second measure of the timing of cup closure, we used depletion of FM4-64 fluorescence to quantify the timing of Rab5 localization. FM4-64 is a lipophilic

dye that is used to label the outer leaflet of exposed membrane surfaces. Although its fluorescence is negligible in water, FM4-64 fluorescence increases significantly upon binding to plasma membranes (Yoshida et al., 2009). Consequently, FM4-64 can be used to label membranes even in dye-containing medium. Additionally, FM4-64 has low photostability, causing it to bleach quickly. In the outer cell membrane, bleached molecules are rapidly replaced by non-bleached molecules from the medium. A closed macropinosome, however, has a much more limited supply of FM4-64 molecules. Consequently, continuous photobleaching will exhaust the fluorescent molecules in the macropinosome faster than in the outer cell membrane, leading to decreased fluorescence. The inflection point of FM4-64 fluorescence intensity can then be used to identify the timing of cup closure (Yoshida et al., 2009). We tested FM4-64 depletion in BMMs expressing CFP-MEM and Citrine-Rab5. The inflection point in FM4-64 depletion occurred 100s after the formation of the macropinocytic cup (Fig. 3.2A and B). Rab5 expression did not peak until 80s later, or 180s after cup formation (Fig. 3.2A and C). These results suggest that peak Rab5 localization occurs on fully closed intracellular vacuoles, and that Rab5 localization can thus be used to monitor the end of the membrane cup phase.

3.3.2 A Phosphoinositide Cascade Directs Macropinocytosis

With time markers for the beginning (circular ruffles) and end (intracellular vesicle) of the membrane cup phase, we were now able to measure the relative timing of different signaling events. All of these experiments used ratiometric

imaging, in which fluorescence intensity due to recruitment of the protein of interest was compared to the baseline fluorescence caused by path length. Path length fluorescence was measured by expression and visualization of an unbound, monomeric fluorescent molecule, typically mCerulean. The protein of interest was usually tagged with Yellow Fluorescent Protein (YFP), or its variant mCitrine. Additionally, mCherry-Rab5 was coexpressed as the late macropinocytic time marker. Phase-contrast imaging was used to identify the first timepoint of cup formation (*t=0s*) and the size of the macropinosome. Cherry-Rab5/Cerulean ratios were used to monitor cup closure. YFP-[probe]/Cerulean ratios were used to observe various signaling proteins.

In determining the macropinocytic signaling pathway, we first looked at phosphoinositides (PIs). PIs are plasma membrane phospholipids that contribute to various signaling pathways. PIs function to recruit the cytoplasmic proteins that carry out the enzymatic reactions that comprise cellular processes (DiNitto and Lambright, 2006; Krauss and Haucke, 2007b). While they are not direct effectors, their ability to recruit proteins means that PIs are essential in the spatial organization of membrane reactions. Additionally, PI-dependent signaling might control the timing of signaling events. PI signaling is a rapid process predicated on conversion between PI species (De Matteis and Godi, 2004). PI conversion involves phosphorylation and dephosphorylaton, which does not require protein synthesis and the associated time delays. Different PI species interact with different proteins, and a cell can precisely control the recruitment or activation of effectors by cycling between PI species (DiNitto and Lambright, 2006). The benefits of PI-dependent

signaling align with the timing of macropinosome formation, which occurs within one or two minutes of cup assembly.

Citrine-tagged PI-binding domains can be used to visualize the localization of PIs. These domains are adapted from the effector proteins that naturally interact with the different PI species, and are highly specific. Of these, BtkPH recognizes phosphatidylinositol 3,4,5-trisphosphate (PIP_3); PLCδ1PH recognizes phosphatidylinositol 4,5-bisphosphate ($PI(4,5)P_2$); Tapp1PH recognizes phosphatidylinositol 3,4-bisphosphate ($PI(3,4)P_2$); and FYVE recognizes phosphatidylinositol 3-phosphate (PI(3)P) (DiNitto and Lambright, 2006).

A previous report showed that PIP_3 is formed shortly after the formation of the circular ruffle (Yoshida et al., 2009). PIP_3 is commonly generated in response to receptor stimulation, usually by phosphorylation of $PI(4,5)P_2$ (Kotani et al., 1994). Therefore, we sought to determine if formation of $PI(4,5)P_2$ preceded that of PIP_3. We observed a distinct spike in $PI(4,5)P_2$ localization immediately after formation of the membrane cup (Fig. 3.3A). Further, temporal comparisons confirmed that $PI(4,5)P_2$ formed before PIP_3 (Fig. 3.3B and E), suggesting $PI(4,5)P_2$ as the precursor molecule.

Several mechanisms of localized $PI(4,5)P_2$ synthesis have been hypothesized, mostly involving differential activation of PIP(5)K isoforms (Krauss and Haucke, 2007a). We focus here, however, on how an initial $PI(4,5)P_2$ flux can be maintained throughout a signaling cascade. The first step in the cascade was the conversion of $PI(4,5)P_2$ into PIP_3. PIP_3 expression was transient, and its rapid disappearance was

indicative of dephosporylation or hydrolysis. PIP_3 can be dephosphorylated at the 3', 4', and 5' positions of its inositol ring, and one possibility was that the inositol 5-phosphatase SHIP1 converted PIP_3 into $PI(3,4)P_2$. Indeed, $PI(3,4)P_2$ followed the disappearance of PIP_3, peaking 100s after ruffle closure (Fig 3.3C and E), roughly coincident with cup closure.

$PI(3,4)P_2$ is functionally redundant with PIP_3 (Franke et al., 1997), and likely acts as an intermediary molecule in the phosphoinositide cascade. Accordingly, $PI(3,4)P_2$ might be dephosphorylated into PI(3)P, which is a known occupant of endosomal membranes. PI(3)P is thought to function in a positive feedback loop with Rab5 (Zerial and McBride, 2001), wherein each molecule facilitates the localization of the other to recently formed intracellular vesicles. Indeed, we found that PI(3)P appeared gradually and coincidently with Rab5, peaking after the peak of $PI(3,4)P_2$ localization (Fig 3.3D and E).

These experiments show a clear spatiotemporal organization of PI signaling molecules. All of the molecules are localized exclusively to the forming macropinosome, suggesting their importance in directing cup closure. These findings accord with an earlier observation that a diffusion barrier exists in the perimeter of macropinocytic cups. The barrier was previously identified as limiting protein diffusion, but these results suggest it also controls the distribution of membrane lipids. Spatial diffusion barriers maintain the $PI(4,5)P_2$ orientation, allowing for localized production of all subsequent phosphoinositides. The result is

a dynamic series of changes in the chemical environment of the membrane domain. This wave of membrane chemistries directs the macropinocytic signaling proteins.

3.3.3 GTPase Activity during Macropinocytosis

The versatility of PIs as signaling molecules relates partly to the diversity of the effector proteins with which they interact. Chief among these are small GTPases, a broad family of proteins participating in a wide variety of cellular behaviors. Additionally, GTPases exist in discrete "on" and "off" states, and conversion between the two allows for rapid activation and deactivation. Rab5 is a GTPase that, based on the timing of its localization, likely participates in macropinocytic trafficking or maturation. Several other GTPases might participate in macropinocytosis.

Earlier reports suggested that Rac1 might be activated at different points during macropinocytosis. In one, Rac1 activity was believed to precede and contribute to formation of $PI(4,5)P_2$ (He et al., 1998). In contrast, another showed Rac1 activity as following the formation of PIP_3 (Yoshida et al., 2009). We visualized Rac1 activity using the p21-binding domain (PBD) of Pak1 a protein that interacts with only the active, GTP-bound form of Rac1 (Hoppe and Swanson, 2004). Ratiometric localization of YFP-PBD indicated that peak Rac1 activation occured after the conversion of $PI(4,5)P_2$ to PIP_3 (Fig. 3.4A and D), which suggests that Rac1 has little role in the generation of $PI(4,5)P_2$. The timing of PIP_3 formation and Rac1 activation suggested that PIP_3 contributes to Rac1 activation. The inositol headgroup of PIP_3 is known to interact with the guanosine nucleotide dissociation

inhibitor (GDI) for Rac1 (Ugolev et al., 2008). GDIs inhibit both the activation and membrane localization of GTPases. PIP_3 might therefore liberate Rac1 from its GDI, thereby allowing the distinct spike in Rac1 activity in the forming macropinosome. Rac1 functions mostly in cytoskeletal reorganization, and its activity might contribute to the morphological changes of cup closure.

Rac2 and Cdc42 are other Rho GTPases that affect cytoskeletal reorganization (Bustelo et al., 2007), and might have contributed to the morphological changes of macropinocytosis. Further, $PI(4,5)P_2$ is thought to coordinate actin polymerization through Cdc42. A proposed mechanism is that $PI(4,5)P_2$ cooperates with the Rho GTPase Cdc42 to activate N-WASP and the Arp2/3 complex (Rohatgi et al., 2000). We therefore sought to determine if Cdc42 is activated following the formation of $PI(4,5)P_2$. However, using FRET microscopy to specifically monitor the activity of Rac2 and Cdc42, we found that neither GTPase was significantly activated at any point during macropinosome formation (Fig 3.4B and C). FRET microscopy uses donor and acceptor fluorescence to track the protein of interest, and these experiments did not include coexpression of the Cherry-Rab5 fluorophore.

The Ras GTPase is believed to mediate a variety of signaling networks, and it has a known role in rearrangement of the actin cytoskeleton (Wennerberg et al., 2005). In other growth factor-mediated signaling pathways, Ras is activated soon after receptor activation. Ras has been indicated in the production of both $PI(4,5)P_2$ and, separately, PIP_3 (He et al., 1998). We monitored Ras activity using Ras-binding

domain (RBD), which binds specifically to active Ras. While Ras was activated during macropinocytosis, this activation occurred late in the process, after the peaks of both $PI(4,5)P_2$ and PIP_3. (Fig. 3.5A and D). Interestingly, Ras activation was approximately concurrent with localization of Rab5. This observation accords with evidence that Ras can regulate signaling on formed endosomes (Hancock, 2003). Additionally, Ras regulates RIN1, the guanine nucleotide exchange factor (GEF) that is responsible for activating Rab5 (Tall et al., 2001). Ras activation might therefore contribute to Rab5 activation and the associated maturation of the intracellular macropinosome.

The Arf GTPases are also involved in vesicular transport. Arf6 contributes to trafficking of newly formed intracellular vesicles, shuttling them from the plasma membrane to the Golgi (Donaldson, 2003). Additionally, Arf6 is known to activate PIP5K, and might therefore contribute to the early formation of $PI(4,5)P_2$ (Honda et al., 1999). Arf1 also guides vesicular trafficking, but in the opposite direction as Arf6. It functions mainly to provide new membrane from the Golgi to the plasma membrane (Donaldson and Jackson, 2011). Arf1 might therefore mediate the insertion of membrane into the forming macropinocytic cup. We visualized Arf activity using FRET microscopy, and found that neither Arf1 nor Arf6 were appreciably activated during macropinocytosis (Fig. 3.5B and C). As with the FRET measurements of Rho GTPases, these experiments did not include coexpression of the Cherry-Rab5 fluorophore.

3.3.4 The Diacylglycerol Pathway

In addition to phosphorylation into PIP_3, the $PI(4,5)P_2$ that is formed early in macropinocytosis might also be converted to other compounds. Specifically, the γ isoform of phospholipase C (PLCγ) is known to cleave $PI(4,5)P_2$ into inositol 1,4,5-trisphosphate (IP_3) and diacylglycerol (DAG) (Hinchliffe et al., 1998).

DAG can be localized using fluorescent chimeras of C1 domains, which are DAG-binding domains of protein kinase C (Azzi et al., 1992). Visualizing DAG formation using Citrine-tagged C1δ (from PKCδ), we observed that DAG peaked shortly after the disappearance of $PI(4,5)P_2$. The timing of peak DAG formation corresponded approximately with the peak of PIP_3, indicating that $PI(4,5)P_2$ is converted into both molecules concurrently (Fig 3.6 A and D). Visualization of YFP-PLCγ showed that it did not localize to macropinocytic cups during $PI(4,5)P_2$ hydrolysis. However, it is important to note that YFP-PLCγ localization does not necessarily correspond to PLCγ activity. In terms of differential DAG formation, PLC might have been continuously present, but only as its $PI(4,5)P_2$ substrate was formed was it able to generate DAG.

DAG is a membrane lipid that recruits and activates cytosolic proteins such as members of the Protein Kinase C (PKC) family. PKC proteins are known to participate in processes relevant to macropinocytosis, including actin polymerization (van Blitterswijk and Houssa, 2000). We observed a pattern of PKCα localization similar to that of Rab5 (Fig. C and D), consistent with a role for PKCα in regulating Rab5, or vice versa.

3.3.5 Calphostin C Inhibits Macropinocytosis

The pattern of PKCα localization was also similar to that for Ras activation. It was recently shown that DAG contributes to Ras activation during phagocytosis. Specifically, DAG interacts with RasGRP3, a Ras GEF (Botelho et al., 2009). We therefore tested if Ras activation requires PKCα activity.

Calphostin C is a highly specific inhibitor that prevents DAG from binding to its protein effectors (Lorenzo et al., 2000). It was thus useful for identifying the downstream effectors of the DAG pathway. We first looked at PKCα localization, finding that calphostin C abrogates PKCα recruitment (Fig. 3.7A). This finding supports the notion that PKCα is directly recruited through interaction with DAG. The effects of calphostin C on Ras activation were ambiguous. Measuring YFP-RBD localization to cups, we found that Ras was still activated in calphostin C, but at a much lesser amount than in control experiments (Fig. 3.7B). This could be consistent with a mechanism in which DAG interacts with the Ras GEF, but the results are not conclusive.

Calphostin C also allowed us to assess of the importance of the DAG pathway in macropinocytosis. Calphostin C inhibited macropinocytic cup closure, indicating that the DAG-dependent signaling is essential (data not shown). Macropinocytosis was not completely inhibited, as circular ruffles still formed. Additionally, Rab5 localized to these cups at lowered amounts, suggesting some recruitment. The DAG

pathway thus appears to be important in the late stages of macropinosome formation.

3.4 Discussion

A central goal of this study was to gain insight into the signaling network that drives macropinosome formation. Figure 3.8 provides a hypothetical schematic of the organization of signaling events in macropinocytic cups. The events that dictate Ras activation are still unclear, although the interaction of Ras with RIN1 does suggest its importance for Rab5 activation. A key area of future research is to test the placement of molecules in the proposed schematic, which could be done by inhibiting different interactions and monitoring the effects.

The most novel aspect of the signaling network outlined herein is the PI pathway. PI-dependent signaling has previously been described as driven by fluctuations in levels of individual PIs (Di Paolo and De Camilli, 2006). We present here a mechanism in which PI fluctuations work in concert. Spatiotemporal imaging of fluorescent protein chimeras confirmed four PI species involved in the macropinocytic cascade. Further, the PIs demonstrated waves of chemistries, in which one species was apparently converted into another. In combination with imaging of the membrane lipid DAG and various effector proteins, PI behavior during macropinocytosis is an example of how transient fluctuations in PI concentrations can be organized into a complete, coordinated cellular behavior.

Membrane ruffles act as local barriers that coordinate the stochastic signaling activities by confining them to cup-shaped domains of the plasma membrane.

Previous reports have suggested that PIs control cell morphology (such as in cell growth, chemotaxis, etc.) (Di Paolo and De Camilli, 2006). Many of these proposed mechanisms involve a PI coordinating actin polymerization through effector proteins. Our work supports a different dynamic, in which changes in cytoskeletal and membrane organization define PI localization. The first PI to demonstrate a localized amplification- $PI(4,5)P_2$- peaked after formation of the circular membrane ruffle. We showed previously that these membrane subdomains functionally amplify receptor signaling into downstream protein activation. The data presented here extends those findings to membrane lipids. Macropinocytosis is thus self-organized through distortions in the plasma membrane.

While membrane morphology controls PI distribution, PIs apparently regulate the actual signaling events. In our schematic, formation of $PI(4,5)P_2$ is the first step in macropinocytosis. Phosphatidylinositol 4-phosphate (PI(4)P), the likely substrate in the synthesis of $PI(4,5)P_2$, is widely distributed in the plasma membrane. Therefore, the appearance of $PI(4,5)P_2$ is perhaps the beginning of the regulated macropinocytic signaling cascade.

$PI(4,5)P_2$ immediately precedes formation of DAG and PIP_3, and the temporal overlap in the formation of these molecules might indicate a regulatory control mechanism. The PIP_3 headgroup interacts with and activates PLCγ (Xie et al., 2005). As early conversion of $PI(4,5)P_2$ to PIP_3 occurs, PLCγ might be activated to hydrolyze

$PI(4,5)P_2$. Both the DAG and the PIP_3 pathways are presumably essential for the completion of macropinocytosis. Activation of the PLCγ by PIP_3 might ensure that at least some of $PI(4,5)P_2$ precursor molecules are hydrolyzed to DAG. An undiscovered effect of DAG on PI3k might balance this effect, ensuring adequate formation of PIP_3.

An interesting observation is that the early signaling lipids are apparently depleted as part of the signaling cascade. Following their peak intensities, the membrane distributions of $PI(4,5)P_2$, PIP_3, and DAG all drop below their baseline, pre-spike levels (data not shown). Depletion of the early membrane lipids might act as a "refractory period" with significance in the regulation of macropinocytosis. This would prevent macropinocytosis from immediately re-initiating in the same region of the membrane where it had just occurred, presumably with the benefit of allowing the cell to better sample its extracellular environment.

3.5 Materials and Methods

3.5.1 Cell Culture

Bone marrow-derived macrophages (BMMs) were generated as previously described (Araki et al., 2003; Swanson, 1989). Bone marrow exudate was obtained from femurs of C57BL/6J mice. Marrow was cultured in medium (DMEM with 20% FBS and 30% L cell-conditioned medium) promoting the differentiation of macrophages. Bone marrow cultures were differentiated for 1 week with additions

of fresh differentiation medium at days 3 and 6. Following differentiation, macrophages were transfected and plated onto 25-mm circular coverslips. Cultures were incubated overnight in medium lacking M-CSF (RPMI 1640 with 20% heat-inactivated FBS). All experiments were performed the day after plating.

Calphostin C was used as an inhibitor in some experiments. When indicated, calphostin C was added to cell culture at a concentration of 0.1 μM 15 minutes before the addition of M-CSF, and was kept at the same concentration for the duration of the imaging experiment.

3.5.2 Constructs and Cell transfection

BMMs were transfected with plasmids encoding fluorescent protein chimeras via Amaxa Nucleofector II, using automated protocol Y-01. The conditions and reagents for macropinocytosis observation were 200 ng/mL M-CSF (R&D Systems) in Ringer's Buffer (155 mM NaCl, 5 mM KCl, 2 mM $CaCl_2$, 1 mM $MgCl_2$, 2 mM NaH_2PO_4, 10 mM glucose and 10 mM HEPES at pH 7.2). All imaging experiments were temperature controlled at 37°C.

3.5.3 Fluorescence Microscopy

Fluorescence images were collected using a Nikon Eclipse TE-300 inverted microscope with a 60x numerical aperture 1.4, oil-immersion PlanApo objective

lens (Nikon, Tokyo, Japan) and a Lambda LS xenon arc lamp for epifluorescence illumination (Sutter Instruments, Novato, CA). Fluorescence excitation and emission wavelengths were selected using a JP4v2 filter set (Chroma Technology, Rockingham, VT) and a Lambda 10-2 filter wheel controller (Shutter Instruments) equipped with a shutter for epifluorescence illumination control. Images were recorded with a Photometrics CoolSnap HQ cooled CCD camera (Roper Scientific, Tucson, AZ). Image acquisition and processing were performed using MetaMorph v6.3 (Molecular Devices, Sunnyvale, CA).

3.5.4 Ratiometric Imaging

Ratiometric imaging was used to correct for variations in optical path length caused by changes in cell morphology and volume. Specifically, fluorescence intensities for images of a fluorescent chimera were divided by fluorescence intensities of a non-chimeric fluorescent volume marker (e.g. Cit-BtkPH/Cer). All ratiometric images were generated using MetaMorph processing software.

3.5.5 FM4-64 Microscopy Experiments

FM4-64 was applied to cells at a concentration of 1 μg/mL in Ringer's Buffer. Images were collected every 20 seconds, with 1 second exposures, using a 555-nm excitation filter and a 605-nm emission filter.

3.5.6 FRET Microscopy

Measurement of Rac2 activation used cells transfected with Citrine-Rac2 and Cerulean-PBD. Measurement of Cdc42 activation used cells transfected with Citrine-Cdc42 and Cerulean-PBD. Measurement of Arf1 activation used cells transfected with Citrine-Arf1 and Cerulean-NGAT. Measurement of Arf6 activation used cells transfected with Citrine-Arf6 and Cerulean-NGAT.

FRET microscopy was carried out as previously described (Hoppe et al., 2002; Yoshida et al., 2009). Briefly, collected images were background-subtracted and shading-corrected. E_A images were then calculated using published FRET stoichiometry equations (Beemiller et al., 2006; Hoppe et al., 2002).

3.5.7 Fluorescence Intensity Measurements

Quantification of all microscopy experiments was conducted using MetaMorph. Measurements of intensity were made using the "draw region" and "region measurement" tools. For each signaling event, measurements were collected starting two frames (-40s) before the identification of ruffle closure (0s). Measurements were collected until after Rab5 had reached its peak intensity, typically around 180s after ruffle closure.

For each condition, whole cell fluorescence was averaged and subtracted from experimental readings, removing "baseline" noise. Comparison of the timing of different signaling events relied on normalized "peak intensities." Peak intensity

was identified as the highest measured fluorescence ratio during the sequence. All other timepoints were divided by the peak intensities, so that the "Relative Normalized Fluorescence" indicates the relative strength of a signaling molecule, with respect to that molecule's peak intensity. All peak intensities therefore had a value of 1.0 and indicated the point at which that signaling molecule was most prevalent during macropinocytosis.

3.5.8 4D Reconstruction Microscopy

Cells expressing CFP-MEM and mCherry-Rab5 fluorophores were imaged using an Olympus FV-500 Confocal microscope fitted with a 100x 1.45 NA oil immersion objective. The microscope was equipped with argon (for CFP imaging), and HeNe green (for mCherry imaging) lasers. Image collection used Fluoview FV500 imaging software. Image Z-stacks used a step size of 250 nm between planes. Images were collected continuously in line sequential scanning mode.

Image stacks were deconvolved using Huygens Essential (Scientific Volume Imaging, Hilversum, Netherlands). Resulting images were reconstructed into 4D image stacks. Ratiometric image stacks of mCherry-Rab5/CFP-MEM were created using MetaMorph. Stacks were visualized using the 4D viewer and linescan function in MetaMorph.

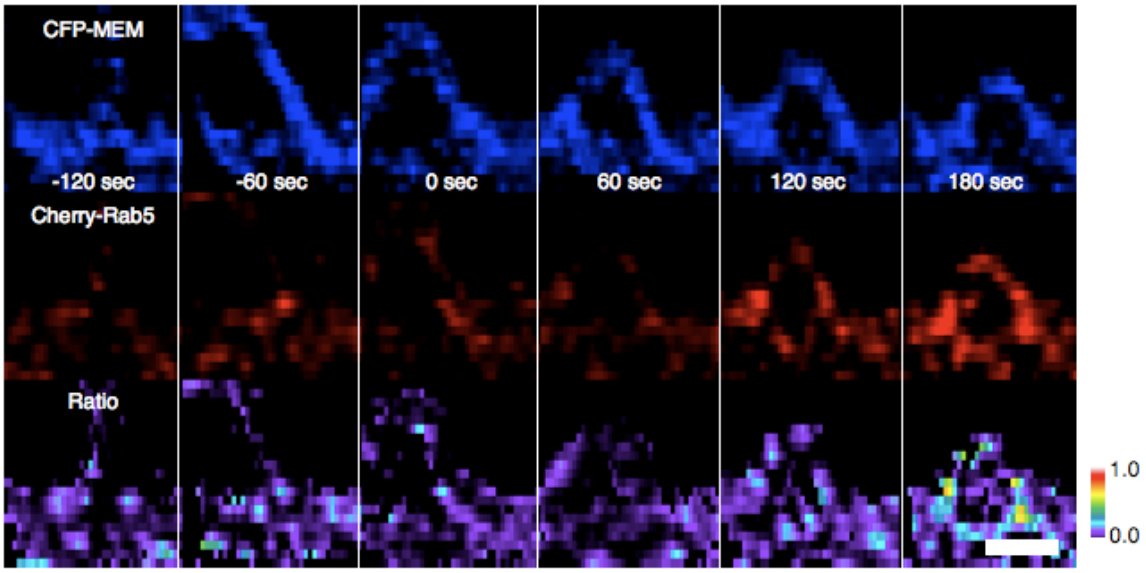

Figure 3.1 4D reconstruction of Cherry-Rab5 localization during macropinocytosis. Through-focus z-stacks were collected of CFP-MEM and mCherry-Rab5 at regular intervals during M-CSF-stimulated macropinocytosis. Cross-sections of macropinocytic cups showing distribution of CFP-MEM (blue, top row), Cherry-Rab5 (red, middle row) and Cherry/CFP ratio (pseudocolor). Time points are separated by 60s, with the "0s" marking the point at which cup closure is evident. Rab5 localization increased significantly after complete cup closure.

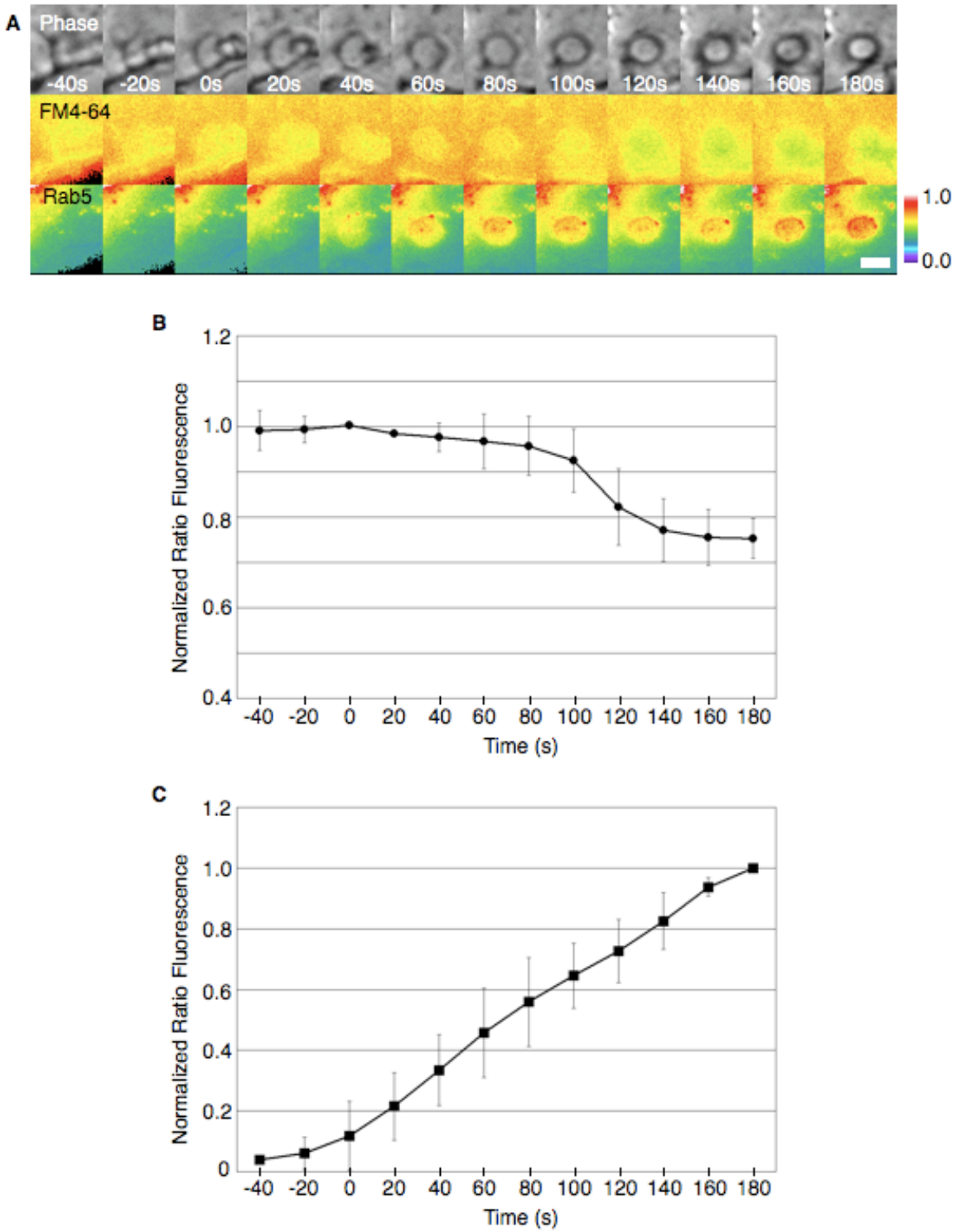

Figure 3.2 Photobleaching of FM4-64 in macropinosomes revealed the timing of cup closure relative to Rab5 localization. (A) Macrophages expressing CFP-MEM and Citrine-Rab5 imaged in the presence of M- CSF and 1μg/ml FM4-64. The top row shows phase-contrast images of the stages of macropinosome formation. The

middle row shows the intensity of ratiometric FM4-64/CFP-MEM. The bottom row shows the intensity of ratiometric Citrine-Rab5/CFP-MEM. Time *t=0* indicates the point of ruffle closure. FM4-64 photobleaching increased significantly at *t=100s*, indicating that as the point of cup closure. Rab5 localization increased steadily until *t=180s*. Scale bars = 3.0 μm. Color bars indicate relative fluorescence intensities of ratio images. (B) Plot of ratiometric FM4-64/CFP-MEM intensity during macropinosome formation. Inflection point occurred at *t=100s*. (C) Plot of ratiometric Cit-Rab5/CFP-MEM intensity during macropinosome formation. Rab5 localization peaked at *t=180s*, after the formation of the intracellular macropinosome. Error bars indicate standard deviation. $n \geq 9$ for each curve.

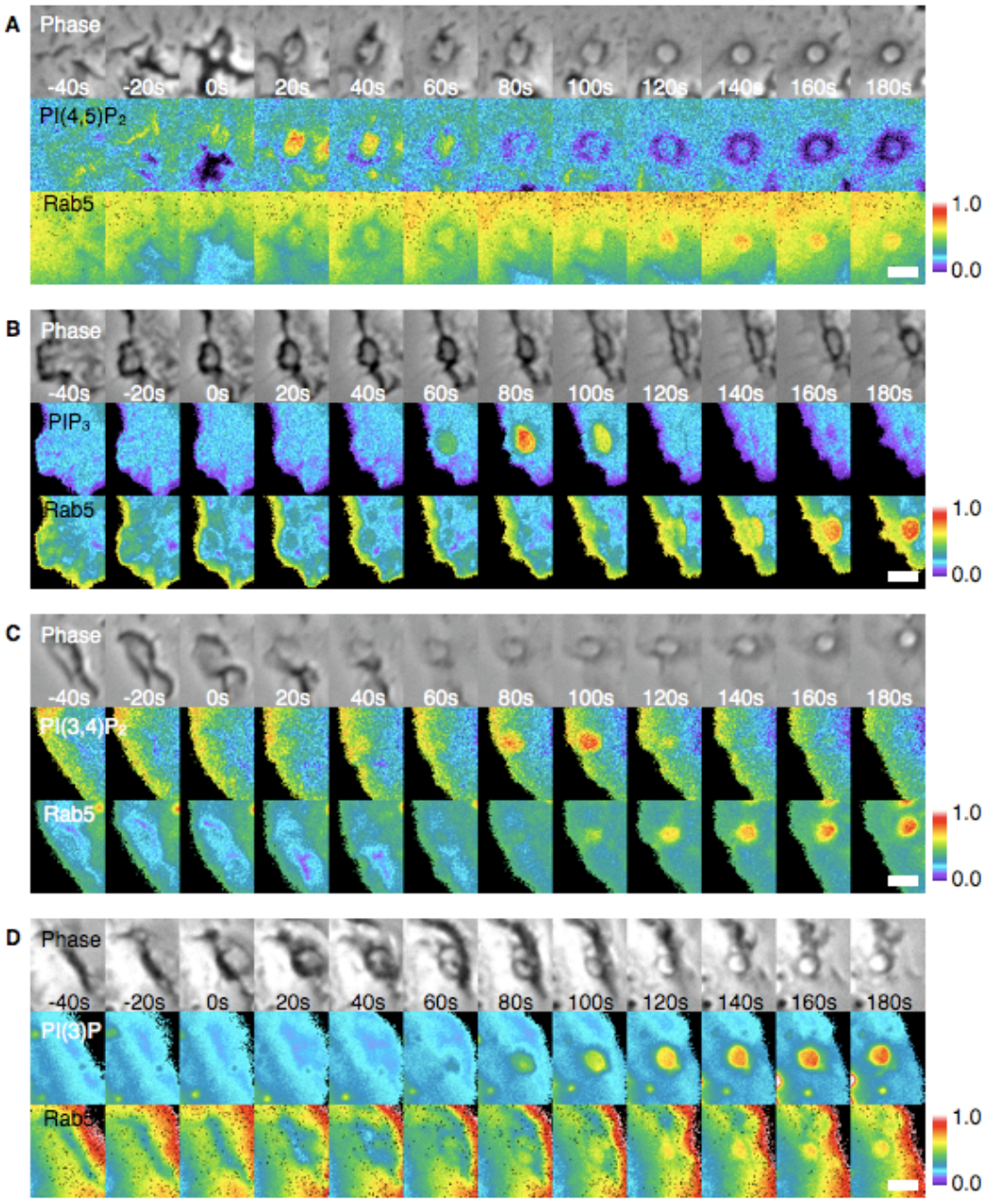
A
Phase
-40s
-20s
0s
20s
40s
60s
80s
100s
120s
140s
160s
180s
PI(4,5)P2
Rab5
1.0
0.0
B
Phase
PIP3
Rab5
C
Phase
PI(3,4)P2
Rab5
D
Phase
PI(3)P
Rab5
E
PI(4,5)P2
PIP3
PI(3,4)P2
PI(3)P
Rab5
Normalized Relative Fluorescence
Time (s)

Figure 3.3 Fluorescence imaging of phosphoinositide localization during macropinocytosis. (A-D) Macrophages were transfected with mCerulean, mCherry-Rab5, and a Citrine-tagged phosphoinositide probe. Localization of the phosphoinositide probe was imaged during M-CSF-stimulated macropinocytosis. The top row shows phase-contrast images of the stages of macropinocytosis. The middle row shows the ratiometric intensity of the Citrine-tagged fluorophore/mCerulean. The bottom row shows the ratiometric intensity of mCherry-Rab5/mCerulean. Time *t=0* indicates the point of ruffle closure. Scale bars = 3.0 μm. Color bars indicate relative fluorescence intensities of ratio images. (A) Fluorescence imaging of Citrine-PLCδ1PH, a probe for $PI(4,5)P_2$. Intensity peaked at *t=20s*. (B) Fluorescence imaging of Citrine-BtkPH, a probe for PIP_3. Intensity peaked at *t=80s*. (C) Fluorescence imaging of Citrine-Tapp1PH, a probe for $PI(3,4)P_2$. Intensity peaked at *t=100s*. (D) Fluorescence imaging of Citrine-FYVE, a probe for PI(3)P. Intensity peaked at *t=180s*. (E) Plot comparing relative timing of formation of different phosphoinositides. Quantitation showed that peak formation of PIP_3 is spread from *t=60-80s*. $n \geq 9$ for each curve. Error bars indicate standard deviation.

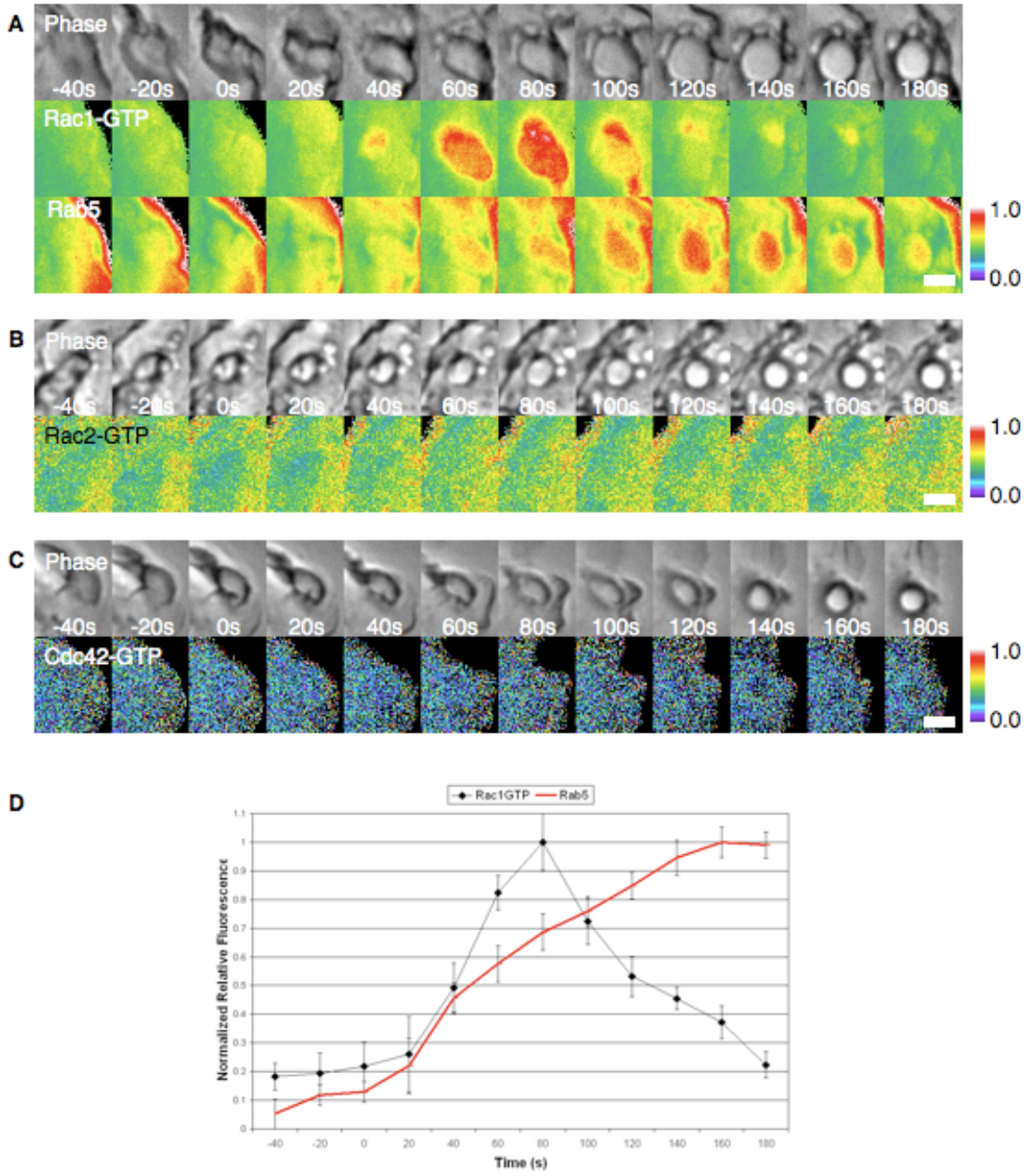

Figure 3.4 Imaging of Rho GTPase activity during macropinocytosis. (A) Macrophages were transfected with mCerulean, mCitrine-PBD, and mCherry-Rab5. PBD is a probe for Rac1-GTP, and therefore shows the localization of Rac1 activity. Cells were imaged during M-CSF-stimulated macropinocytosis. The top row shows phase-contrast images of the stages of macropinocytosis. The middle row shows the ratiometric intensity of the Citrine-PBD/mCerulean. The bottom row shows the ratiometric intensity of mCherry-Rab5/mCerulean. Time *t=0* indicates the point of ruffle closure. Rac1 activity peaked around *t=80*s. Scale bars = 3.0 μm. Color bar indicates relative fluorescence intensities of ratio images. (B and C) FRET

microscopy of GTPase activity. Cells were transfected with Cerulean-PBD, mCherry, and a Citrine-tagged GTPase. FRET interactions between Cerulean and Citrine demonstrate activity of the GTPase being tested. The top row shows phase-contrast images of the stages of macropinocytosis. The bottom row shows the FRET value E_A. Color bars indicate relative intensities of FRET interactions. Time *t=0* indicates the point of ruffle closure. Scale bars = 3.0 μm. (B) FRET imaging for Rac2. Cells expressed Citrine-Rac2. No FRET was observed, suggesting that Rac2 is not active during macropinocytosis. (C) FRET imaging for Cdc42-GTP. Cells expressed Citrine-Cdc42 No FRET was observed, suggesting that Cdc42 is not active during macropinocytosis. (D) Plot showing relative timing of Rac1 activation. Quantitation showed that peak activation of Rac1 occurred at *t=80s*. $n \geq 9$.

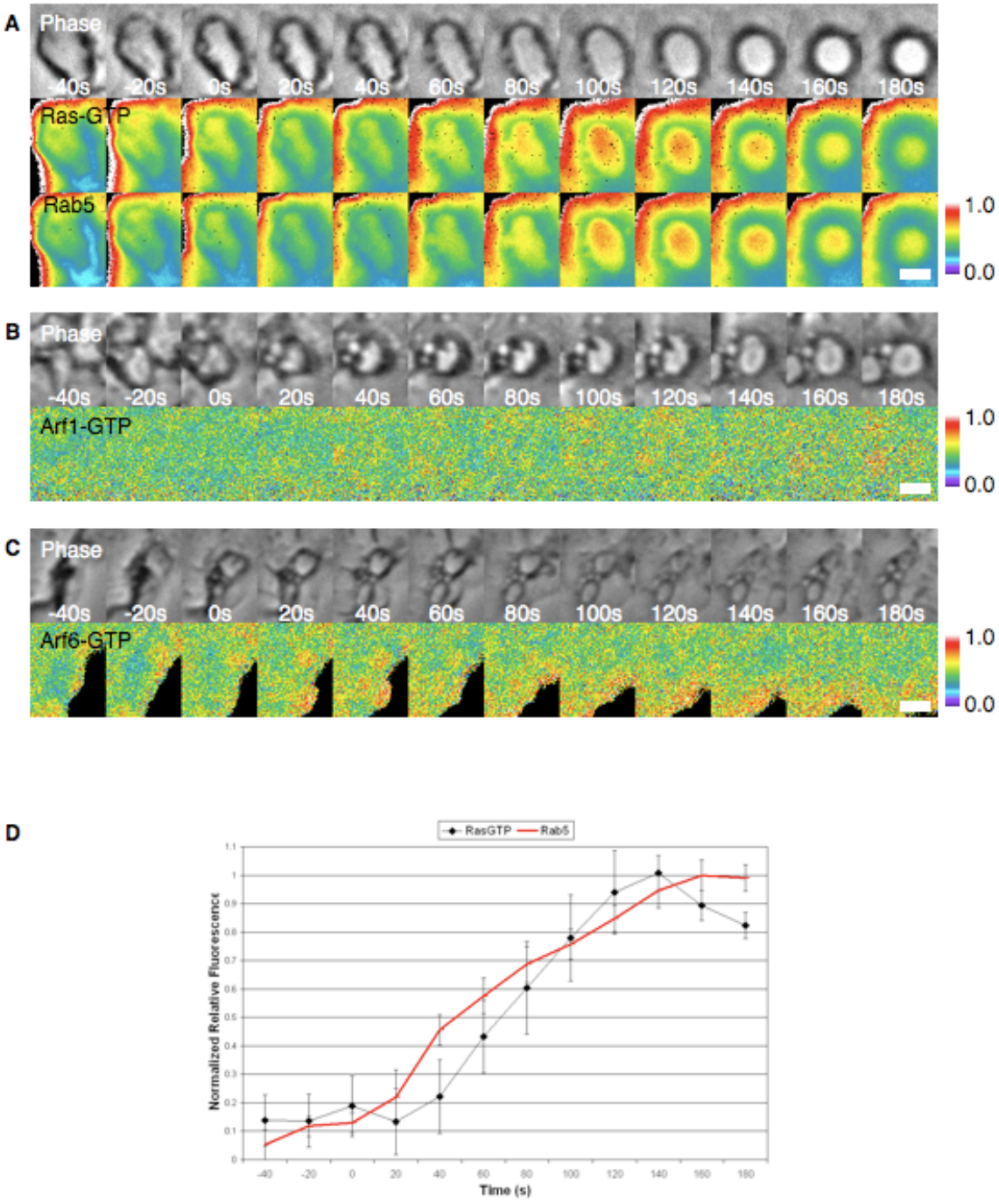

Figure 3.5 Imaging of Ras and Arf GTPase activity during macropinocytosis. (A) Macrophages were transfected with mCFP-RBD, mCitrine, and mCherry-Rab5. RBD is a probe for Ras-GTP, and therefore shows the localization of Ras activity. Cells were imaged during M-CSF-stimulated macropinocytosis. The top row shows phase-contrast images of the stages of macropinocytosis. The middle row shows the ratiometric intensity of the CFP-RBD/mCerulean. The bottom row shows the ratiometric intensity of mCherry-Rab5/mCerulean. Time *t=0* indicates the point of ruffle closure. Scale bars = 3.0 μm. Color bar indicates relative fluorescence

intensities of ratio images. (B and C) FRET imaging of GTPase activity. Cells were transfected with Cerulean-NGAT, mCherry, and a Citrine-tagged GTPase. FRET interactions between Cerulean and Citrine demonstrate activity of the GTPase being tested. The top row shows phase contrast images of the stages of macropinocytosis. The bottom row shows the FRET value E_A. Color bars indicate relative intensities of FRET interactions. Time *t=0* indicates the point of ruffle closure. Scale bars = 3.0 μm. (B) FRET imaging for Arf1-GTP. Cells expressed Citrine-Arf1. No FRET was observed, suggesting that Arf1 is not active during macropinocytosis. (C) FRET imaging for Arf6-GTP. Cells expressed Citrine-Arf6. No FRET was observed, suggesting that Arf6 is not active during macropinocytosis. (D) Plot showing relative timing of Ras activation. Quantitation showed that peak activation of Ras has broad activation, with the peak occurring at *t=180s*. $n \geq 9$.

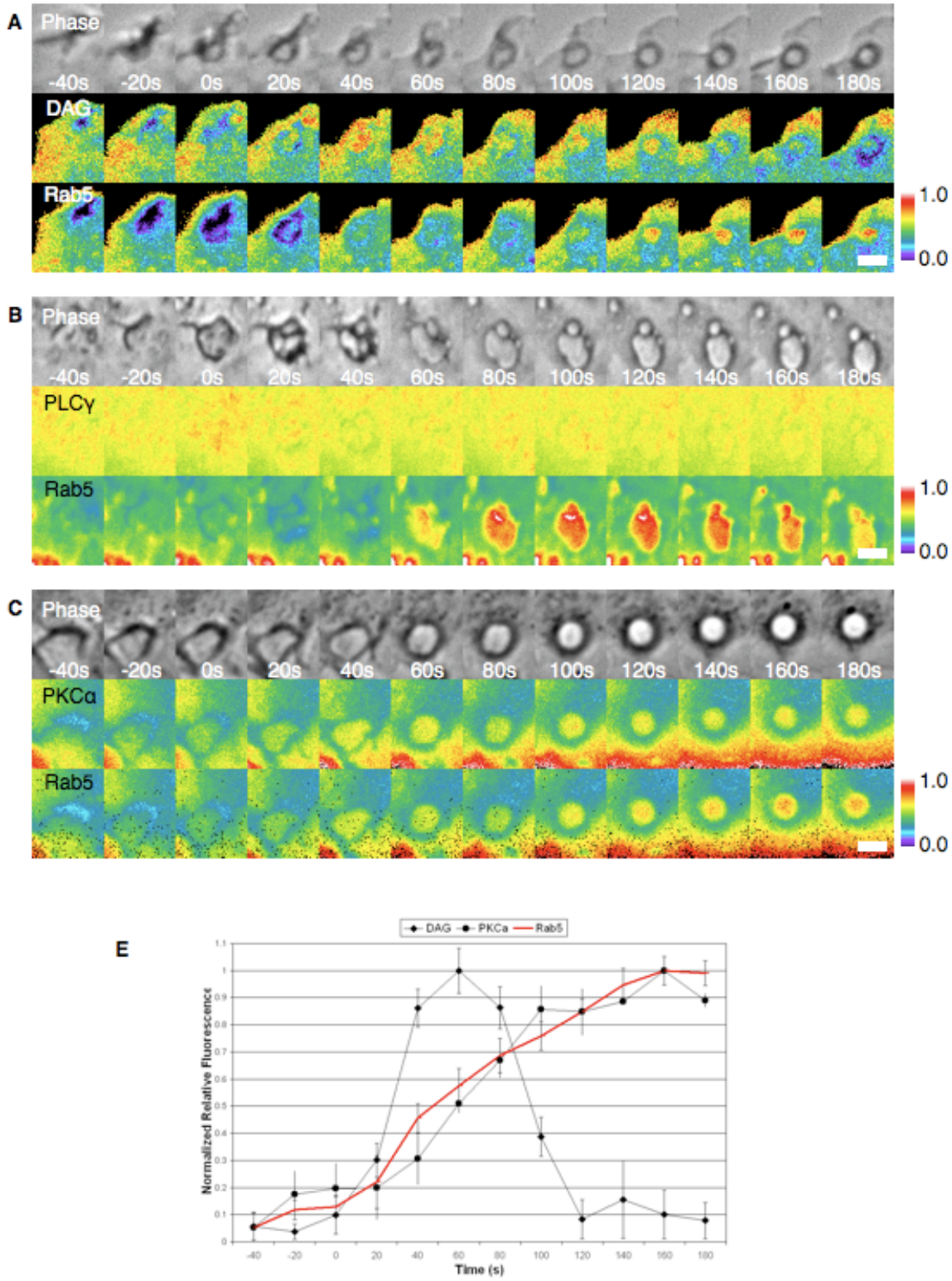

Figure 3.6 Fluorescence imaging of the DAG pathway during macropinocytosis. (A-C) Macrophages were transfected with mCerulean, mCherry-Rab5, and a Citrine-tagged probe. Probes were imaged during M-CSF-stimulated macropinocytosis. The

top row shows phase-contrast images of the stages of macropinocytosis. The middle row shows the ratiometric intensity of the Citrine-tagged fluorophore/mCerulean. The bottom row shows the ratiometric intensity of mCherry-Rab5/mCerulean. Time *t=0* indicates the point of ruffle closure. Scale bars = 3.0 μm. Color bars indicate relative fluorescence intensities of ratio images. (A) Fluorescence imaging of Citrine-C1δ, a probe for DAG. Intensity peaked at *t=40s*. (B) Fluorescence imaging of Citrine-PLCγ, a probe for PIP_3. PLCγ did not demonstrate differential localization during macropinocytosis. (C) Fluorescence imaging of Citrine-PKCα. PKCα localization mirrored that of Rab5. (D) Plot comparing relative timing of signaling events in the DAG pathway. Quantitation showed that peak formation of DAG occurs at *t=40s*. PKCa localization to the forming macropinosome peaks at *t=180s*. $n \geq 9$ for each curve. Error bars indicate standard deviation.

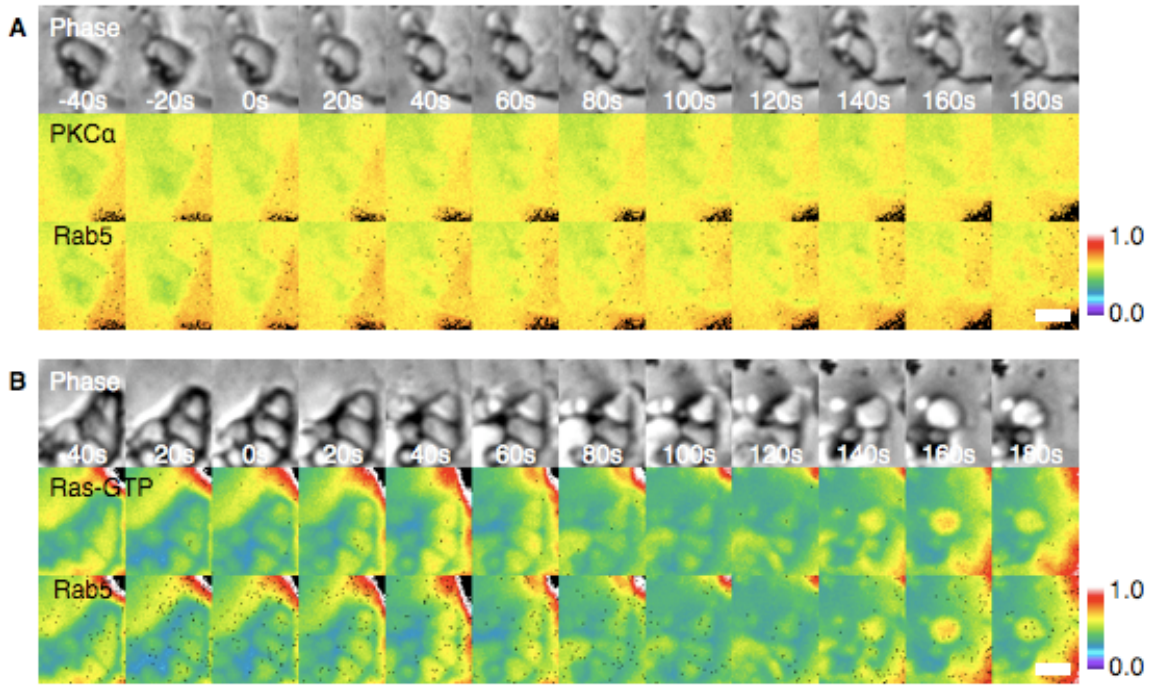

Figure 3.7 Effect of calphostin C treatment on late signaling molecules. (A and B) Macrophages were treated with 0.1 μM calphostin C during M-CSF-stimulated macropinocytosis. (A) Cells were transfected with mCerulean, mCitrine-PKCα, and mCherry-Rab5. The top row shows phase-contrast images of the stages of macropinocytosis. The middle row shows the ratiometric intensity of the Citrine-tagged fluorophore/mCerulean. The bottom row shows the ratiometric intensity of mCherry-Rab5/mCerulean. PKCα localization was abrogated by the calphostin C treatment. Additionally, localization of Rab5 was apparently reduced. Time *t=0* indicates the point of ruffle closure. Scale bars = 3.0 μm. Color bars indicate relative fluorescence intensities of ratio images. (B) Cells were transfected with CFP-RBD, mCitrine, and mCherry-Rab5. Other conditions are same as in (A). Calphostin C also reduced the activation of Ras.

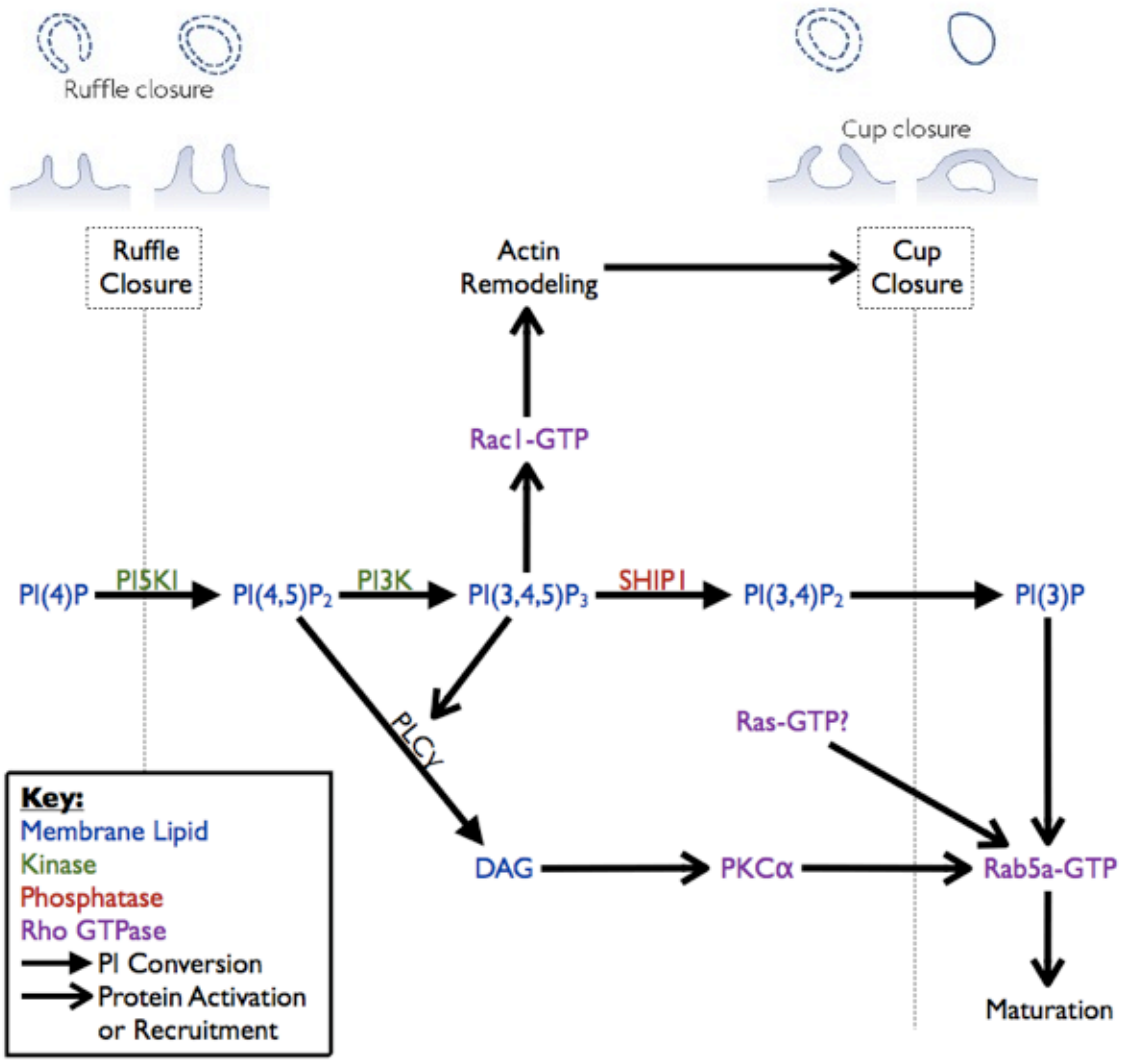

Figure 3.8. Hypothetical Schematic of the Macropinocytic Signaling Network

3.6 References

Araki, N., T. Hatae, A. Furuka, and J.A. Swanson. 2003. Phosphoinositide-3-kinase-independent contractile activities associated with fcgamma-receptor-mediated phagocytosis and macropinocytosis in macrophages. *Journal of Cell Science*. 116:247-257.

Azzi, A., D. Boscoboinik, and C. Hensey. 1992. The protein kinase C family. *Eur J Biochem*. 208:547-557.

Beemiller, P., A.D. Hoppe, and J.A. Swanson. 2006. A phosphatidylinositol-3-kinase-dependent signal transition regulates ARF1 and ARF6 during Fcgamma receptor-mediated phagocytosis. *PLoS biology*. 4:e162.

Botelho, R.J., R.E. Harrison, J.C. Stone, J.F. Hancock, M.R. Philips, J. Jongstra-Bilen, D. Mason, J. Plumb, M.R. Gold, and S. Grinstein. 2009. Localized diacylglycerol-dependent stimulation of Ras and Rap1 during phagocytosis. *The Journal of biological chemistry*. 284:28522-28532.

Bustelo, X.R., V. Sauzeau, and I.M. Berenjeno. 2007. GTP-binding proteins of the Rho/Rac family: regulation, effectors and functions in vivo. *Bioessays*. 29:356-370.

De Matteis, M.A., and A. Godi. 2004. PI-loting membrane traffic. *Nat Cell Biol*. 6:487-492.

Di Paolo, G., and P. De Camilli. 2006. Phosphoinositides in cell regulation and membrane dynamics. *Nature*. 443:651-657.

DiNitto, J.P., and D.G. Lambright. 2006. Membrane and juxtamembrane targeting by PH and PTB domains. *Biochimica et biophysica acta*. 1761:850-867.

Donaldson, J.G. 2003. Multiple roles for Arf6: sorting, structuring, and signaling at the plasma membrane. *The Journal of biological chemistry*. 278:41573-41576.

Donaldson, J.G., and C.L. Jackson. 2011. ARF family G proteins and their regulators: roles in membrane transport, development and disease. *Nature reviews*. 12:362-375.

Franke, T.F., D.R. Kaplan, L.C. Cantley, and A. Toker. 1997. Direct regulation of the Akt proto-oncogene product by phosphatidylinositol-3,4-bisphosphate. *Science*. 275:665-668.

Hancock, J.F. 2003. Ras proteins: different signals from different locations. *Nature reviews*. 4:373-384.

He, H., T. Watanabe, X. Zhan, C. Huang, E. Schuuring, K. Fukami, T. Takenawa, C.C. Kumar, R.J. Simpson, and H. Maruta. 1998. Role of phosphatidylinositol 4,5-bisphosphate in Ras/Rac-induced disruption of the cortactin-actomyosin II complex and malignant transformation. *Molecular and cellular biology*. 18:3829-3837.

Hinchliffe, K.A., A. Ciruela, and R.F. Irvine. 1998. PIPkins1, their substrates and their products: new functions for old enzymes. *Biochimica et biophysica acta*. 1436:87-104.

Honda, A., M. Nogami, T. Yokozeki, M. Yamazaki, H. Nakamura, H. Watanabe, K. Kawamoto, K. Nakayama, A.J. Morris, M.A. Frohman, and Y. Kanaho. 1999.

Phosphatidylinositol 4-phosphate 5-kinase alpha is a downstream effector of the small G protein ARF6 in membrane ruffle formation. *Cell*. 99:521-532.

Hoppe, A., K. Christensen, and J.A. Swanson. 2002. Fluorescence resonance energy transfer-based stoichiometry in living cells. *Biophys J*. 83:3652-3664.

Hoppe, A.D., and J.A. Swanson. 2004. Cdc42, Rac1, and Rac2 display distinct patterns of activation during phagocytosis. *Molecular Cell Biology*. 15:3509-3519.

Kerr, M.C., and R.D. Teasdale. 2009. Defining macropinocytosis. *Traffic*. 10:364-371.

Kotani, K., K. Yonezawa, K. Hara, H. Ueda, Y. Kitamura, H. Sakaue, A. Ando, A. Chavanieu, B. Calas, F. Grigorescu, and et al. 1994. Involvement of phosphoinositide 3-kinase in insulin- or IGF-1-induced membrane ruffling. *The EMBO journal*. 13:2313-2321.

Krauss, M., and V. Haucke. 2007a. Phosphoinositide-metabolizing enzymes at the interface between membrane traffic and cell signalling. *EMBO reports*. 8:241-246.

Krauss, M., and V. Haucke. 2007b. Phosphoinositides: regulators of membrane traffic and protein function. *FEBS Lett*. 581:2105-2111.

Lanzetti, L., A. Palamidessi, L. Areces, G. Scita, and P.P. Di Fiore. 2004. Rab5 is a signalling GTPase involved in actin remodelling by receptor tyrosine kinases. *Nature*. 429:309-314.

Lorenzo, P.S., M. Beheshti, G.R. Pettit, J.C. Stone, and P.M. Blumberg. 2000. The guanine nucleotide exchange factor RasGRP is a high -affinity target for diacylglycerol and phorbol esters. *Mol Pharmacol*. 57:840-846.

Rohatgi, R., H.Y. Ho, and M.W. Kirschner. 2000. Mechanism of N-WASP activation by CDC42 and phosphatidylinositol 4, 5-bisphosphate. *The Journal of cell biology*. 150:1299-1310.

Simons, K., and D. Toomre. 2000. Lipid rafts and signal transduction. *Nature Reviews Molecular Cell Biology*. 1:31-39.

Singer, S.J., and G.L. Nicolson. 1972. The fluid mosaic model of the structure of cell membranes. *Science*. 175:720-731.

Swanson, J.A. 1989. Phorbol esters stimulate macropinocytosis and solute flow through macrophages. *Journal of Cell Science*. 94:135-142.

Swanson, J.A. 2008. Shaping cups into phagosomes and macropinosomes. *Nature Reviews Molecular Cell Biology*. 9:639-649.

Swanson, J.A., and C. Watts. 1995. Macropinocytosis. *Trends in cell biology*. 5:424-428.

Tall, G.G., M.A. Barbieri, P.D. Stahl, and B.F. Horazdovsky. 2001. Ras-activated endocytosis is mediated by the Rab5 guanine nucleotide exchange activity of RIN1. *Developmental cell*. 1:73-82.

Ugolev, Y., Y. Berdichevsky, C. Weinbaum, and E. Pick. 2008. Dissociation of Rac1(GDP).RhoGDI complexes by the cooperative action of anionic liposomes containing phosphatidylinositol 3,4,5-trisphosphate, Rac guanine nucleotide exchange factor, and GTP. *The Journal of biological chemistry*. 283:22257-22271.

van Blitterswijk, W.J., and B. Houssa. 2000. Properties and functions of diacylglycerol kinases. *Cell Signal*. 12:595-605.

Wennerberg, K., K.L. Rossman, and C.J. Der. 2005. The Ras superfamily at a glance. *J Cell Sci*. 118:843-846.

Xie, Z., P.A. Singleton, L.Y. Bourguignon, and D.D. Bikle. 2005. Calcium-induced human keratinocyte differentiation requires src- and fyn-mediated phosphatidylinositol 3-kinase-dependent activation of phospholipase C-gamma1. *Molecular biology of the cell*. 16:3236-3246.

Yoshida, S., A.D. Hoppe, N. Araki, and J.A. Swanson. 2009. Sequential signaling in plasma-membrane domains during macropinosome formation in macrophages. *Journal of Cell Science*. 122:3250-3261.

Zerial, M., and H. McBride. 2001. Rab proteins as membrane organizers. *Nature reviews*. 2:107-117.

Chapter Four:
Discussion

4.1 Summary of Thesis Findings

The overall goal of this thesis was to investigate the signaling dynamics that drive macropinocytosis. Macropinocytosis is a complex response that requires minimal environmental guidance. Like phagocytosis and chemotaxis, macropinocytosis involves large morphological changes in response to an extracellular stimulus. However, macropinocytosis does not benefit from the spatial guidance provided by an ingested particle or chemical gradient (Swanson, 2008). A primary focus was thus to determine how macropinosome formation is spatially organized. By testing membrane and diffusion dynamics, we showed that macropinocytosis effectively relies on the cell creating a membrane subdomain with inhibited diffusion.

The shape and size of the macropinocytic subdomain makes it unlike other membrane structures, which led us to examine its functional significance. We specifically wanted to look at how it related to macropinocytic signaling. We found that the membrane cup is essentially a self-contained signaling platform. The result is that macropinocytic signaling is a highly ordered process that relies on temporal

conversion between phosphoinositide species. The temporal regulation most likely relies on the spatial organization provided by the membrane diffusion barriers.

One hope in our study was that the specifics of macropinosome formation might have general applicability to cellular signaling and behavior. We have shown here the cells are capable of creating large-scale membrane subdomains for the purpose of localizing and amplifying signaling networks. As part of that, we provided evidence that membrane shape is an important consideration in signaling networks.

4.1.1 Identification of a Macropinocytic Membrane Diffusion Barrier

The inspiration for this thesis was an observation by Yoshida et al. that the signaling molecules PIP_3 and Rac1-GTP demonstrate "spikes" localized to the membrane cup during macropinocytosis (Yoshida et al., 2009). An immediate question was whether the distribution of these molecules was dependent on the macropinocytic cup. Membrane structures are based on actin polymerization, so we looked at the effect of Latrunculin B, an actin depolymerizing agent, on the formation of Rac1-GTP. Latrunculin B generally inhibited Rac1 activation, and completely inhibited the Rac1-GTP spikes evident in macropinocytic cups.

We were next interested in assessing which aspect of the membrane cups allowed for the Rac1-GTP localization. We considered that some aspect of the cups inhibited diffusion of membrane molecules into the surrounding membrane. We

measured diffusion dynamics using a photoactivatable probe, and found that diffusion of proteins on the inner leaflet of the plasma membrane was indeed inhibited by macropinocytic cups.

It was important for us to characterize the nature of this inhibited diffusion. First, was diffusion inhibited throughout the entire membrane cup? We found that molecules diffused at a normal rate in the central base of the cup, but became inhibited near the perimeter of the cup. This supported a model in which molecules were diffuse and interact within the membrane cup, but cannot diffuse out of the cup. A possible implication of this is to concentrate signaling activities. Studies on receptor activation kinetics suggest that a controlled signaling environment like this could maximize interactions between activated surface receptors. A possible result of such environments is the localized positive-feedback amplification of downstream signals, as we saw with PIP_3 and Rac1-GTP.

We then tried to determine the location of the barrier in the wall of the macropinocytic cup. In 4-Dimensional (4-D) imaging experiments, our fluorescent probe persisted and diffused slowly throughout the entire cell wall. This suggested that some property of the walls made them diffusion barriers. The nature of the diffusion barrier remains unknown and is an area of potential future research.

4.1.2 Characterization of Signaling Dynamics within Macropinocytic Cups

Our experimentation was next directed towards the functional implication of the macropinocytic cup diffusion barrier. As mentioned, the diffusion barrier had implications in maximizing the downstream effects of local receptor activation, so we characterized the macropinocytic signaling network using fluorescence imaging.

The first molecules we investigated were phosphoinositides (PIs). Macropinocytosis relies on a variety of molecules being recruited to a discrete membrane structure over time. For differential recruitment to occur over time, the molecular composition of the membrane was likely changing continuously. PIs are efficiently converted between species, and each species has a distinct shape recognized by different effector molecules (Di Paolo and De Camilli, 2006). We found that four PIs and DAG were synthesized in macropinocytic cups. Further, these PIs had a clear temporal order that corresponded with the progression of signaling during macropinocytosis, and that overlapped with sequences of Rac1, Ras, and Rab5 activation and localization.

4.2 Experimental Limitations

All of the experimental work in this thesis was subject to the limitations of fluorescence live cell imaging. Fluorescence imaging involves transfecting cells with fluorescently-tagged proteins of interest. An initial concern is the nature of macrophage transfection itself. Likely due to their importance in the immune response to infection, macrophages are resistant to DNA insertion. As a result, macrophage transfection is an inefficient process. Further, bone marrow-derived

macrophages are transfected using electroporation, a violent process that kills many cells. Cell health is an importance consideration when trying to determine normal cellular signaling mechanisms. Fortunately, healthy cells were transfected nonetheless. We were careful to image only cells that demonstrated normal morphology and growth factor responsiveness. Based on subjective assessment, the cells that were imaged were no less adept at macropinocytosis than non-transfected cells.

Another problem with transfection is that it causes the proteins of interest to become overexpressed in the cell, which can inadvertently alter the signaling process being studied. This thesis looked at the localization of various proteins. It is possible that overexpression of these proteins caused them to localize to regions of interest at higher concentrations than they naturally do. Overexpression can also interfere with PI-dependent activities (Holz et al., 2000). One method for correcting for this is in the statistical analysis. Background subtraction and normalization processes help address high expression problems, although not completely.

Adding fluorescent tags to proteins can alter protein function. It is possible that a fluorescent tag interferes with protein responsiveness. Since they greatly outnumber their endogenous counterparts, the fluorescent-tagged proteins might behave like dominant-negative mutants. Such problems are primarily addressed in the basic design of the fluorescent chimera. Signaling proteins often have distinct and well-characterized binding and catalytic domains that mediate much of their activity. Protein function artifacts can be avoided simply by inserting the fluorescent

tag in a region of the protein where it will not alter conformation or accessibility of the functional domains. Crystallography is commonly used to forecast whether a fluorescent tag will have deleterious effects.

A goal of Chapter Three was to monitor the formation of different phosphoinositide (PI) species during macropinocytosis. Fluorescent tagging of PIs is impractical, forcing us to use proxies to visualize PI dynamics. Myriad cellular processes rely on PH and FYVE domains recognizing different PIs with high specificity. However, the localization of these domains is still only an approximation of PI formation (DiNitto and Lambright, 2006). We have no reason to think this occurred in our experiments, but a variety of factors could disallow a PI-binding domain from recognizing its intended target.

PI-binding domains might also have interfered with macropinocytic signaling. As a fluorescent probe bound to its target PI, it might have blocked access to that molecule. Consequently, endogenous effectors would not be properly activated, and normal PI conversion might not occur. In such instances, one would expect PI-binding probes to slow or inhibit the pattern of macropinocytosis. However, we do not think this was a significant effect in our studies because the rate of macropinocytic formation was apparently consistent regardless the probes being expressed.

Important observations in both Chapters Two and Three were made using 4-D imaging. 4-D imaging helped characterize spatial patterns in macropinocytic signaling, but the observations were not quantifiable. The imaging software simply

does not include relevant quantification tools for 4-D images. In both instances where 4-D imaging was used, the observations were confirmed using independent quantitative methods.

Computer modeling was used in Chapter Two to provide key insights. An immediate drawback with computer modeling is that it does not completely account for the complexity of any cellular behavior. No cell response has been entirely characterized, and any corresponding computer model lacks certain information. Our experiments relied on modeling the three-dimensional nature of membrane cups. Membrane cups are not perfectly consistent, varying in size and depth of curvature. We designed our computer models based on averages between cells, which allowed us to look at general trends.

4.3 Future Experimental Directions

This thesis has provided some new insights into general cell signaling behavior and into the molecules involved in macropinocytosis. However, we feel that the experimental results raised at least as many questions as they have answered. Some of those questions could be addressed in future research.

4.3.1 Characterization of the Diffusion Barrier

The molecular nature of the diffusion barrier remains unclear. What is the molecular nature of the diffusion barrier? In Chapter Two, we discussed three

possibilities: physical interaction between actin filaments and the membrane, membrane curvature, and a “fence” molecule.

Of these, investigation of the fence molecule would be the most straightforward. It would involve monitoring the macropinocytic localization of different molecular candidates, looking for molecules that localize to the walls of macropinocytic cups. Once a molecule is identified, it could be deleted or inhibited. Diffusion dynamics would be re-tested, and deviations from previous diffusion dynamics would suggest a role for that molecule in the inhibition of diffusion. Cadherins were recently shown to participate in the regulation of macropinocytosis. Cadherins also mediate cell-cell junctions, which are regions of the membrane in which diffusion is similarly inhibited (Sabatini et al., 2011). As such, cadherins would be strong candidates for such testing.

Membrane curvature and actin polymerization are highly interdependent, and it would be difficult to test them individually. One possible method would be through use of optical tweezers, which are focused laser beams that generate attractive or repulsive forces (Poole and Losert, 2007). Those forces can be used to distort the membrane in ways similar to macropinocytosis. If diffusion dynamics were altered in the absence of actin polymerization, it would strengthen the notion that the membrane curvature itself creates the diffusion barrier.

4.3.2 Characterization of the Macropinocytic Signaling Pathway

The macropinocytic signaling pathway proposed in Figure 3.8 is incomplete. There are likely many other molecules involved in the regulation of macropinocytosis, as well as uncharacterized relationships between those molecules. The immediate goal of future research is thus the continued investigation of macropinocytic signaling events.

WASP and Arp2/3 are proteins that are known to function in actin polymerization. These proteins interact with Rho GTPases and phosphoinositides, and might contribute to macropinocytic cytoskeletal reorganization(Kolluri et al., 1996; Suetsugu et al., 2002). Additionally, actin depolymerizaton is also involved in macropinocytosis, and it would be interesting to see which molecules mediate that process.

Dynamin is a GTPase that is thought to mediate the scission of the forming macropinosome from the plasma membrane (Swanson, 2008). Additionally, it recognizes several of the PIs studied in Chapter Three, PI(4,5)P_2, PIP3, and PI(3,4)P_2 (DiNitto and Lambright, 2006). Dynamin might contribute to macropinocytosis, and could provide information on the timing of macropinosome closure.

4.4 Conclusions

Macropinocytosis is a dynamic and self-organized process. We used fluorescence imaging to characterize the mechanisms that govern the formation of the intracellular macropinosome. We showed that organization of the

macropinocytic signaling network depends on a diffusion barrier in the forming macropinosome. The diffusion barrier has the ability to localize signaling molecules, facilitating their cooperation and interconversion. This is best exemplified in the waves of phosphoinositide formation that correlate with the progression of macropinocytosis. These results provide novel insights into the spatial and temporal regulation of signaling networks.

4.5 References

Di Paolo, G., and P. De Camilli. 2006. Phosphoinositides in cell regulation and membrane dynamics. *Nature*. 443:651-657.

DiNitto, J.P., and D.G. Lambright. 2006. Membrane and juxtamembrane targeting by PH and PTB domains. *Biochimica et biophysica acta*. 1761:850-867.

Holz, R.W., M.D. Hlubek, S.D. Sorensen, S.K. Fisher, T. Balla, S. Ozaki, G.D. Prestwich, E.L. Stuenkel, and M.A. Bittner. 2000. A pleckstrin homology domain specific for phosphatidylinositol 4, 5-bisphosphate (PtdIns-4,5-P2) and fused to green fluorescent protein identifies plasma membrane PtdIns-4,5-P2 as being important in exocytosis. *The Journal of biological chemistry*. 275:17878-17885.

Kolluri, R., K.F. Tolias, C.L. Carpenter, F.S. Rosen, and T. Kirchhausen. 1996. Direct interaction of the Wiskott-Aldrich syndrome protein with the GTPase Cdc42. *Proceedings of the National Academy of Sciences of the United States of America*. 93:5615-5618.

Poole, C., and W. Losert. 2007. Laser tweezer deformation of giant unilamellar vesicles. *Methods Mol Biol*. 400:389-404.

Sabatini, P.J., M. Zhang, R.V. Silverman-Gavrila, and M.P. Bendeck. 2011. Cadherins at cell-autonomous membrane contacts control macropinocytosis. *J Cell Sci*. 124:2013-2020.

Suetsugu, S., H. Miki, and T. Takenawa. 2002. Spatial and temporal regulation of actin polymerization for cytoskeleton formation through Arp2/3 complex and WASP/WAVE proteins. *Cell Motil Cytoskeleton*. 51:113-122.

Swanson, J.A. 2008. Shaping cups into phagosomes and macropinosomes. *Nature Reviews Molecular Cell Biology*. 9:639-649.

Yoshida, S., A.D. Hoppe, N. Araki, and J.A. Swanson. 2009. Sequential signaling in plasma-membrane domains during macropinosome formation in macrophages. *Journal of Cell Science*. 122:3250-3261.